

NRL Report 8025

**Wideband, Noncoherent, Frequency-Hopped
Waveforms and Their Hybrids in
Low-Probability-of-Intercept Communications**

JOHN D. EDELL

*Special Communications Branch
Communications Sciences Division*

November 8, 1976

**APPROVED FOR PUBLIC
RELEASE - DISTRIBUTION
UNLIMITED**



**NAVAL RESEARCH LABORATORY
Washington, D.C.**

SECURITY CLASSIFICATION OF THIS PAGE (When Date Entered)

REPORT DOCUMENTATION PAGE		READ INSTRUCTIONS BEFORE COMPLETING FORM	
1. REPORT NUMBER NRL Report 8025	2. GOVT ACCESSION NO.	3. RECIPIENT'S CATALOG NUMBER	
4. TITLE (and Subtitle) WIDEBAND, NONCOHERENT, FREQUENCY-HOPPED WAVEFORMS AND THEIR HYBRIDS IN LOW- PROBABILITY-OF-INTERCEPT COMMUNICATIONS		5. TYPE OF REPORT & PERIOD COVERED Interim report on a continuing NRL problem	
		6. PERFORMING ORG. REPORT NUMBER	
7. AUTHOR(s) John D. Edell		8. CONTRACT OR GRANT NUMBER(s)	
9. PERFORMING ORGANIZATION NAME AND ADDRESS Naval Research Laboratory Washington, D.C. 20375		10. PROGRAM ELEMENT, PROJECT, TASK AREA & WORK UNIT NUMBERS NRL Prob R01-88 Project RF21-222.403	
11. CONTROLLING OFFICE NAME AND ADDRESS Office of Naval Research Arlington, Va. 22217		12. REPORT DATE November 8, 1976	
		13. NUMBER OF PAGES 89	
14. MONITORING AGENCY NAME & ADDRESS (if different from Controlling Office)		15. SECURITY CLASS. (of this report) Unclassified	
		15a. DECLASSIFICATION/DOWNGRADING SCHEDULE	
16. DISTRIBUTION STATEMENT (of this Report) Distribution limited to U.S. Government Agencies only; test and evaluation; November 1976. Other requests for this document must be referred to the Commanding Officer, Naval Research Laboratory, Washington, D.C. 20375.			
17. DISTRIBUTION STATEMENT (of the abstract entered in Block 20, if different from Report)			
18. SUPPLEMENTARY NOTES			
19. KEY WORDS (Continue on reverse side if necessary and identify by block number)			
Frequency-hopped waveforms		Quality factors	
Low probability of intercept		Filter bank combiner	
Optimum detectors		Radiometer	
20. ABSTRACT (Continue on reverse side if necessary and identify by block number)			
<p>Frequency hopping is a commonly used technique for achieving wide spread spectrum bandwidths in intercept-resistant and interference-resistant communications. This report develops the techniques necessary to determine the contribution of a frequency-hopped modulation to communication system detectability, independent of such scenario-related parameters as relative geometry, antenna gains, and link margins.</p>			

(Continued)

A variety of frequency-hopped modulation schemes, associated processing techniques, and losses are discussed. Optimum intercept receivers are considered in order to place a theoretical bound on signal detectability. This, in turn, leads to the development of quality factors which permit an analysis of the impact of waveform parameters alone on covertness.

A parametric analysis is performed in terms of these quality factors for a large family of modulations. The result is a small subset of signals optimized for covertness, consisting of fast hop pulsed waveforms and slow hop continuous waveforms, both with pseudonoise hop bandwidth spreading. Selection of the final modulation must ultimately depend on such additional system synchronization time, implementation complexity, and jam resistance. The impact of these factors is discussed qualitatively.

CONTENTS

I. INTRODUCTION	1
II. FREQUENCY-HOPPED MODULATIONS AND SIGNAL PROCESSING	1
Frequency-Hopped Waveforms	2
Pure Frequency Hopping	2
Pulsed Transmission	3
Frequency Hop/Pseudonoise	3
Frequency Hopping With Binary and Higher Order Orthogonal Modulations	3
Orthogonal M -ary Modulation	3
Frequency-Hopped M -ary Frequency Shift Key	4
Frequency-Hopped M -ary Time Shift Key	6
Frequency-Hopped M -ary Code Shift Key	7
Signal Processing Techniques and Processing Losses	8
Coherent Multiple-Hop Detection, Known Initial Phase	8
Coherent Multiple-Hop Detection, Unknown Initial Phase	9
Noncoherent Multiple-Hop Detection	11
Noncoherent Combining Loss	11
Frequency Offset Losses	15
Doppler Compensation	15
Frequency-Hop/Pseudonoise Demodulation	17
Digital Correlator Matched Filters	18
III. FREQUENCY-HOPPED AND HYBRID WAVEFORM QUALITY FACTORS	19
Optimum Intercept Detectors for Spread-Spectrum Signals .	19
Energy Detector	19
Optimum Hop Detector	24
Filter Bank Combiner	36

Detectability Scenario and Quality Factors	38
Detectability Scenario	38
Synoptic Detectability Criteria and Message Quality Factor	40
Hop Quality Factor	41
IV. COVERTNESS: PARAMETRIC ANALYSIS	42
Quality Factors and Waveform, Parameters	42
Covertiness: The Best Choice	58
Pure-Frequency Hopping	58
Pulsed Transmission	61
Pseudonoise Hop Spreading	62
M-ary Modulation	64
V. CONCLUSION	
ACKNOWLEDGMENTS	65
REFERENCES	65
APPENDIX A — Filter Bank Combiner Performance	67
SYMBOLS	84

WIDEBAND, NONCOHERENT, FREQUENCY-HOPPED WAVEFORMS AND THEIR HYBRIDS IN LOW-PROBABILITY-OF-INTERCEPT COMMUNICATIONS

I. INTRODUCTION

Spread-spectrum communications techniques are widely used in interference- and intercept-resistant communications. This report describes the role of noncoherent frequency-hopped waveforms and their hybrids in low-probability-of-intercept wideband spread-spectrum systems. A large family of continuous-wave and pulsed waveform structures is considered, and the relative contribution of each to covertness is analyzed in terms of scenario-independent detectability quality factors for optimum or near-optimum detector models. A parametric analysis is performed in terms of these quality factors, to determine the effects on detectability of such waveform parameters as frequency-hop rate, duty cycle, pseudonoise hop bandwidth spreading, and modulation efficiency. The family of waveforms and modulation schemes considered here is not exhaustive, but the analytical techniques can be extended without difficulty to a virtually unlimited number of other candidates.

This report is divided into three main sections. The first describes basic frequency-hopped waveform structures, frequency-hopped orthogonal high-order M -ary modulations, and signal processing techniques, with their associated losses. The losses are extremely important because covertness depends ultimately on modulation efficiency. Noncoherent combining losses and losses due to relative transmit and receive frequency offsets (doppler shifting and local oscillator drift) are key considerations in the design of a noncoherent frequency-hopped modulation scheme. To assess their full impact on efficiency, one must clearly understand the underlying phenomena. Cost and complexity must also be considerations in the design of a frequency-hopped modulation. Although not discussed specifically in these terms, the signal processing considerations presented should provide insight into this area.

The second section describes theoretically optimum and near-optimum intercept receivers, the detectability scenario, and, finally, the development of scenario-independent detectability quality factors.

The last section presents a parametric analysis for a large family of frequency-hopped waveforms in terms of detectability quality factors. The result is a small subset of frequency-hopped waveforms optimized for covertness. Final waveform selection depends on such constraints as cost, complexity, jam resistance, and synchronization, which are treated only qualitatively here.

II. FREQUENCY-HOPPED MODULATIONS AND SIGNAL PROCESSING

Before techniques for quantifying the effects of modulation on system covertness (the modulation quality factor) are discussed, it is useful to review the basic concept of

spread-spectrum communication signals and to describe some of the covert waveforms and demodulation techniques available to the system designer. The purpose of any covert spread-spectrum modulation is to distribute signal energy in frequency, so as to force an unauthorized listener to observe a much wider bandwidth than actually required for communication. An authorized receiver knows the manner in which the energy was distributed and therefore need not blindly search the entire spread spectrum.

Two fundamental techniques for bandwidth spreading are (a) direct-sequence pseudo-noise modulation (DS) and (b) frequency hopping. Of the two, DS is less vulnerable to detection. It could be generated, for example, by phase modulation of an RF carrier with a high-bit-rate, pseudorandom sequence; this results in an effective bandwidth approximately equal to the sequence bit rate. The technique while devoid of any unique characteristics that would make it more detectable by means other than an energy detector, has the disadvantage of requiring large coherent bandwidths in the propagation medium and phase tracking at the receiver if extremely wide bandwidths are used. This imposes a severe hardware constraint on the receiver.

The second technique, frequency hopping, entails switching, or hopping the RF carrier to a different frequency at regular intervals, determined by the frequency-hopping rate. This technique can achieve extremely wide bandwidths and can be efficiently detected at the receiver without the need for phase coherence across the full spread bandwidth; it thus requires simpler hardware. However, unlike direct-sequence spreading, frequency hopping generally can be detected by exploiting individual hop characteristics. Actual hop detection techniques and their relation to covertness will be discussed later.

Frequency-Hopped Waveforms

The following symbols are used throughout this section:

W_s = total spread-spectrum bandwidth,

W_p = bandwidth occupied by a single hop,

t_p = dwell time of a single hop,

N = total number of frequency cells to which carrier can be switched ($N = W_s/W_p$),

t_m = message duration,

f_H = rate at which carrier is switched or hopped,

M = total number of hops per message ($M = t_m f_H$).

Pure Frequency Hopping (FH)

Frequency-hopped waveforms are most easily described in terms of time-frequency diagrams. Such a diagram is shown in Fig. 1 for pure frequency hopping. In this scheme the carrier is switched, or hopped, to a new frequency occupying a new bandwidth cell of width W_p every $1/f_H$ s. No effort is made to expand the bandwidth of the hop pulse W_p beyond its intrinsic value of approximately $1/t_p$, or to reduce the pulse duration t_p to anything less than $1/f_H$.

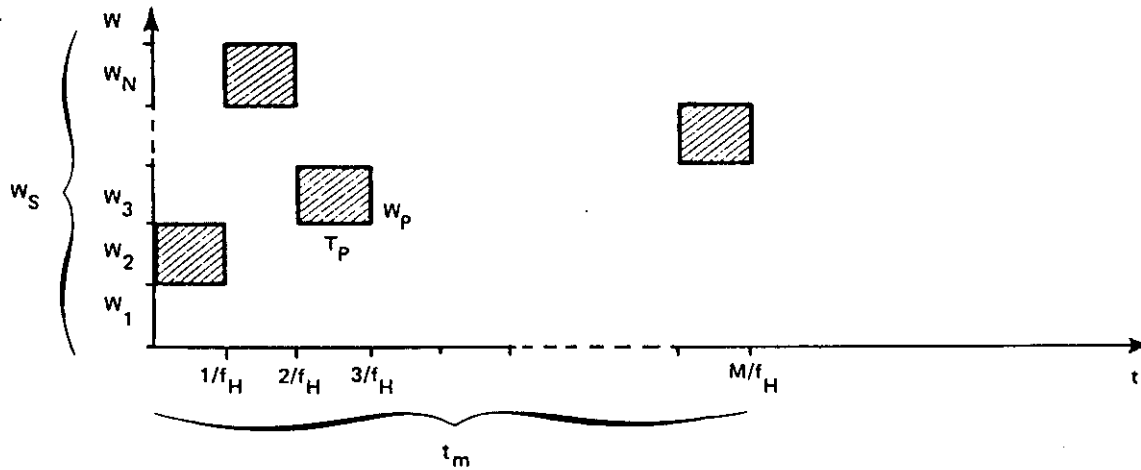


Fig. 1—Pure frequency hopping

Pulsed Transmission

The time-frequency diagram for a pulsed transmission is identical to that of the pure frequency hop waveform (Fig. 1) except that hop pulsewidth t_p is less than $1/f_H$. Carrier duty cycle α is defined as follows:

$$\alpha = \frac{t_p}{1/f_H} = t_p f_H = M t_p / t_m .$$

Pulsed transmission transmits more carrier power for a shorter period of time than pure frequency hopping. In both cases, however, average carrier power transmitted remains the same. Pulsed transmission also expands the pulse bandwidth to $1/t_p$, rather than f_H as in the pure frequency hop case.

Frequency Hop/Pseudonoise

For this FH/PN scheme, the time-frequency diagram is again identical to that for pure frequency hopping, except that hop bandwidth W_p is increased beyond its intrinsic value of approximately $1/t_p$. This is accomplished by phase modulating the hop carrier by a pseudo-random (PN) binary stream at a rate greater than f_H . The effective bandwidth of the hop is then approximately equal to the clock rate of the PN stream.

One can easily envision a combination of pulsed transmission and PN spreading; the effects of such combinations are discussed later.

Frequency Hopping With Binary and Higher Order Orthogonal Modulations

Orthogonal M-ary Modulation

Orthogonal M -ary modulation is a technique in which one of M possible symbols is transmitted, each representing one of the possible combinations of $\log_2 M$ binary data bits.

The simplest example of this type of modulation is binary, or "2-ary," frequency shift keying (FSK). Here the carrier frequency is shifted to one of two frequencies, depending on whether the data bit to be transmitted is a binary 1 or 0. If this were extended to 8-ary FSK, the carrier frequency would be shifted to one of 2^3 , or 8, frequencies, corresponding to the binary state of the three data bits to be transmitted. Curves for M -ary modulation schemes are well known and yield the required ratio of bit energy to noise density, E_b/N_0 for a given probability of bit error in a Gaussian communications channel.

The advantage of higher order M -ary modulation is that it reduces the E_b/N_0 required to achieve a given bit error probability. The probability of a symbol error P_s is given as follows [1]:

$$P_s = \frac{1}{M} \sum_{i=2}^M (-1)^i \binom{M}{i} \exp \left[\frac{(1-i)}{iN_0} E_s \right]$$

$\frac{E_s}{N_0}$ = the ratio of energy per symbol to noise density.

The corresponding probability of bit error is

$$P_b = \frac{2^{[(\log_2 M)-1]}}{2^{\log_2 M} - 1} P_s = \frac{M}{2(M-1)} P_s.$$

Thus the required E_b/N_0 for a specified P_b can be determined, because

$$\frac{E_b}{N_0} = \frac{E_s/N_0}{\log_2 M}.$$

Curves showing the effective required E_b/N_0 for a given probability of bit error are shown in Fig. 2 for various values of M . The improvement in E_b/N_0 decreases as M becomes larger and approaches a limit of $E_b/N_0 = -1.6$ dB as M goes to infinity. Improvement is gained very slowly beyond $M = 64$. M -ary modulations can be made in both time and frequency. Several of these techniques, combined with frequency hopping, will now be discussed.

Frequency-Hopped M-ary Frequency Shift Key

Figure 3 shows a time-frequency diagram of an M -ary FSK-modulated frequency-hopped waveform. In its simplest form, the transmitted carrier frequency is shifted to one of M relative frequencies, each at fixed offsets from the carrier and each representing one of the M states of $\log_2 M$ data bits. Thus the signal energy can occupy one of M possible positions (bandwidth cells) about the actual transmitted carrier frequency, forming an M -ary FSK symbol. Without frequency hopping, the carrier would be shifted to one of the M possible positions, and the transmitter would remain at this frequency for the duration of $\log_2 M$ data bits or $\log_2 M/r_D$ s, where r_D is the data rate. With frequency hopping, the carrier frequency is hopped at intervals of $1/f_H$ s. In essence this hops the

NRL REPORT 8025

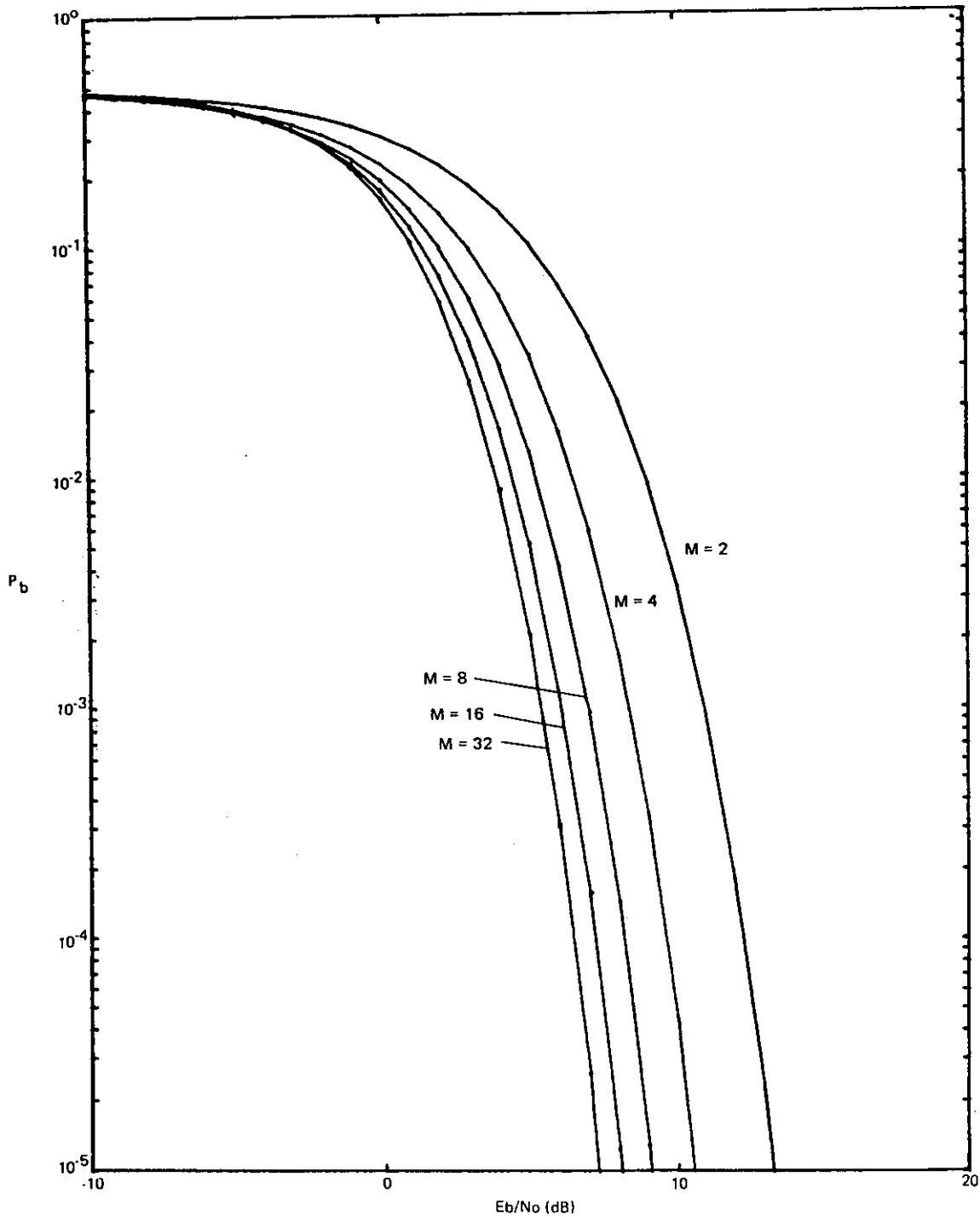


Fig. 2—Bit error probability for orthogonal M -ary modulation, noncoherent reception

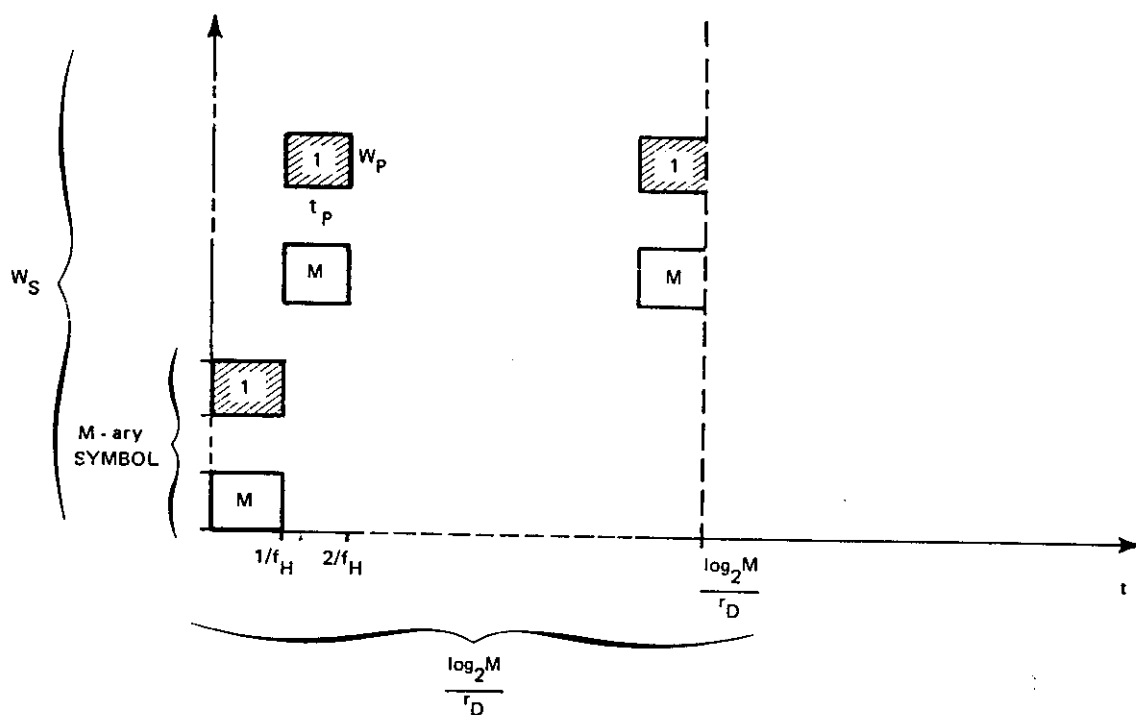


Fig. 3—*M*-ary FSK frequency hopping

entire *M*-ary symbol over the spread bandwidth. The actual number of hops per symbol equals $f_H \log_2 M / r_D$.

One could, of course, envision more sophisticated schemes, for which each of the *M* possible transmitted frequencies would be pseudorandomly selected. That is, during each hop interval a different set of *M* pseudorandom frequencies (not contiguous or related as before) would be selected to form the *M*-ary symbol. This would require a more complex receiver but could have considerable advantages over certain jamming threats. Pulsed transmission and PN hop bandwidth spreading could be used with this type of modulation.

Frequency-Hopped M-ary Time Shift Key

Figure 4 shows a time-frequency diagram of an *M*-ary time shift key (TSK) modulated, frequency-hopped waveform. This is equivalent to pulse-position modulation with superimposed frequency hopping. In the scheme depicted in Fig. 4A an *M*-ary symbol is made up of *M* time slots, each representing one of the *M* possible states of the $\log_2 M$ data bits. The duration of each time slot is equal to the duration of $\log_2 M$ data bits divided by *M*, the number of slots required. The frequency-hopped carrier is transmitted only during the time slot representing the state of the $\log_2 M$ data bits. The number of hops transmitted during the time slot is equal to hopping rate f_H multiplied by slot duration $\log_2 M / Mr_D$. Transmitter duty cycle α is equal to $1/M$.

Figure 4B depicts another *M*-ary TSK modulation technique. In this case the frequency-hopped carrier is divided into *N* groups of *M* hops. Each group represents a

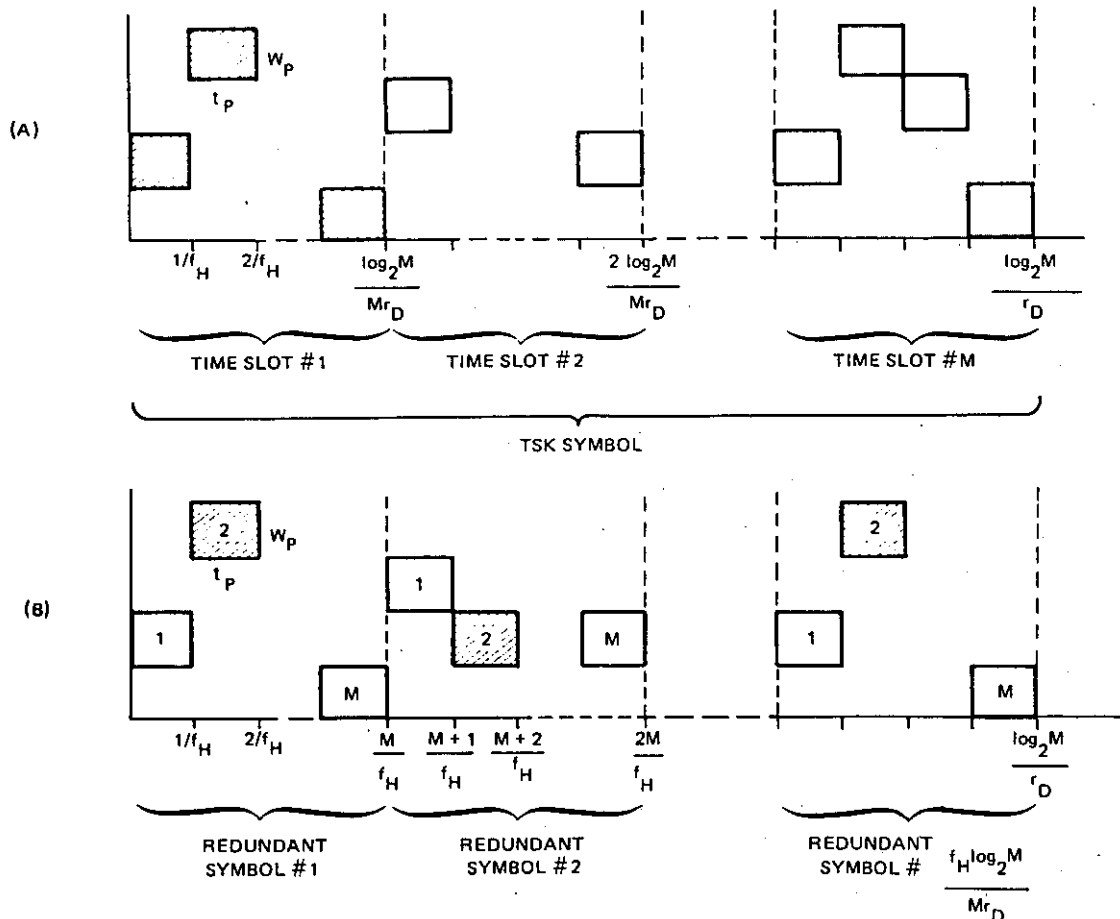


Fig. 4— M -ary TSK frequency hopping—A and B

redundant TSK symbol, and the carrier is transmitted during time interval $1/f_H$, corresponding to the state of the $\log_2 M$ data bits it represents. This symbol is then repeated $N = (f_H \log_2 M / Mr_D)$ times during the symbol period. Duty cycle α is again equal to $1/M$.

Ordinarily, some form of pseudorandom time hopping would be used to avoid vulnerability to a time-gated receiver. Pulsed transmission (reduction in α) and PN spreading can also be applied to this modulation scheme.

Frequency-Hopped M -ary Code Shift Key

A frequency-hopped M -ary code shift key (CSK) waveform is identical in form to pure frequency hopping with pseudonoise hop spreading added. However, one of M fixed codes is added to the hop spreading PN to represent the state of the $\log_2 M$ data bits. The receiver must determine (through correlation) which code was transmitted. Pulsed transmission also can be used with this modulation scheme.

Signal Processing Techniques and Processing Losses

A frequency-hopped transmission is in essence a transmitted series of pulses, and the detection of such a waveform is analogous to pulse train detection in radar theory [2]. The results of radar analysis can therefore be applied to the detection of frequency-hopped waveforms.

A transmitted frequency-hopped waveform can be represented as

$$s(t) = A \cos(\omega_i t + \phi_i)$$

where

- $i = 0, 1, 2, \text{ etc.},$ represents the frequency-hop interval
- $\omega_i =$ carrier frequency transmitted during hop interval i
- $\phi_i =$ unknown initial phase of the carrier frequency ω_i
- $A =$ carrier amplitude.

Received signal $S_R(t)$ is transmitted signal $s(t)$ corrupted by white Gaussian noise $n(t)$. It is represented as

$$S_R(t) = s(t) + n(t).$$

In the following discussion it is assumed that transmitter and receiver are synchronized in time so that the frequency-hop synthesizer in the receiver will select the carrier ω_i at the appropriate time. To demonstrate the techniques, hop detection will be treated in the same way as the detection of multiple pulses in radar theory. Actual demodulation of frequency-hopped waveforms incorporates the accumulation of multiple hops, such that the total energy in a transmitted data bit or M -ary symbol may be recovered. Once this energy is accumulated a decision is made as to which data bit or symbol was actually transmitted. These decision circuits will not be discussed explicitly; they are merely indicated by the label "Decision" in the receiver diagrams that follow.

Coherent Multiple-Hop Detection, Known Initial Phase

A coherent frequency-hopped waveform is one in which the carrier phase remains continuous when the frequency is changed. (The discussion in this section applies equally well to a waveform in which the phase is known, but not necessarily continuous, after the carrier is switched.) A typical receiver for optimum detection of such a waveform when the starting phase of the first hop is known is shown in Fig. 5. In this case, $\phi_i = 0$, corresponding to coherent hopping and known phase.

The frequency-hop synthesizer produces an exact replica of the transmitted signal $s(t)$, including phase. This is multiplied by incoming signal $S_R(t)$ and integrated over the desired number of hops k (again, the desired number of hops depends on the modulation scheme). The integrator output is then sampled at its maximum value $Ak/2f_H$, which occurs at time k/f_H , and this value is sent to the decision circuit.

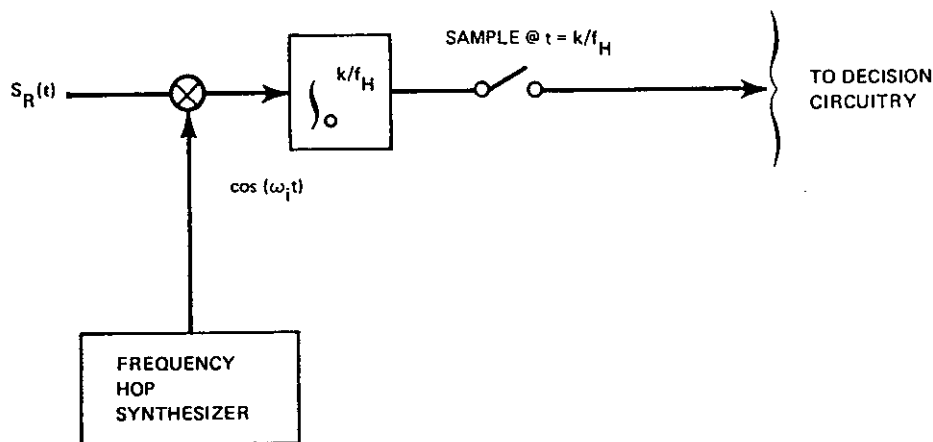


Fig. 5—Coherent frequency-hop detection when initial phase is known

The multiplier and integrator form a filter matched to the transmitted waveform containing k hops. This is sometimes referred to as a coherent matched filter, indicating that the phase of the signal is known exactly. In reality, the initial signal phase is not likely to be known. In addition, rather severe hardware constraints would be involved in implementing a coherently hopped waveform.

Coherent Multiple-Hop Detection, Unknown Initial Phase

An example of a receiver for optimum detection of a coherently hopped waveform when the initial phase is unknown as shown in Fig. 6. Now, $\phi_i = \phi_1 = \phi_F$, which corresponds to a constant but unknown phase offset of the initial hop (and hence every hop).

In this case received signal $S_R(t)$ is simultaneously dehopped and split into in-phase (I) and quadrature (Q) components through multiplication by the respective outputs of the frequency-hop synthesizer. The maximum output of the integrator in the I channel is given by

$$I(t) = \frac{Ak}{2f_H} \cos \phi_F$$

and in the Q channel by

$$Q(t) = \frac{Ak}{2f_H} \sin \phi_F .$$

The output of each integrator is, therefore, exactly the same as when the initial phase is known, except that it is now reduced by the cosine and sine of the phase offsets, respectively. The reduction in output due to this phase offset can be resolved by forming the square root of the sum of the squares of the outputs of each channel. This yields a maximum output at time k/f_H of

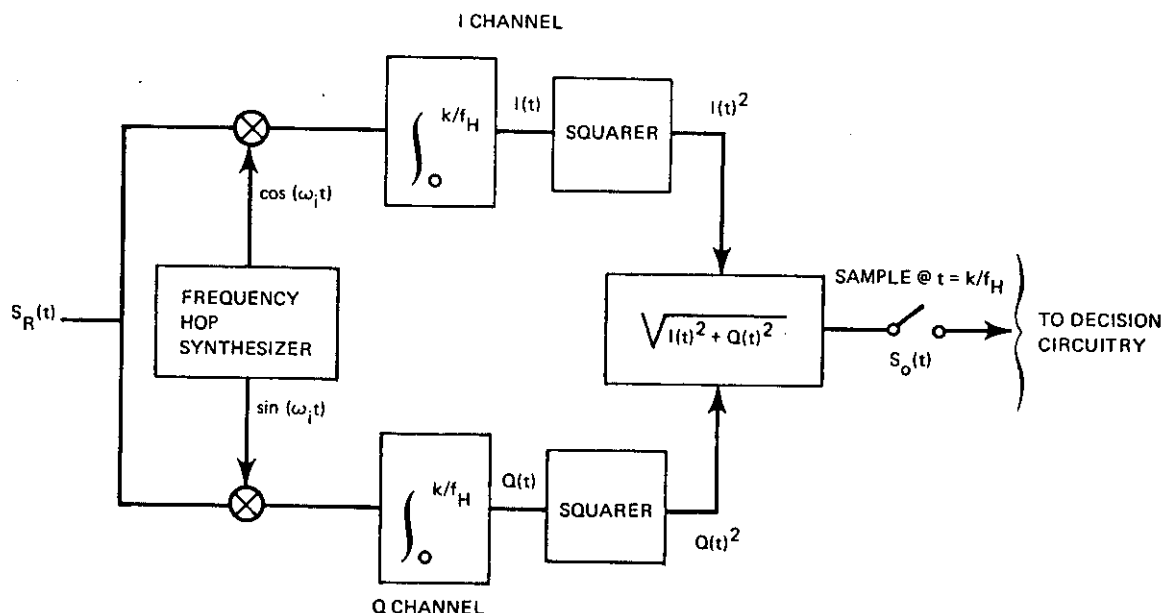


Fig. 6—Coherent frequency-hop detection when initial phase is not known

$$S_0\left(\frac{k}{f_H}\right) = \left[\left(\frac{Ak}{2f_H}\right)^2 \cos^2 \phi_F + \left(\frac{Ak}{2f_H}\right)^2 \sin^2 \phi_F \right]^{1/2}$$

$$= \frac{Ak}{2f_H},$$

which is identical to that of the known phase receiver.

The process of forming the square root of the sum of the squares is known as envelope detection, so called because it need not use the absolute phase of the transmitted signal to recover the transmitted energy. Instead, it forms the envelope of the signal, which is independent of initial phase. Because phase information is not used, one would expect the envelope detector to be inferior in performance to the coherent detector, and indeed this is the case. The reason is that the envelope detector processes both in-phase and quadrature components of the incoming signal, and therefore processes noise that is both in phase and in quadrature with the signal. The known-phase coherent detector processes only the in-phase signal component and thus only in-phase noise. Generally, for a narrowband Gaussian process, the in-phase and quadrature noise components are independent. This reduces the likelihood that the two will be large simultaneously with respect to a large carrier amplitude A . As would be expected, for a large transmitted carrier power the performance of the envelope detector is very close to that of the coherent detector. However, when A is small the received signal must compete with both components of noise, and the performance of the envelope detector falls below that of the coherent detector.

NRL REPORT 8025

The multiplier and integrator in each receiver channel of Fig. 6 form filters that are matched to the in-phase and quadrature components of the incoming waveform containing k hops, except that the relative phase offset is unknown. It is important to note that this detector will resolve an initial phase offset only, and not a continuously varying phase offset, as would be encountered if the frequency-hop synthesizer were slightly off frequency or if the incoming signal had a doppler offset. These cases are discussed later.

Noncoherent Multiple-Hop Detection

A noncoherently hopped waveform is one in which the carrier phase is not continuous as the frequency is changed. In other words, the initial phase ϕ_i of each hop is a random variable. A typical receiver for near-optimum detection of such a waveform is shown in Fig. 7. A comparison with Fig. 6 (the receiver for a waveform of k coherent hops with unknown initial phase) indicates that now each of the k hops is detected individually in the same manner (envelope detection) as the entire coherent waveform was processed previously. After each hop output $S_0(t)$ is sampled and accumulated in the video or post-detection integrator. Finally, after k hops have been accumulated, the output of the video integrator is sampled and fed to the demodulator. This process is generally known as noncoherent combining and post-detection or video integration.

Noncoherent Combining Loss

The detection of k coherent hops with the receiver in Fig. 6 yields exactly the same output as would be expected if all the carrier power were transmitted at one frequency for time interval k/f_H . There is no loss in output when coherent frequency hopping is used. However, when k hops (either coherent or noncoherent) are processed with the receiver in Fig. 7, that is, when each hop is noncoherently (envelope) detected and then combined (video integrated), there is a net loss relative to k coherently processed hops. The source of this degradation will now be examined.

Recall that for small carrier amplitudes envelope detector performance is poorer than that of the coherent detector because the former must process noise that is both in phase and in quadrature with the signal. The in-phase and quadrature noise samples may be considered zero-mean, independent, Gaussian random variables. Let the in-phase and quadrature noise samples be represented by N_I and N_Q , respectively. If the standard deviation of these random variables is much less than carrier amplitude A , then, intuitively, both noise samples would not be large simultaneously with respect to A . For white Gaussian noise of power spectral density N_0 the standard deviations of N_I and N_Q are

$$\sqrt{N_I^2} = \sqrt{N_Q^2} = \sqrt{BN_0}$$

where B is the noise bandwidth of interest. The matched filter integrators in the receivers of Figs. 5, 6, and 7, often referred to as "integrate and dump" filters, have an effective noise bandwidth approximated by the reciprocal of integration time t . That is,

$$B \approx 1/t.$$

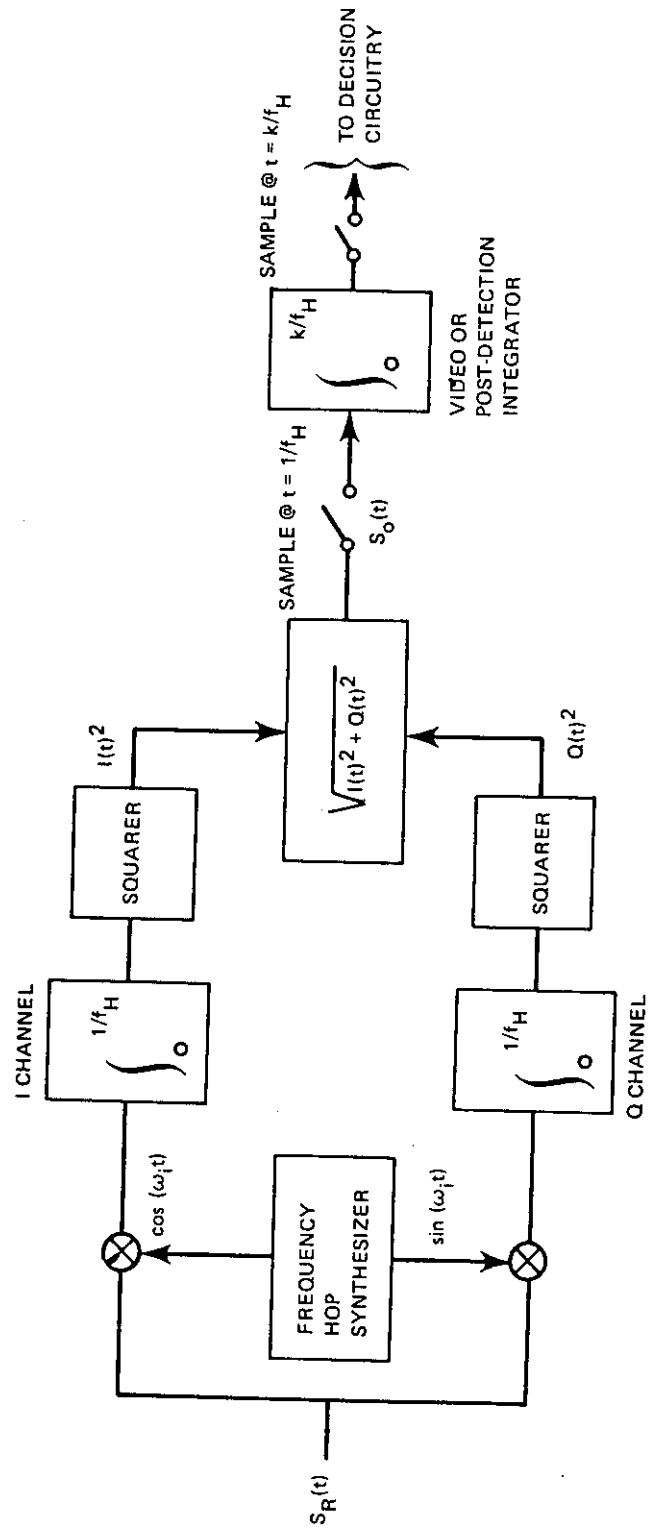


Fig. 7—Noncoherent frequency-hop detection

NRL REPORT 8025

The standard deviation of the noise samples is then inversely proportional to the integration time. Shorter integration times result in larger standard deviations and thus increase the probability that both noise samples will be large relative to carrier amplitude A . This provides intuitive insight into why the noncoherent processing of k hops is inferior to coherent processing, or equivalently inferior to the processing of one pulse of the same duration as all k pulses. In the last two cases matched filter integrator duration t is equal to k/f_H , and the corresponding noise bandwidth B is

$$B \approx 1/t = f_H/k,$$

whereas in the noncoherent combining case,

$$B \approx 1/t = f_H.$$

The standard deviation of the noise samples in the coherent combining case is approximately \sqrt{k} smaller than in the noncoherent case. It would therefore be expected that for the latter the likelihood of both noise samples being large simultaneously is much greater, and therefore the output per hop will be much less.

Another way of expressing NCL is to consider the decision output when the energy that would normally be transmitted in one noncoherently processed hop is divided into k shorter hops transmitted over the same time interval, each of which is noncoherently detected. These losses have been computed for a square-law envelope detector and are presented in Fig. 8. There are a number of curves showing various values of S/N , the post-detection signal-to-noise ratio, required for given probabilities of error and particular modulation schemes. (Bernstein [3] has shown the applicability of these noncoherent combining curves to M -ary modulation applications.) If one pulse were transmitted and noncoherently processed, it would yield a particular value of post-detection S/N at the receiver output. However, if this pulse is broken into k smaller pulses that are noncoherently detected and combined, then the video integrator output after k pulses will be less than the one-pulse S/N by the amount indicated on the vertical axis for k pulses. This is the noncoherent combining loss.

As would be expected from the previous discussion, the losses are larger for smaller values of single-pulse S/N (smaller carrier amplitude A). For large k , all curves have a slope approximately equal to \sqrt{k} .

The foregoing discussion of noncoherent combining losses is anything but rigorous. Its main purpose is to provide some intuitive feel for the source of these losses, not to present a formal derivation in which the physical rationale is obscured. For the sake of clarity the suppression effects that occur in the envelope detector (suppression of signal by noise for small signal-to-noise ratios) have not been discussed analytically; these effects degrade performance and actually result in a thresholding effect. It has been shown [4] that above threshold,

$$\frac{S_{out}}{N_{out}} \propto k_1 \frac{S_{in}}{N_{in}}; \quad \frac{S_{in}}{N_{in}} \gg 1,$$

and below threshold,

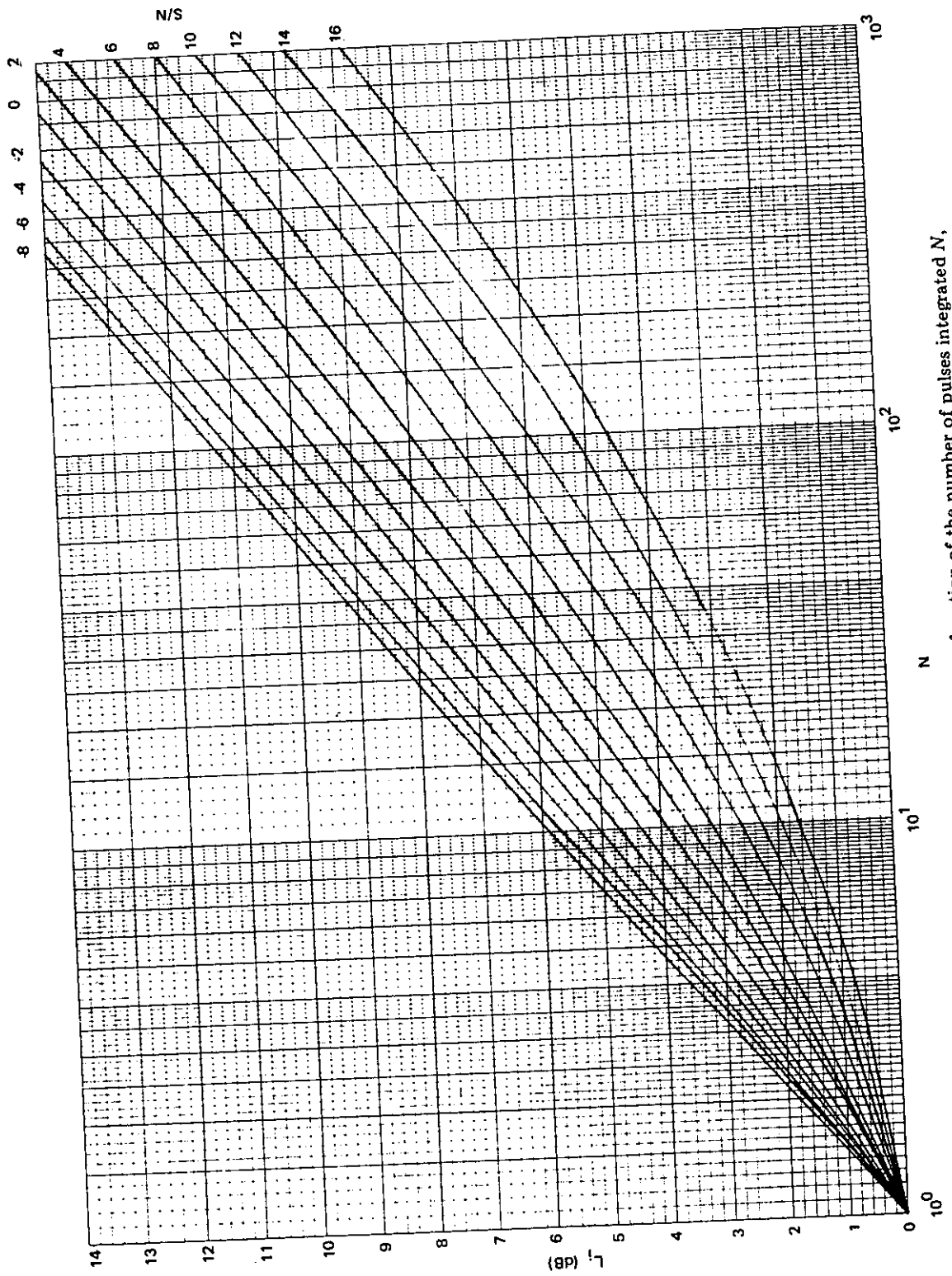


Fig. 8—Noncoherent combining loss L_i , as a function of the number of pulses integrated N , for various values of post-detection signal-to-noise ratio S/N

$$\frac{S_{\text{out}}}{N_{\text{out}}} \propto k_2 \left[\frac{S_{\text{in}}}{N_{\text{in}}} \right]^2 ; \quad \frac{S_{\text{in}}}{N_{\text{in}}} \ll 1 ,$$

where $S_{\text{out}}/N_{\text{out}}$ is the output signal-to-noise ratio, $S_{\text{in}}/N_{\text{in}}$ is the input signal-to-noise ratio, and k_1 and k_2 are constants of order unity.

Frequency Offset Losses

In the noncoherent detection techniques discussed so far, the frequency-hop synthesizer was assumed to be at exactly the same frequency as the received hop. Because of relative transmitter and receiver oscillator instabilities and doppler shifting of the received carrier, this is rarely true. A relative frequency offset between the received signal and the frequency-hop synthesizer will cause a loss L_D in the matched filter integrator output. This loss is given by

$$L_D = \left[\frac{\sin \pi \Delta f t}{\pi \Delta f t} \right]^2 ,$$

where t is integration time. A plot of L_D as a function of $\Delta f t$ is shown in Fig. 9.

This relative frequency offset causes a continuously varying phase difference between the received carrier frequency and the receiver-generated frequency. The resultant output is as though the two frequencies were identical but changed in relative phase throughout the multiplication and integration period. Relative phase change $\Delta\phi$ as a function of time is

$$\Delta\phi = \pi \Delta f t .$$

Consider two sinusoids with no initial phase offset. If $\Delta\phi$ is equal to 2π rad at the end of integration time t , the input to the integrator from 0 to $t/2$ will be the negative of the input from $t/2$ to t . The contributions to the integral from the first and second half of the integration time will cancel, and the resultant output will be zero. To prevent serious degradation, the total phase change during integration must be substantially less than π radians. This in turn requires $\Delta f t$ to be small. In the presence of large doppler offsets or long integration periods, some form of carrier tracking or doppler compensation must be used.

Doppler Compensation

A common technique for reducing frequency offset losses warrants discussion at this time. Consider the noncoherent receiver of Fig. 7. A frequency hop with a doppler offset Δf relative to the synthesizer hop frequency will incur a loss L_D at the integrator output. The loss is given by

$$L_D = \left[\frac{\sin \pi \Delta f (1/f_H)}{\pi \Delta f (1/f_H)} \right]^2 .$$

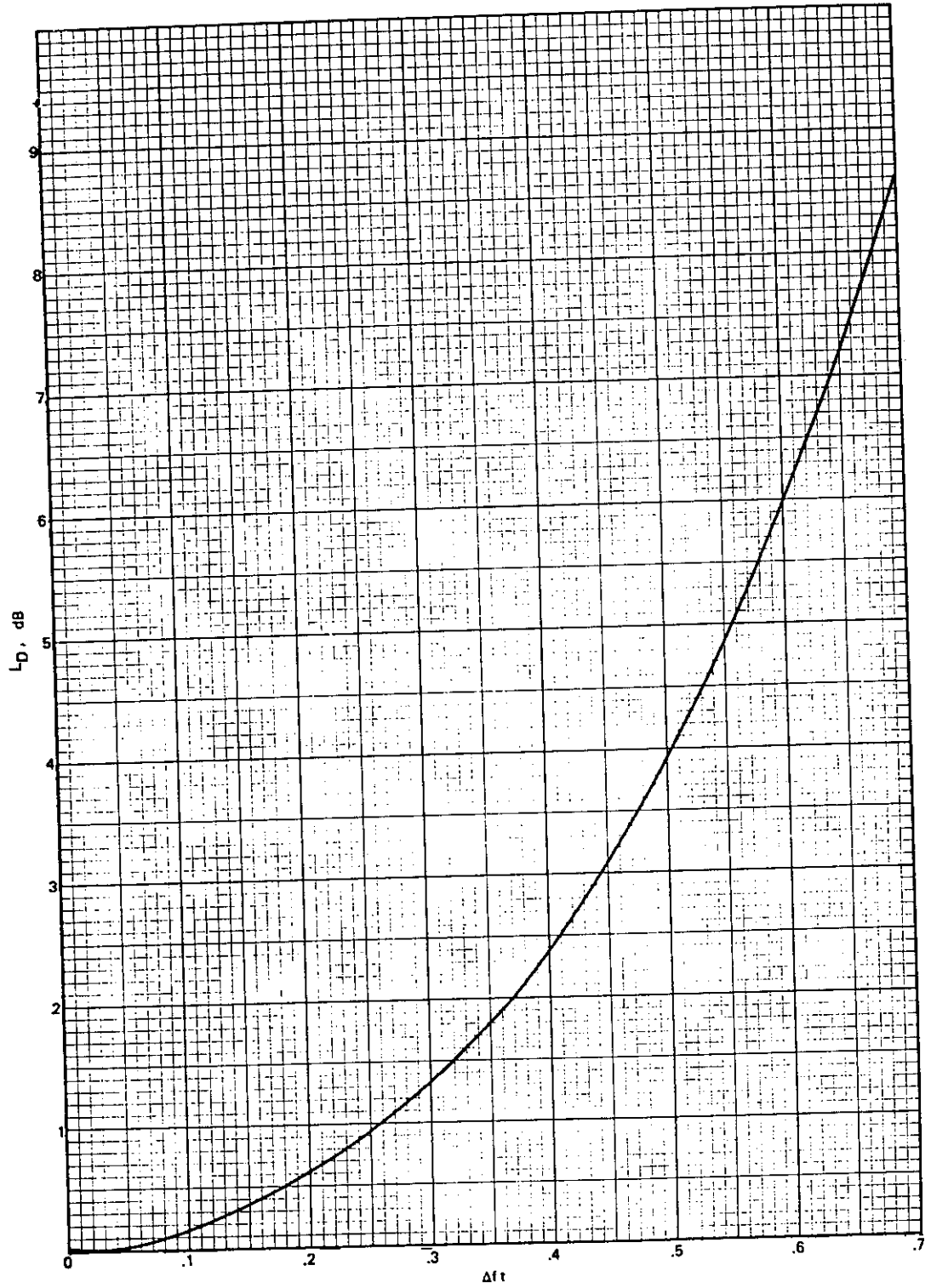


Fig. 9—Frequency offset loss L_D , as a function of frequency offset multiplied by integration time (Δft)

NRL REPORT 8025

Instead of being integrated over the entire hop dwell time $1/f_H$ and sampled at a rate equal to f_H , the individual hop could be divided into J subintervals by integrating over a period of $1/Jf_H$ and sampling at rate Jf_H . The doppler loss per subinterval is then

$$L_D = \left[\frac{\sin \pi \Delta f t (1/Jf_H)}{\pi \Delta f t (1/Jf_H)} \right]^2,$$

which can be substantially less than the previous loss, depending on the value of J . The video integrator must now integrate J pulses during interval $1/f_H$, instead of only one as before. This results in a noncoherent combining loss L_i , dependent on J and the post-detection signal-to-noise ratio required. In the limiting case,

$$L_i \sim \sqrt{\frac{1}{J}},$$

and if

$$\sqrt{\frac{1}{J}} \left[\frac{\sin \pi \Delta f (1/Jf_H)}{\pi \Delta f (1/Jf_H)} \right]^2 \geq \left[\frac{\sin \pi \Delta f (1/f_H)}{\pi \Delta f (1/f_H)} \right]^2,$$

then there will be a net reduction in the overall loss. A little thought (and an examination of Fig. 8) will show that this can easily result in a net reduction in doppler loss of several decibels.

This technique is analogous to widening the IF (matched filter) bandwidth (because the integrator bandwidth is inversely proportional to the integration time) to allow the frequency-shifted input signal energy to reach the detector circuitry (in this case an envelope detector). Even though all the signal energy reaches the detector, so does more noise. This results in degradation in S/N out of the envelope detector, reflected in the higher noncoherent combining losses during video integration. Noise bandwidth B of the video integrator is still

$$B \approx f_H,$$

which is the same as that of the original filter matched to hop interval $1/f_H$. However, due to the envelope detection process and the effectively widened IF bandwidth, the final S/N power ratio is degraded.

Frequency Hop/Pseudonoise Demodulation

The FH/PN waveform is generally implemented by biphase modulation of the hop carrier with a pseudonoise sequence. This is accomplished by pseudo-randomly multiplying the carrier by plus or minus one at a rapid rate. The PN can be removed at the receiver by multiplying the dehopped carrier by a replica of the transmitted PN sequence, assuming that the transmitter and receiver are synchronized in time. Once this is accomplished, the detection process is exactly as previously described. A circuit performing this function is illustrated in Fig. 10 for a noncoherent FH/PN waveform.

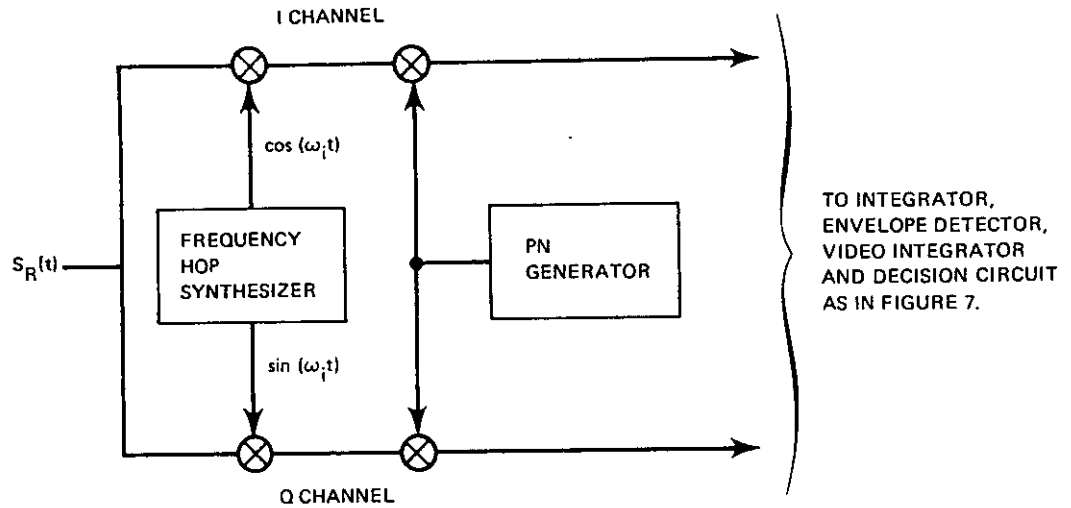


Fig. 10—Noncoherent frequency-hop/pseudonoise demodulation

Digital Correlator Matched Filters

The matched filter (multiplier and integrator) described in the discussion of detection techniques can be implemented with digital logic. A digital implementation of a non-coherent FH/PN receiver is shown in Fig. 11. Here the PN modulation on the carrier need not be removed before correlation and integration. The digital correlation actually multiplies the sampled PN on the carrier with the duplicate PN sequence generated in the receiver, while simultaneously performing the integration. It is interesting to note that the input to the A/D converter need not be at baseband; it could be an intermediate frequency, which would somewhat simplify the hardware.

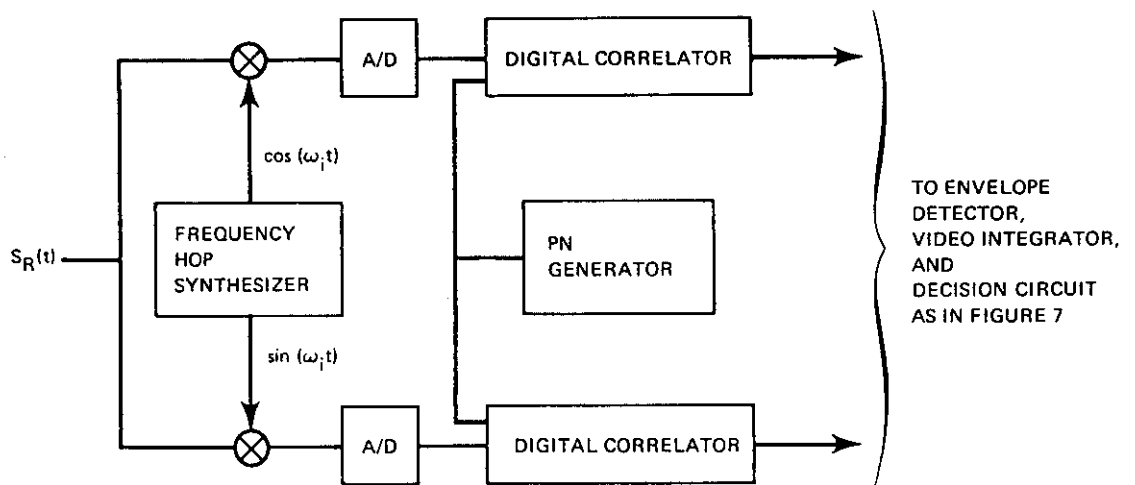


Fig. 11—Noncoherent frequency-hop/pseudonoise digital demodulation

The digital correlator circuitry is applicable to the demodulation of M -ary CSK, because with M correlator pairs (in-phase and quadrature) the received hop with the PN plus code can be correlated against all M possible PN plus code sequences and detected in parallel. The demodulator can then choose the largest of the M outputs to determine the actual transmitted code. A block diagram of such a receiver is in Fig. 12, where $S_I(t)$ and $S_R(t)$ represent the dehopped in-phase and quadrature carrier components and PN represents the output of the PN generator in the receiver.

III. FREQUENCY-HOPPED AND HYBRID WAVEFORM QUALITY FACTORS

Optimum Intercept Detectors for Spread-Spectrum Signals

Energy Detector

The likelihood ratio [5] derivation of an optimum detector for a spread-spectrum signal, when this signal is represented as samples of Gaussian noise, has been performed by Peterson et al. [6]. A block diagram of this detector, often referred to as a wideband radiometer or energy detector, is shown in Fig. 13. The receiver consists of a filter of bandwidth W , a square law (sometimes linear law) detector, and a postdetection integrator.

When there is a signal plus noise at the input to the receiver, the output Y has a non-central chi-square density function with $2tW$ degrees of freedom and a noncentrality

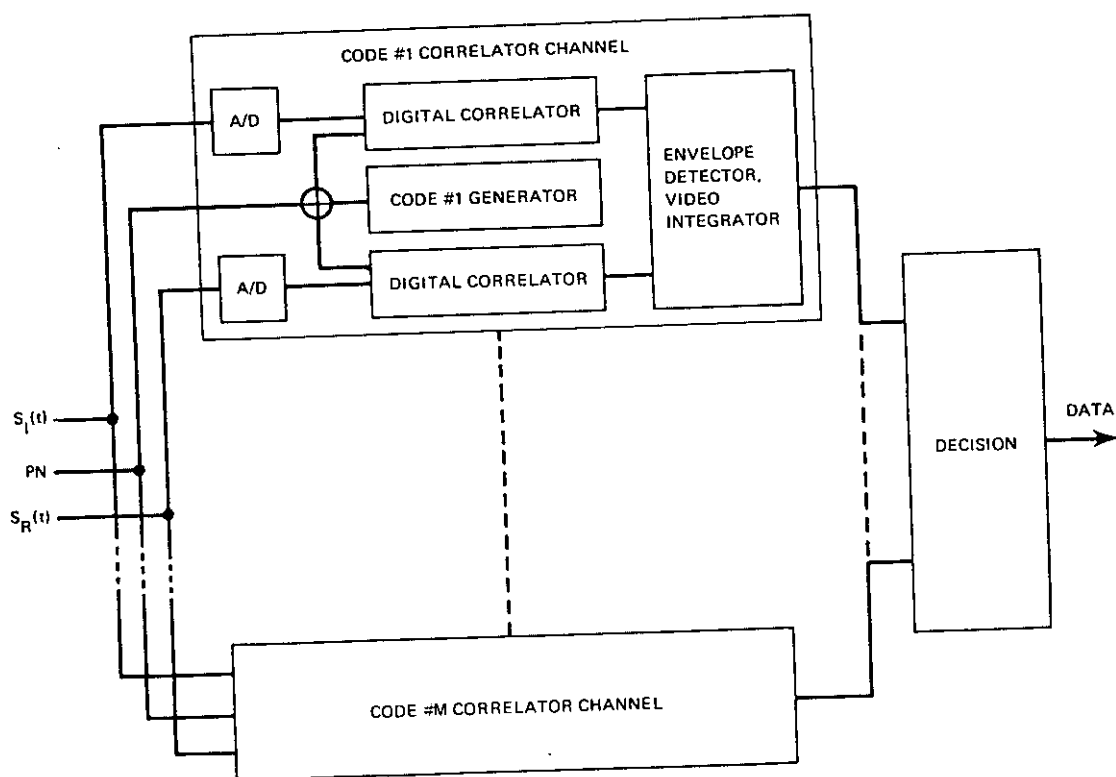


Fig. 12—Noncoherent frequency-hop M -ary code shift key demodulation

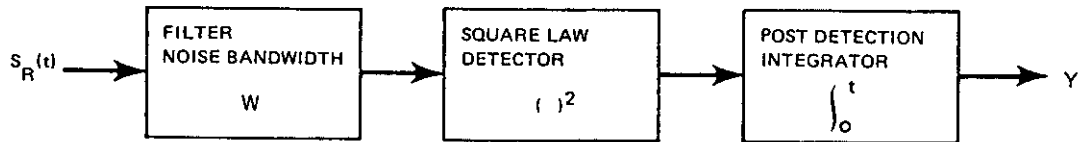


Fig. 13—Simple energy detector

parameter of $2E/N_0$ (twice the ratio of integrated signal energy to input noise power spectral density). With noise only present at the input, the output Y has a chi-square density function with $2tW$ degrees of freedom. When the output Y is compared to a fixed threshold ℓ , the exact probabilities of detection P_D ,* and false alarm P_{FA} † can be calculated from these density functions. The general approach is to determine the allowable false alarm probability and then find the inverse chi-square distribution function. This becomes the threshold. For this threshold value, P_D can be determined as a function of the post-detection signal-to-noise ratio. Another way of looking at the receiver performance is to determine the P_D and P_{FA} for a given post-detection signal-to-noise ratio. This is perhaps a more interesting approach, because reducing the listener's post-detection signal-to-noise ratio forces him to accept a less favorable P_D and P_{FA} . It should be pointed out that the chi-square density functions that describe the behavior of the statistic Y also describe the output of the hop detector of Fig. 7 if the square root of the sum of the squares of the I and Q channels is not taken. (That these statistics are chi-square can be verified in Refs. 2 and 7.) These density functions are quite complicated, and their integrals do not exist in closed form. They must be numerically evaluated. For large time-bandwidth products ($tW \gtrsim 100$), the density functions can be approximated by Gaussian statistics. In this case, assume that the output statistics are Gaussian density functions with mean and variance equal to the mean and variance of the chi-square density functions. Then

$$P_{FA} = \int_{\ell}^{\infty} \frac{1}{\sqrt{2\pi} \sigma_N} e^{-(x-\mu_N)^2/2\sigma_N^2} dx$$

where

$$\mu_N = 2tW$$

$$\sigma_N^2 = 4tW \text{ and}$$

ℓ = the threshold.

$$P_D = \int_{\ell}^{\infty} \frac{1}{\sqrt{2\pi} \sigma_{S+N}} e^{-(x-\mu_{S+N})^2/2\sigma_{S+N}^2} dx$$

where

*The probability that Y will exceed the threshold when the signal is present.

†The probability that Y will exceed the threshold when noise only is present at the input.

NRL REPORT 8025

$$\mu_{S+N} = 2tW + 2E/N_0$$

$$\sigma_{S+N}^2 = 4tW + 8E/N_0.$$

After a change of variables the equations can be written as

$$P_{FA} = \frac{1}{\sqrt{2\pi}} \int_{\frac{(\ell - \mu_N)}{\sigma_N}}^{\infty} e^{-z^2/2} dz$$

and

$$P_D = \frac{1}{\sqrt{2\pi}} \int_{\frac{(\ell - \mu_{S+N})}{\sigma_{S+N}}}^{\infty} e^{-z^2/2} dz.$$

If

$$Q(z) = \frac{1}{\sqrt{2\pi}} \int_z^{\infty} e^{-t^2/2} dt,$$

we have

$$P_{FA} = Q[(\ell - \mu_N)/\sigma_N]$$

$$P_D = Q[(\ell - \mu_{S+N})/\sigma_{S+N}].$$

Solving the P_{FA} equation for ℓ and substituting this into the P_D equation yields

$$P_D = Q \left[\frac{\sigma_N Q^{-1}(P_{FA}) + \mu_N - \mu_{S+N}}{\sigma_{S+N}} \right]$$

or

$$\sigma_{S+N} Q^{-1}(P_D) = \sigma_N Q^{-1}(P_{FA}) + \mu_N - \mu_{S+N}.$$

Therefore,

$$Q^{-1}(P_{FA}) - \frac{\sigma_{S+N}}{\sigma_N} Q^{-1}(P_D) = d$$

where

$$d = \frac{\mu_{S+N} - \mu_N}{\sigma_N}.$$

Now if it is assumed that the variances of the output density functions with signal plus noise and noise only are approximately equal [8] then

$$d = [Q^{-1}(P_{FA}) - Q^{-1}(P_D)] ; \quad \sigma_{S+N} \approx \sigma_N .$$

In view of low-level or threshold signals this assumption is certainly not unreasonable.

Substituting the values for the means and variances in the expression for d yields

$$d = [Q^{-1}(P_{FA}) - Q^{-1}(P_D)] = \frac{2tW + 2E/N_0 - 2tW}{\sqrt{4tW}} = \frac{E}{N_0 \sqrt{tW}} .$$

This expression can be rewritten in terms of a number of related parameters:

$$d = [Q^{-1}(P_{FA}) - Q^{-1}(P_D)] = \frac{E}{N_0 \sqrt{tW}} = \frac{C}{N_0} \sqrt{\frac{t}{W}} = \frac{S}{N} \sqrt{tW}$$

where

$$\frac{C}{N_0} = \text{ratio of input carrier power to noise power}$$

$$\frac{S}{N} = \text{ratio of predetection signal power to noise power.}$$

In the equal-variance Gaussian approximation, the radiometer probability of detection and probability of false alarm are uniquely related by the post-detection signal-to-noise ratio $S/N \sqrt{tW}$ or, equivalently, the ratio C/N_0 of input carrier power to noise density, once the radiometer integration time t and bandwidth W are specified.

Solving for C/N_0 in the above expression results in

$$\frac{C}{N_0} = d \sqrt{\frac{W}{t}} = [Q^{-1}(P_{FA}) - Q^{-1}(P_D)] \sqrt{\frac{W}{t}} .$$

The equal-variance Gaussian assumption, therefore, provides a simple technique for determining the input C/N_0 required for a specified listener P_D and P_{FA} . Values of d have been calculated for a wide range of P_D and P_{FA} and are given in Fig. 14.

Unfortunately, whenever the time-bandwidth product of the radiometer is near unity there is a significant difference between C/N_0 as determined under the Gaussian assumption and the actual C/N_0 , as predicted by the accurate chi-square statistics. A correction factor η may be defined as follows:

$$\eta \equiv \frac{F(\chi^2, P_D, P_{FA}, t, W)}{G(\text{Gaussian}, P_D, P_{FA}, t, W)} = \frac{F(\chi^2, P_D, P_{FA}, t, W)}{d \sqrt{\frac{W}{t}}}$$

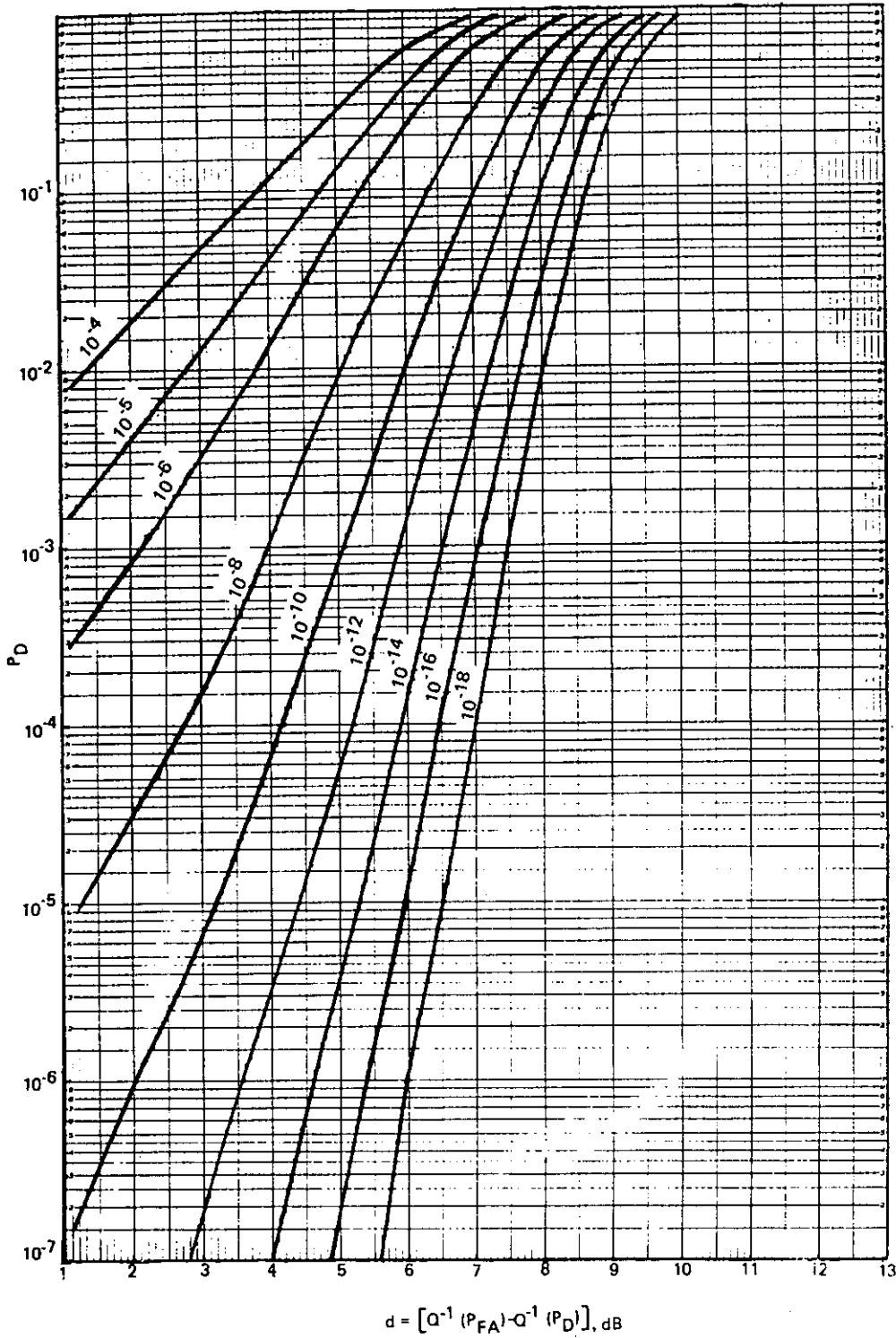


Fig. 14—Radiometer probability of detection P_D and probability of false alarm P_{FA} vs parameter $d = [Q^{-1}(P_{FA}) - Q^{-1}(P_D)]$

where $F(\chi^2, P_D, P_{FA}, t, W)$ is the C/N_0 predicted by the accurate chi-square statistics for the specified P_D, P_{FA}, t , and W , and G (Gaussian, P_D, P_{FA}, t, W) is the value predicted by the equal-variance Gaussian approximation. Values of η have been plotted in Figs. 15a through 15j for a wide range of P_D, P_{FA} , and tW . The figures indicate that the error in the Gaussian assumption (a) increases with decreasing P_{FA} , (b) decreases with decreasing P_D , and (c) decreases rather quickly with increasing tW . For values of tW in excess of about 100, the Gaussian approximation is quite accurate.

The required input C/N_0 can now be written accurately, in terms of the Gaussian approximation and η , as

$$\frac{C}{N_0} = \eta d \sqrt{\frac{W}{t}} = \eta [Q^{-1}(P_{FA}) - Q^{-1}(P_D)] \sqrt{\frac{W}{t}}.$$

Optimum Hop Detector

The likelihood ratio derivation of the optimum detector for a frequency-hopped waveform is shown as a block diagram in Fig. 16. This receiver was derived for a continuous waveform consisting of hops with no pseudonoise spreading. In other words, the tW product of the individual hops is equal to one. The optimum detector consists of a bank of energy detectors, one for each of the N possible hop channels, matched in time and frequency to the individual hops. The receiver takes the square root of each radiometer output*, forms the modified Bessel function, sums the outputs of the N channels, and finally forms the product over M hops. This product is then compared to the threshold ℓ . Unfortunately, the output statistics of the optimum hop detector have not been determined analytically. Peterson has shown that the performance of the receiver in terms of the previously defined parameter d can be obtained as follows:

$$d^2 = M \ln \left[1 - \frac{1}{N} + \frac{1}{N} I_0 \left(\frac{2E_H}{N_0} \right) \right]$$

or

$$I_0 \left(\frac{2E_H}{N_0} \right) = 1 + N [e^{(d^2/M)} - 1],$$

where E_H is the integrated signal energy per hop. It must be remembered that d is useful only when the output statistics are equal-variance Gaussian density functions. Although this does not appear to be true with the receiver configuration of Fig. 16, the detector output can be reconfigured so that this assumption is very well satisfied as the number of channels N becomes large.

The receiver in Fig. 16 is very complex, and its performance is based on a Gaussian assumption valid only as N becomes large. Therefore, the Filter Bank Combiner, a

*Remember that this yields the same statistics as the optimum hop detector of Fig. 6, and the radiometer and square-root function could be replaced by the Fig. 6 receiver.

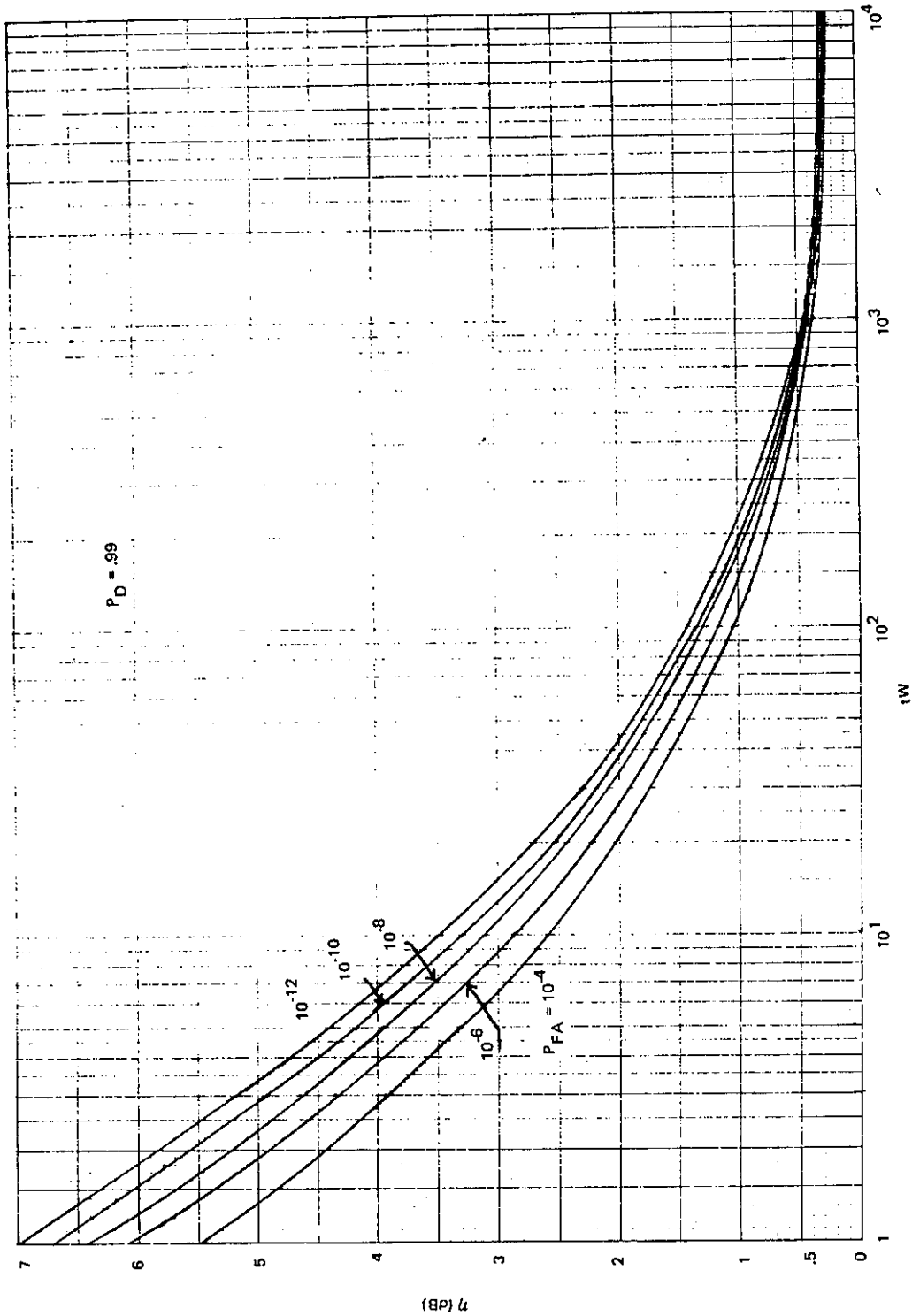


Fig. 1.5a — Correction factor η for Gaussian approximation as a function of time-bandwidth product tW ($P_D = 0$)

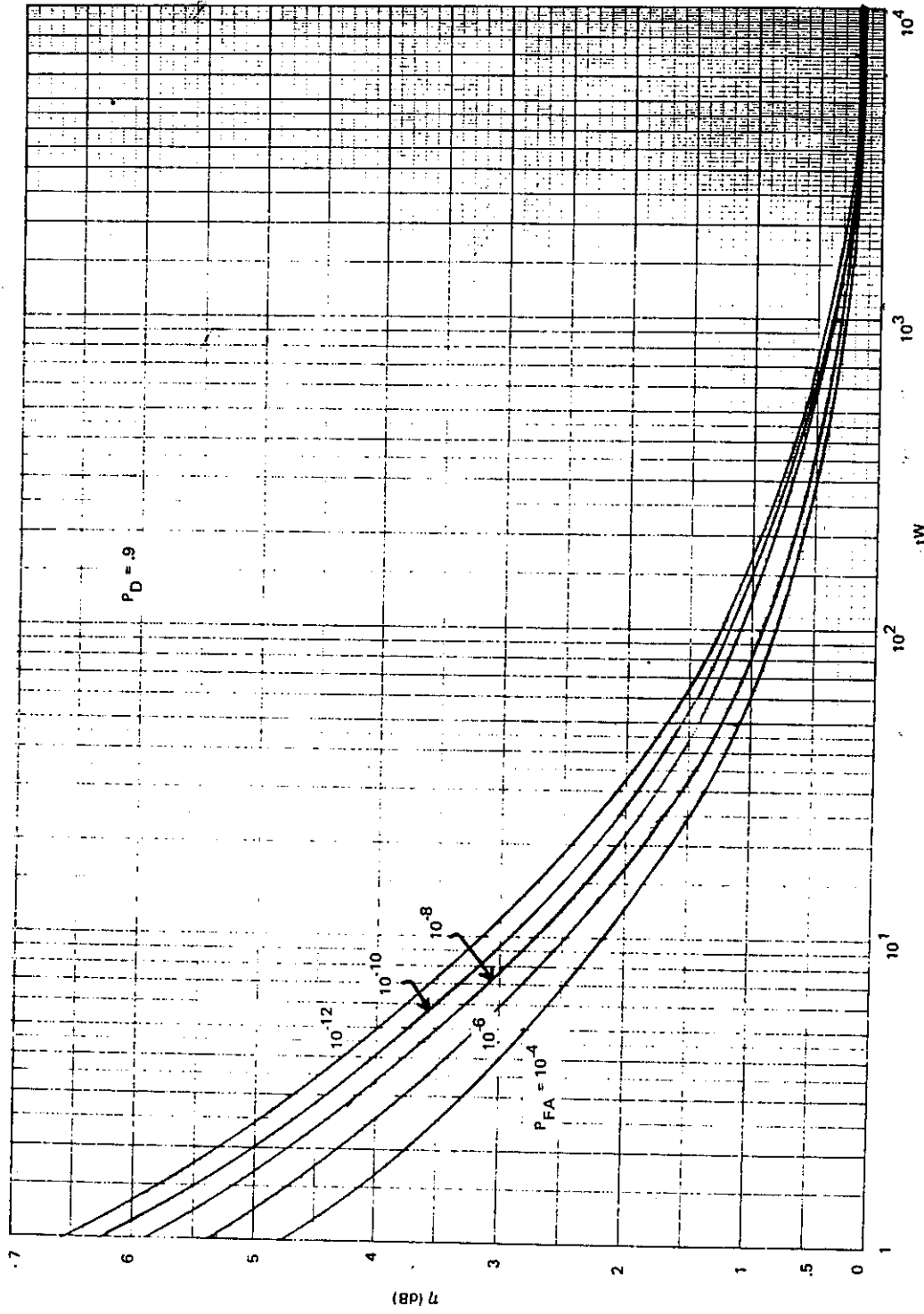


Fig. 15b—Correction factor η for Gaussian approximation as a function of time-bandwidth product tW ($P_D = 0.9$)

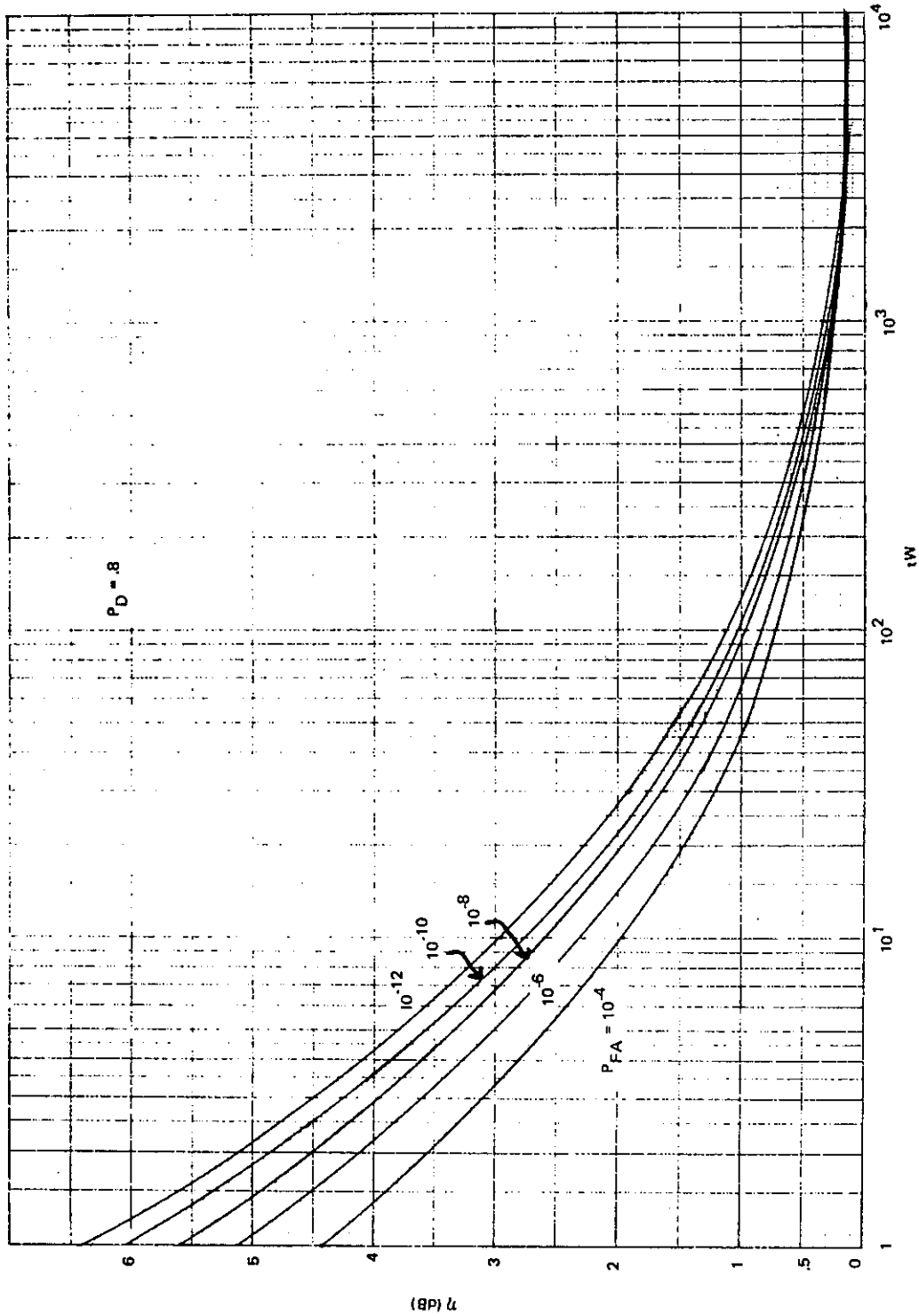


Fig. 15c—Correction factor η for Gaussian approximation as a function of time-bandwidth product tW ($P_D = 0.8$)

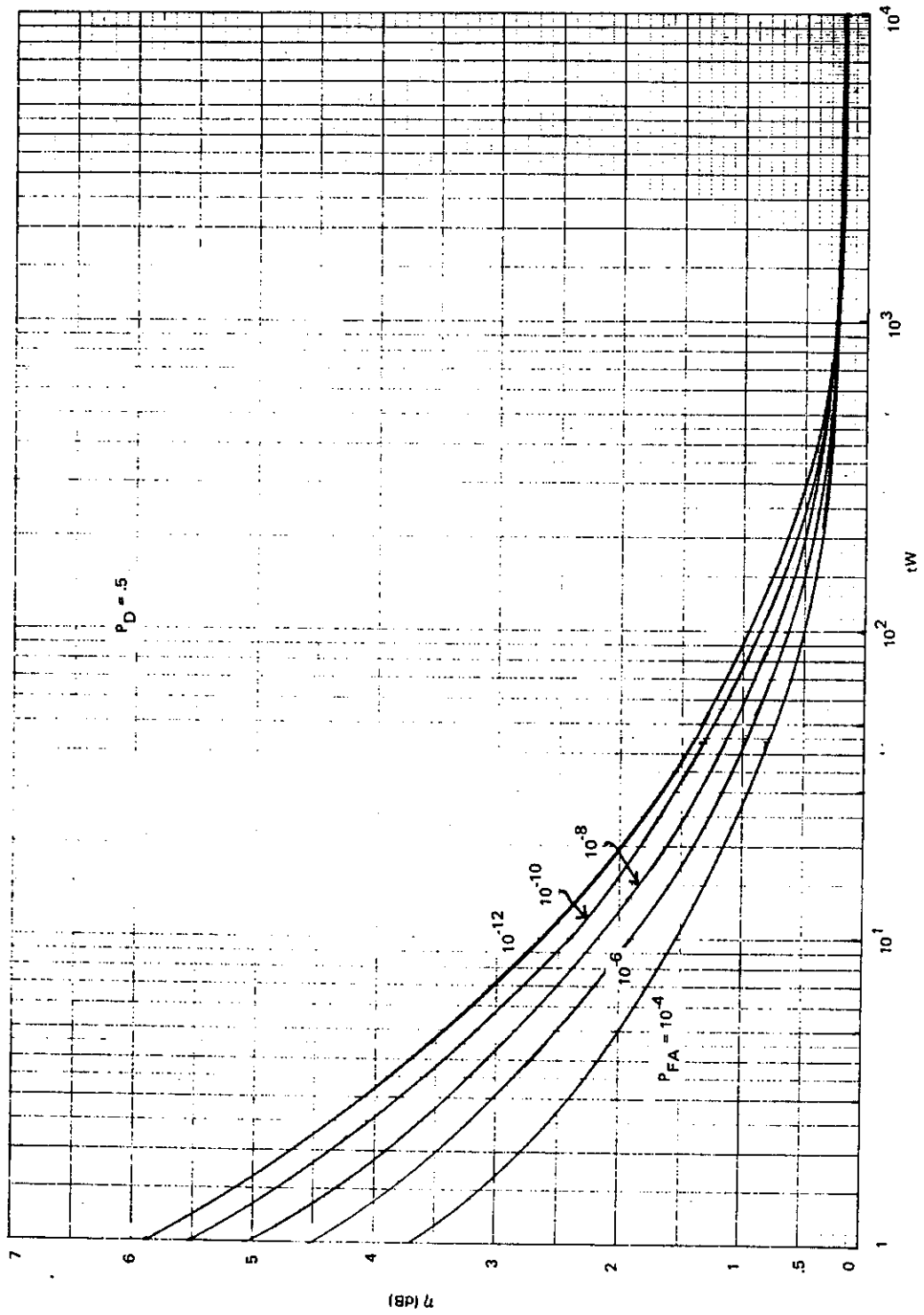


Fig. 15d—Correction factor η for Gaussian approximation as a function of time-bandwidth product tW ($P_D = 0.5$)

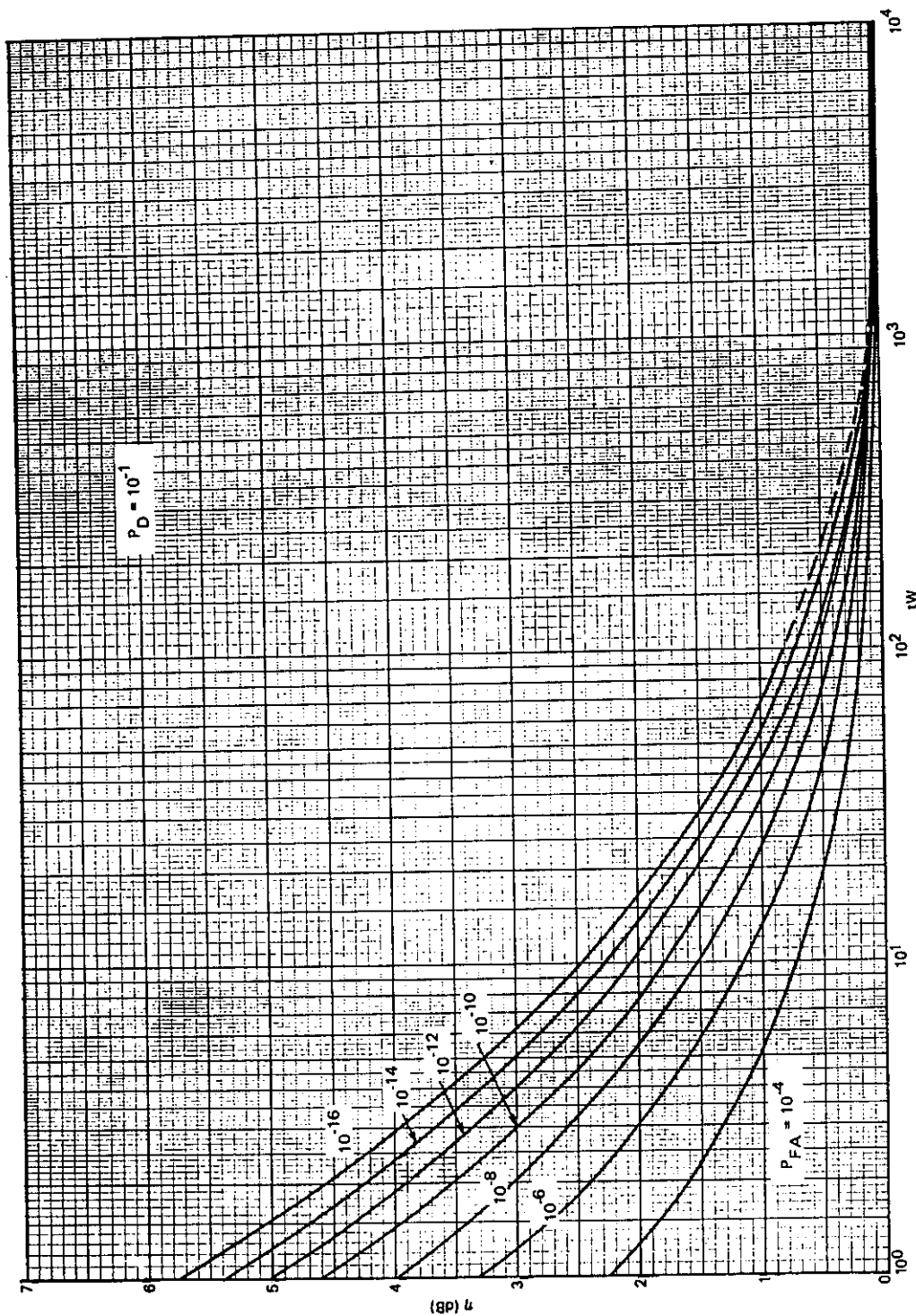


Fig. 15e—Correction factor η for Gaussian approximation as a function of time-bandwidth product tW ($P_D = 10^{-1}$)

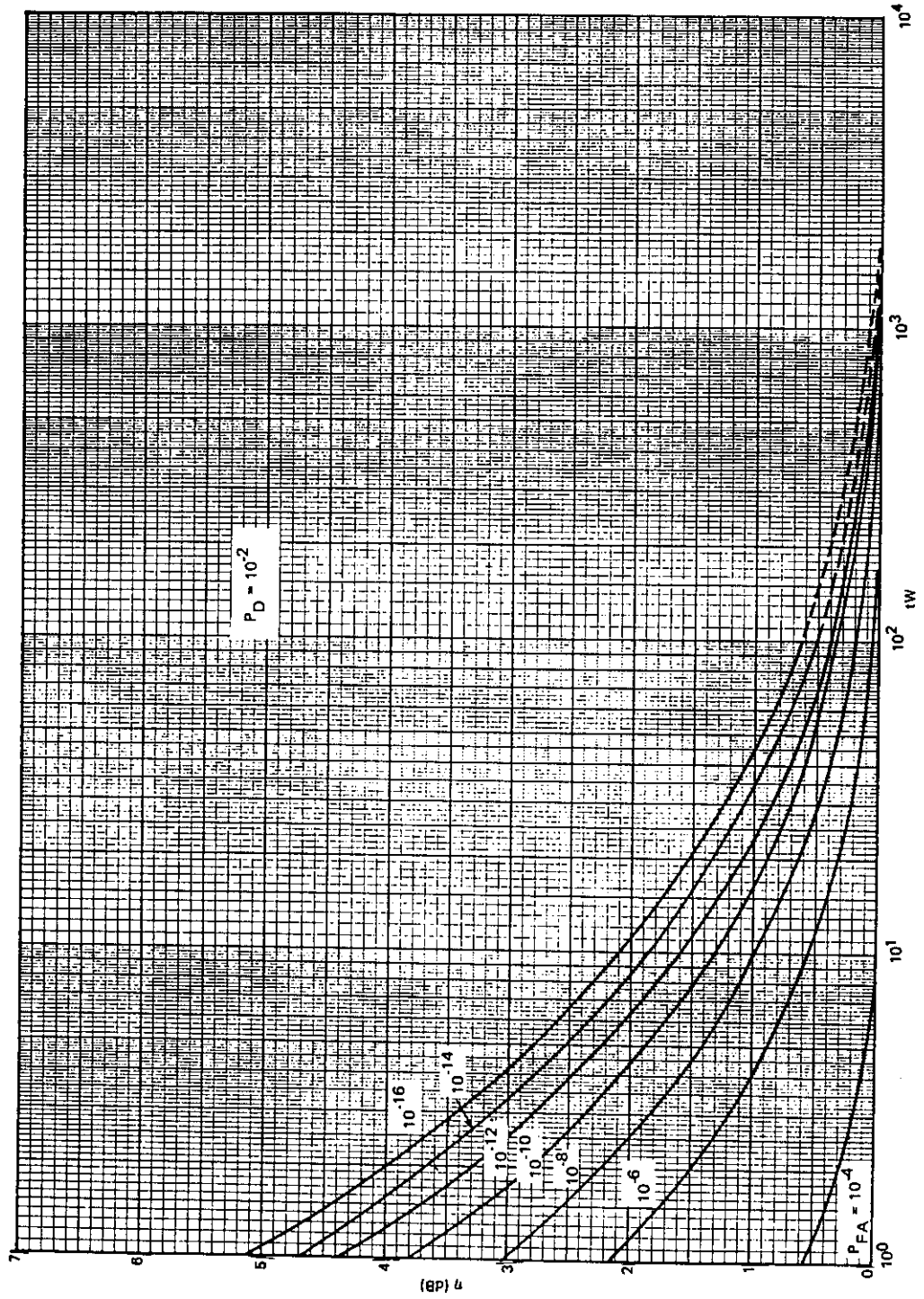


Fig. 15f—Correction factor η for Gaussian approximation as a function of time-bandwidth product tW ($P_D = 10^{-2}$)

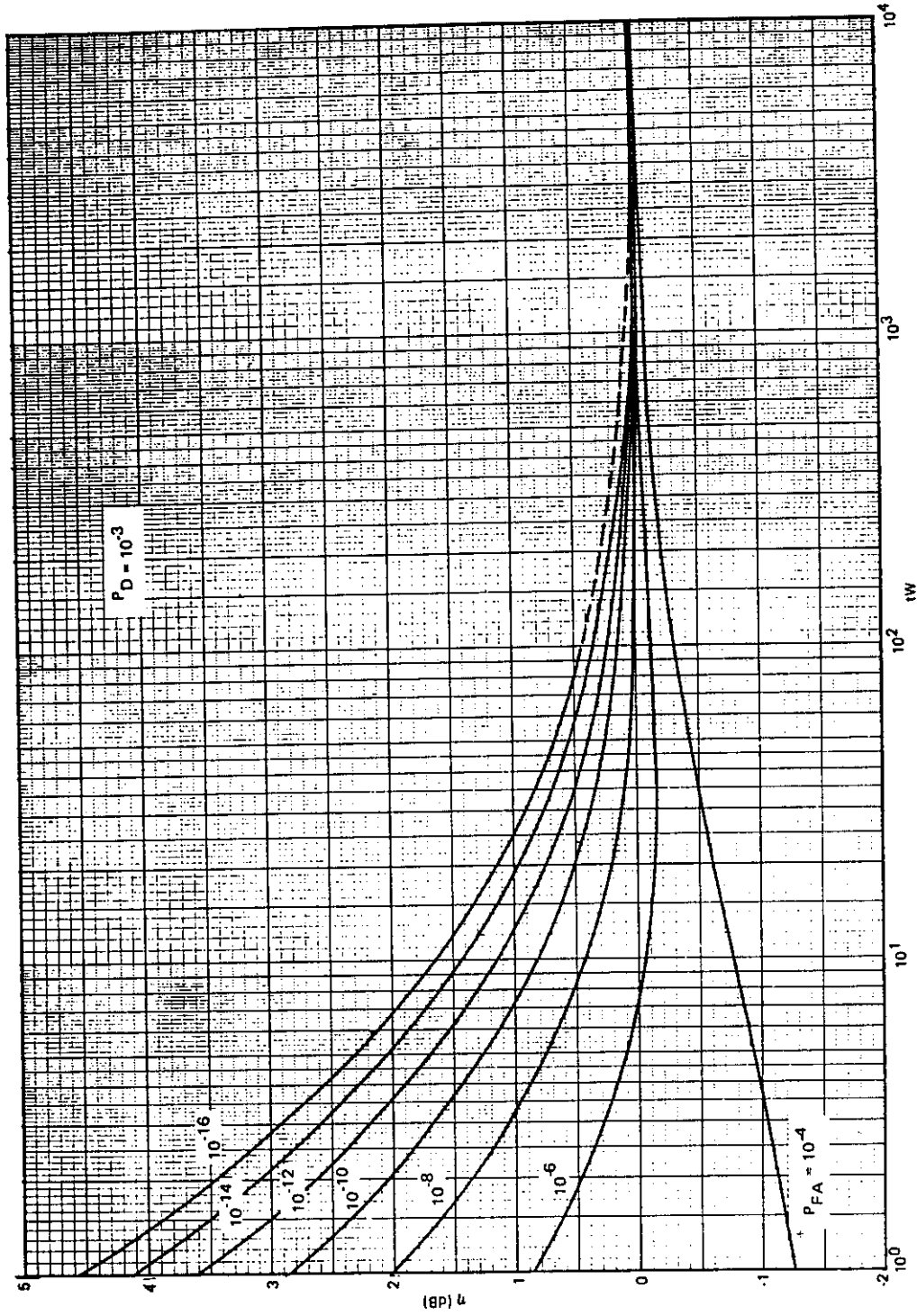


Fig. 15g—Correction factor η for Gaussian approximation as a function of time-bandwidth product tW ($P_D = 10^{-3}$)

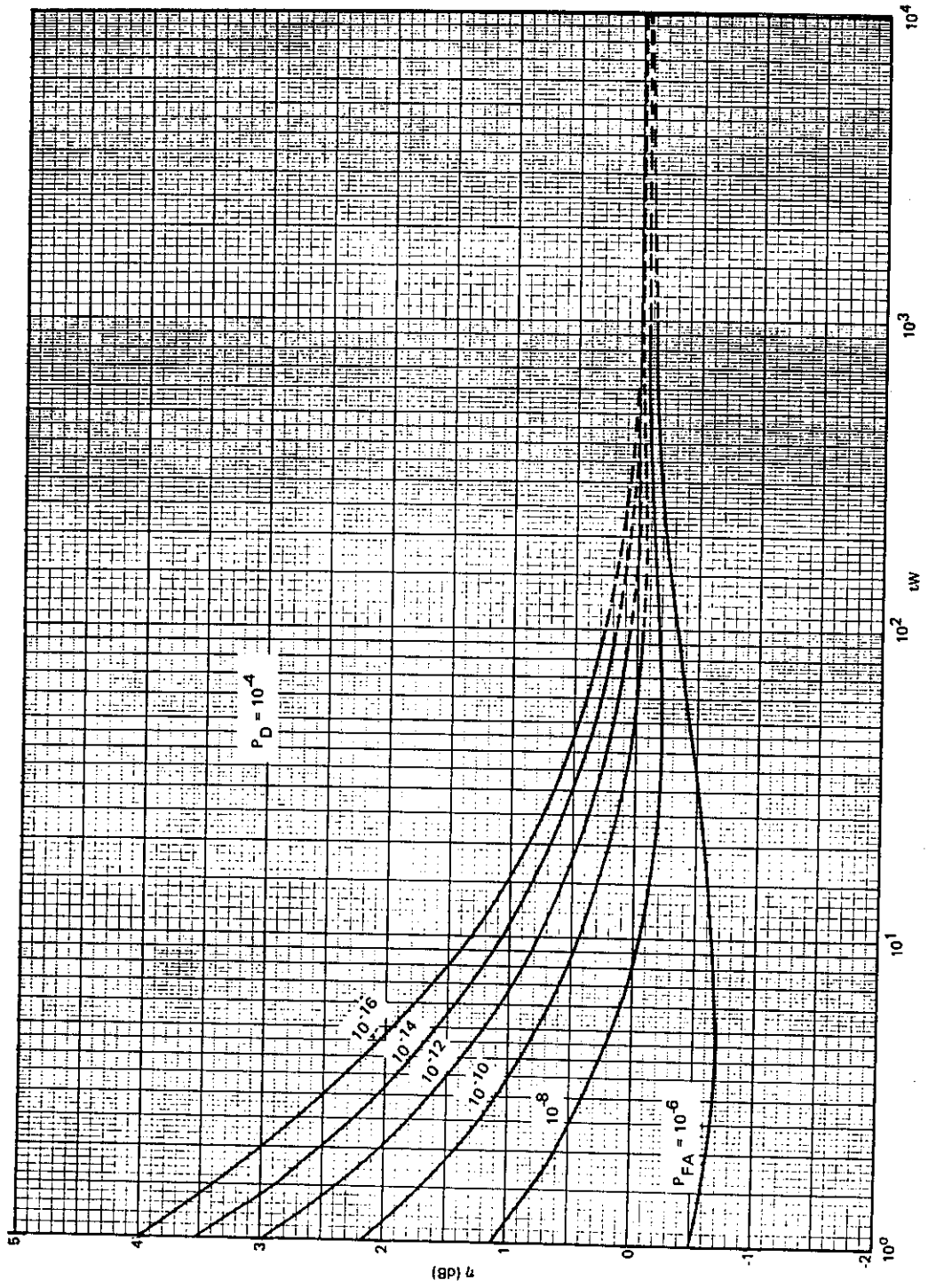


Fig. 15h—Correction factor η for Gaussian approximation as a function of time-bandwidth product τW ($P_D = 10^{-4}$)

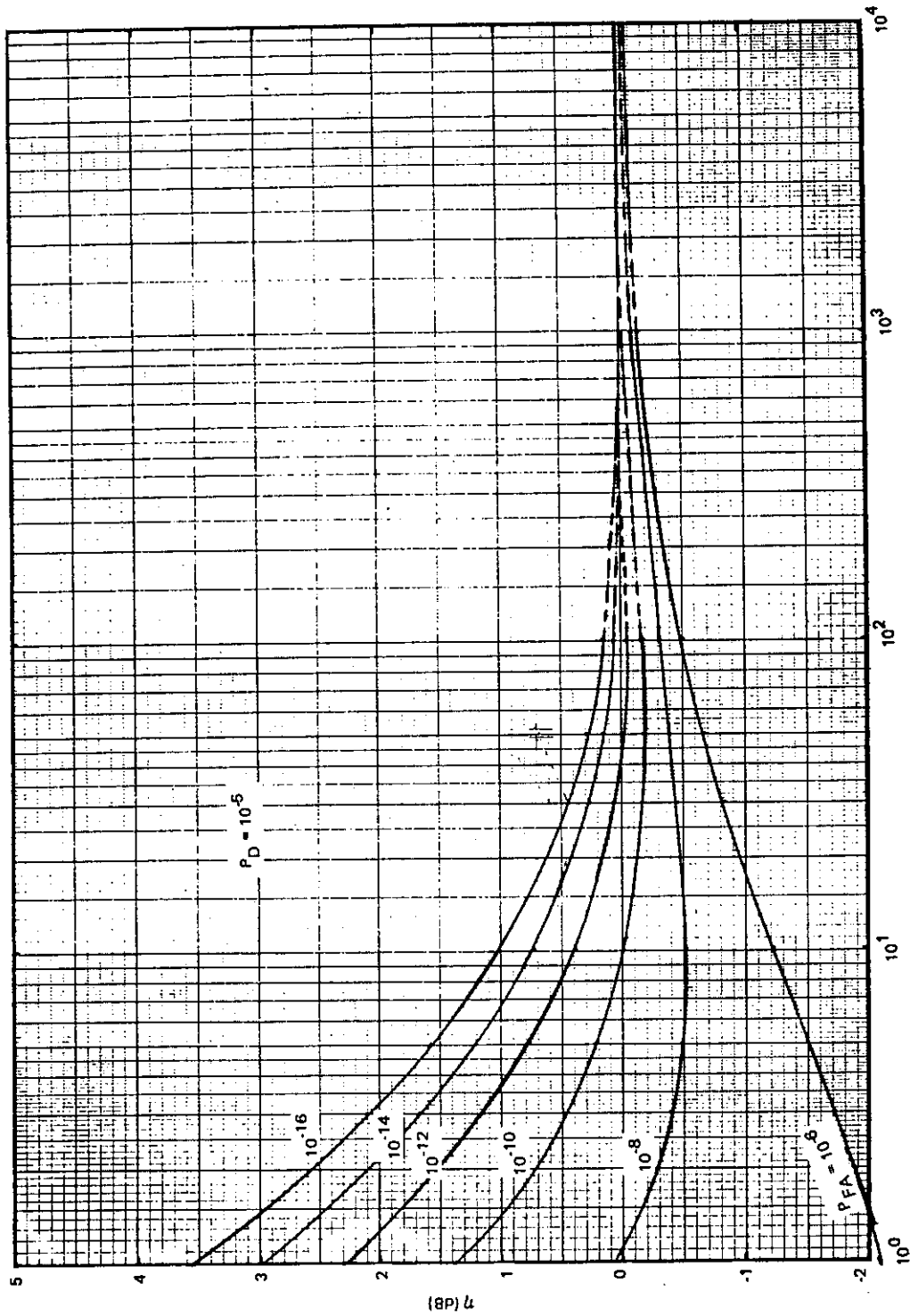


Fig. 16j—Correction factor η for Gaussian approximation as a function of time-bandwidth product tW ($P_D = 10^{-5}$)

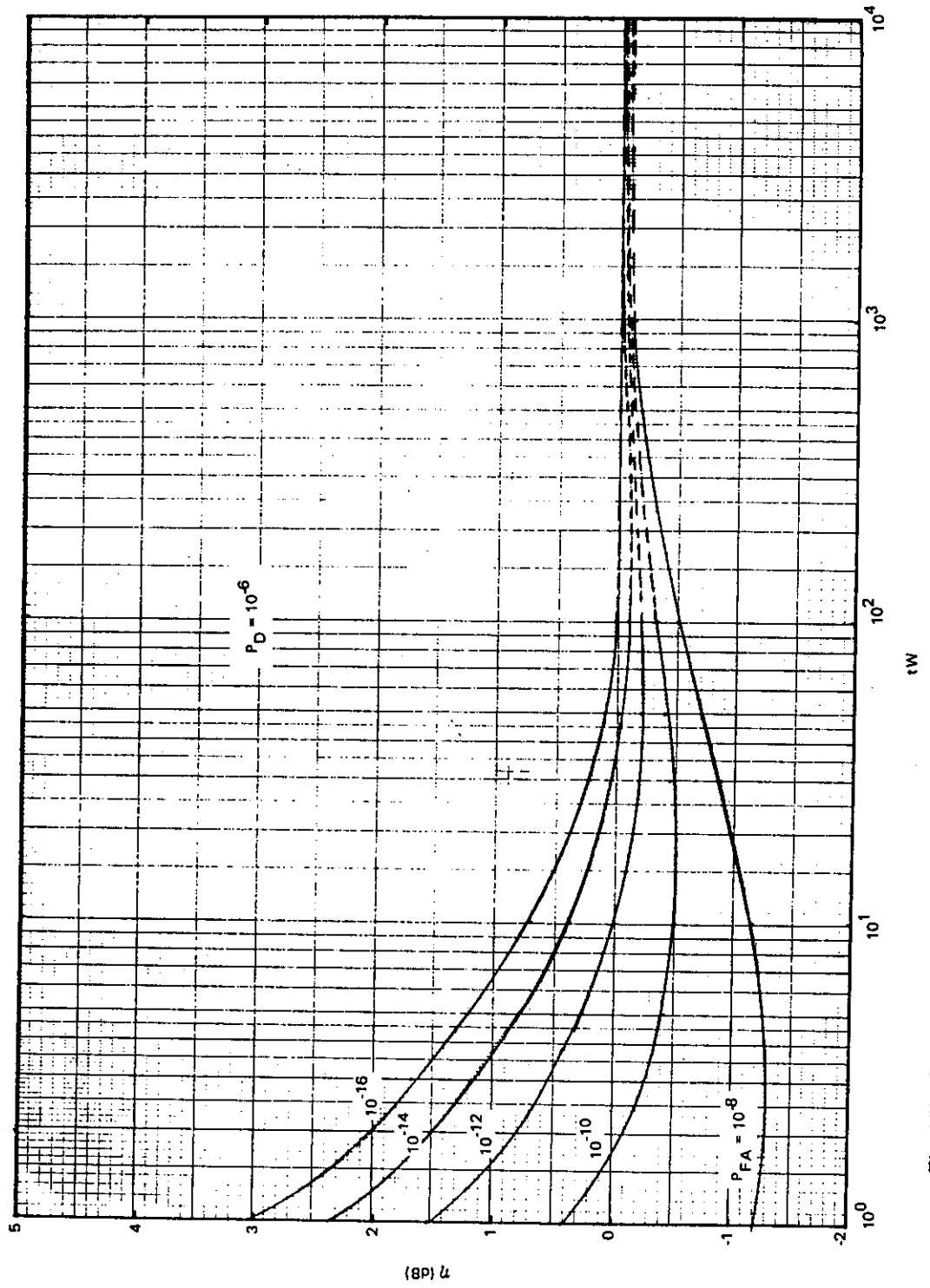


Fig. 15j—Correction factor η for Gaussian approximation as a function of time-bandwidth product tW ($P_D = 10^{-6}$)

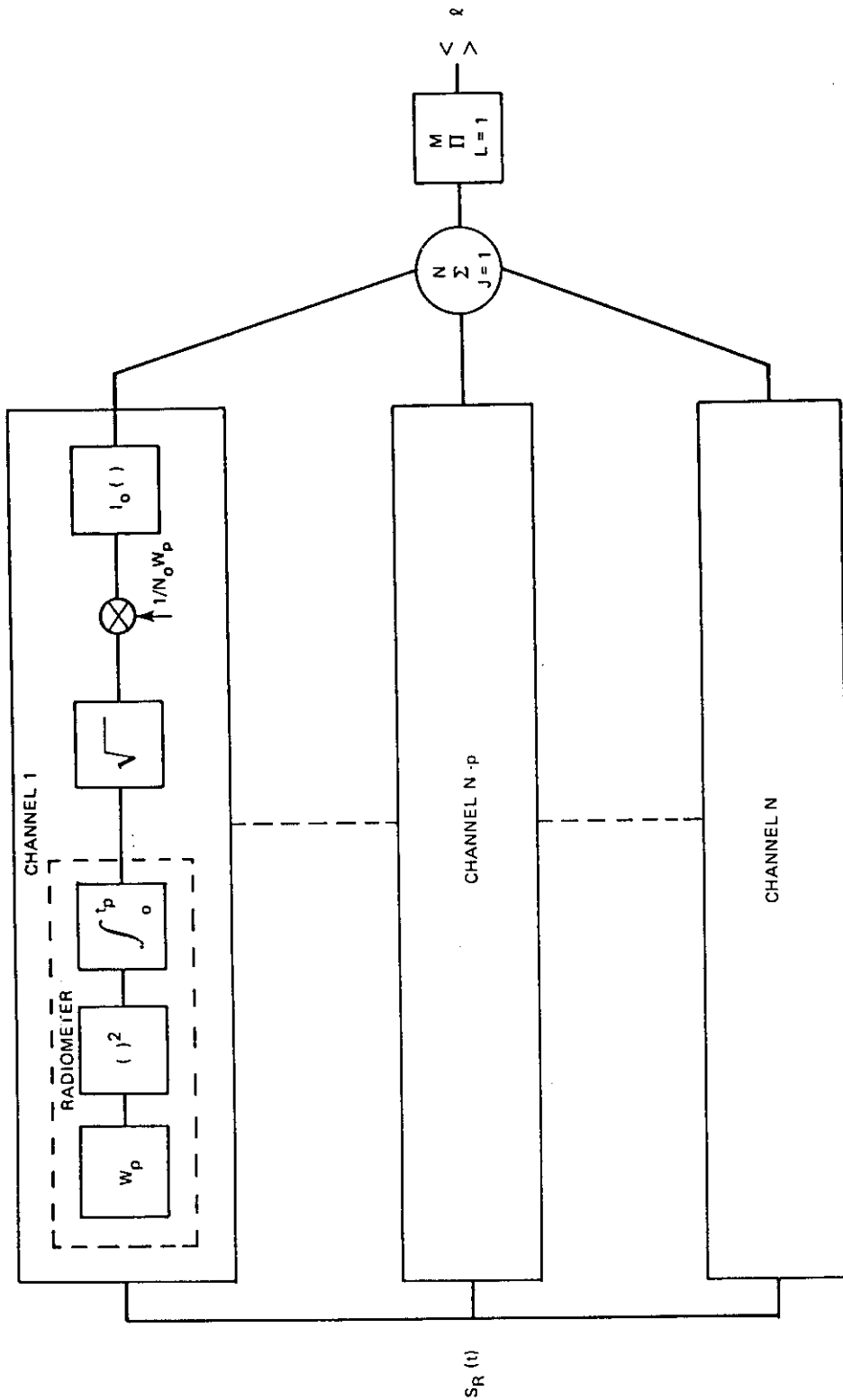


Fig. 16—Optimum detector for a frequency-hopped waveform

suboptimum version for which output statistics can be accurately calculated, will be considered throughout the remainder of the discussion.

Filter Bank Combiner

This technique is described in Ref. 9. A block diagram of the filter bank combiner is shown in Fig. 17. Like the optimum detector, this receiver consists of a bank of energy detectors, one centered at each of the N possible hop frequencies, with integration times matched to pulse duration t_p and bandwidths to pulse bandwidth W_p . Now, however, after each integration interval, a decision is made in each channel as to whether a pulse was detected. These decisions are then logically OR'd, summed over the number of hop intervals M , and finally compared to a threshold λ . If the sum exceeds this final threshold, a detection is announced.

Assuming that the receiver is alined in time with the hops and observes for a duration t , the average carrier power-to-noise density ratio required at the input to the filter bank combiner is

$$\begin{aligned} \left. \frac{\bar{C}}{N_0} \right|_{\text{required}} \Big|_{\text{Hop Detector}} &= \eta_H \alpha \left[\left\{ Q^{-1}(P_{FAI}) - Q^{-1}(P_{DI}) \right\} \sqrt{\frac{W_p}{t_p}} \right] \\ &= \eta_H d_H \alpha \sqrt{\frac{W_p}{t_p}} \end{aligned}$$

where

α = duty cycle

P_{FAI} = probability of false alarm for an individual channel

P_{DI} = probability of detection for an individual channel

$d_H = Q^{-1}(P_{FAI}) - Q^{-1}(P_{DI})$. The subscript H denotes d relative to the individual channel probabilities

η_H = correction factor for Gaussian statistics. The subscript H denotes the correction for the hop detector.

This equation is merely the corrected Gaussian approximation for the energy detector model previously discussed. To compare the performance of the filter bank combiner with that of the wideband radiometer, observing the same total spread bandwidth W , for the same time duration t , both detectors must have the same overall probabilities of detection and false alarm. For the filter bank combiner the following relationships between P_D , P_{DI} , P_{FA} , and P_{FAI} hold:

$$P_D = \sum_{J=0}^{D_1} \binom{D_1}{J} (P_{DI})^J (1 - P_{DI})^{D_1 - J}$$

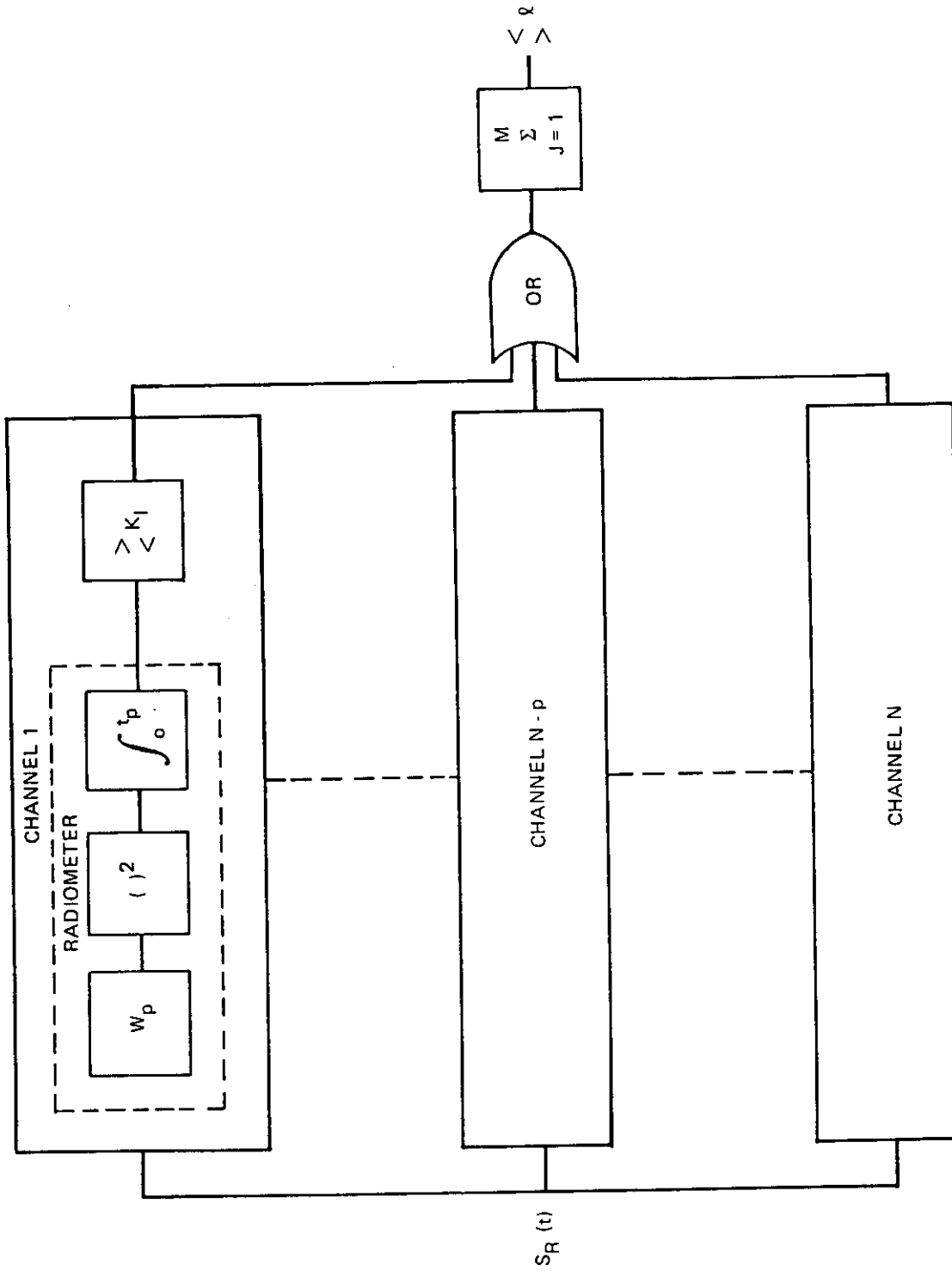


Fig. 17—Filter bank combiner

$$P_{FA} = \sum_{J=\ell}^{D_2} \binom{D_2}{J} \left[1 - (1 - P_{FAI})^N \right]^J \left[(1 - P_{FAI})^N \right]^{D_2 - J}$$

where

D_1 = number of opportunities to detect an individual pulse per message
 = number of pulses per message actually transmitted
 = at/t_p

D_2 = total number of parallel decisions per message
 = total number of opportunities for a false alarm per message interval
 = t/t_p

W = total observed spread bandwidth

W_p = bandwidth of a transmitted pulse

N = number of possible channels to which the carrier may be hopped
 = W/W_p

P_D = probability of detecting the message with a wideband radiometer

P_{FA} = probability of false alarm for a wideband radiometer

ℓ = hop detector decision threshold

$$\binom{D}{J} = D! / J!(D - J)!$$

This expression for P_D ignores the unlikely event of a false alarm occurring during the observation interval, thereby aiding detection. For a given P_D and P_{FA} , three variables, P_{DI} , P_{FAI} , and ℓ , must be determined under the constraint that the ratio of carrier power to noise density required at the input to the hop detector be minimum. This is not simple, because all the system parameters are variables (t , t_p , W , W_H). This optimization must be performed by computer, has been calculated for a large category of system parameters (see Appendix A). It is interesting to note that optimum threshold ℓ is generally between 5 and 25, and is not 1, as might be expected.

Detectability Scenario and Quality Factors

Detectability Scenario

The preceding sections have described the interceptor detector models to be used in the ensuing discussion—the wideband radiometer (energy detector) and the filter bank combiner. Techniques were developed for determining the receiver operating characteristic (relationship of P_D and P_{FA}) as a function of the receiver post-detection signal-to-noise ratio $(S/N)\sqrt{tW}$. This in turn was defined in terms of input C/N_0 , as $(C/N_0)\sqrt{t/W}$. The complete detection scenario can now be treated by determining the uplink C/N_0 present

NRL REPORT 8025

at the input to the listener's receiver as a function of the C/N_0 required for reliable communication between the transmitter and the intended receiver.

For a processing repeater or simple line-of-sight link, with no interference, the required C/N_0 is determined by the modulation alone:

$$\Gamma_U = M_C r_D \frac{E_b}{N_0}$$

where Γ_U is the required communicator's C/N_0 , M_C is the margin communication required to assure reliable communications in the face of uncertainties such as equipment performance and propagation conditions, r_D is the information data rate, and E_b/N_0 is the ratio of bit energy to noise density required by the particular modulation scheme.

The power radiated by the transmitter terminal is

$$P_T = \frac{\Gamma_U k T_R}{G_T L_U G_R},$$

and the C/N_0 at the interceptor is

$$\Gamma_L = \frac{P_T G_T(L) L_U(L) G_{LR}}{k T_L}$$

where

- $\Gamma_L = C/N_0$ at the input to the listener's receiver
- $P_T =$ transmitted power of terminal
- $G_T =$ transmitting antenna gain of terminal
- $L_U =$ uplink path loss
- $G_R =$ gain of receive antenna
- $k =$ Boltzmann's constant
- $T_R =$ receiving system noise temperature
- $G_T(L) =$ gain of the transmitting antenna in the direction of the listener
- $L_U(L) =$ path loss to the listener
- $G_{LR} =$ gain of listener's antenna
- $T_L =$ listener's receiving system temperature.

If P_T and Γ_U are eliminated from the expression for Γ_L , the C/N_0 available to the listener is

$$\Gamma_L = \frac{G_T(L)}{G_T} \frac{L_U(L)}{L_U} \frac{G_{LR}}{G_R} \frac{T_R}{T_L} M_C r_D \frac{E_b}{N_0}.$$

Synoptic Detectability Criteria and Message Quality Factor

A message quality factor (Q_M), based on the performance of the energy detector, is now defined. In terms of input C/N_0 the listener's post-detection signal-to-noise ratio is given as

$$\frac{S}{N} \sqrt{tW} = \frac{\Gamma_L}{\eta} \sqrt{\frac{t}{W}}$$

Suppose the communications system designer assumes an allowable listener post-detection signal-to-noise ratio (receiver operating curve) d_T , defined by the Gaussian approximation to the energy detector's performance. The system then will be detectable if the listener's post-detection signal-to-noise ratio (corrected for accurate chi-square statistics) exceeds d_T . The synoptic detectability criteria will then become

$$\left[\frac{G_T(L)}{G_T} \frac{L_U(L)}{L_U} \frac{G_{LR}}{G_R} \frac{T_R}{T_L} M_C \right] \left[\frac{1}{\eta} r_D \frac{E_b}{N_0} \sqrt{\frac{t}{W}} \right] \geq d_T$$

The first set of brackets contains terms whose values vary widely with geometry and equipment, while the terms in the second set depend only on the modulation scheme and the information data rate.

Rearranging the synoptic detectability equation yields the following criteria: the signal is detectable if

$$\underbrace{\left[\frac{G_T(L)}{G_T} \frac{L_U(L)}{L_U} \frac{G_{LR}}{G_R} \frac{T_R}{T_L} M_C \right]}_{\text{Scenario-dependent factor}} \geq d_T \underbrace{\left[\frac{\eta}{r_D \frac{E_b}{N_0} \sqrt{\frac{t}{W}}} \right]}_{\text{Detectability threshold}}$$

The reciprocal of the modulation-dependent group is now a multiplier on the original detectability threshold and therefore is a convenient measure of the modulation technique's contribution to covertness. The larger this number, the greater the threshold that the listener must exceed to detect the signal. The quantity is defined as modulation quality factor Q_M , such that

$$Q_M = \eta_M \left[r_D \frac{E_b}{N_0} \sqrt{\frac{t_m}{W_M}} \right]^{-1}$$

This quantity permits comparison of modulation schemes without considering scenario factors. Subscript M denotes that the interceptor model is an energy detector observing the entire modulation spread-spectrum bandwidth W_M and integrating over message duration t_m . The subscript will distinguish message quality factor Q_M from hop quality factor Q_H , based on a filter bank combiner threat. It is reasonable to assume that the product

of message time and bandwidth ($t_m W_M$) will be large enough that η_M will be unity. The message quality factor definition now becomes

$$Q_M = \frac{1}{r_D \frac{E_b}{N_0} \sqrt{\frac{t_m}{W_M}}}$$

Hop Quality Factor

The quality factor defined in the previous section is a measure of the covertness of a modulation scheme against interception by an energy detector. To ensure that an interceptor does not gain an advantage by using the more sophisticated filter bank combiner, it is necessary to develop a hop quality factor Q_H that will provide a measure of the modulation vulnerability to such a threat. A waveform designer need only ensure that the message quality factor Q_M (against an energy detector) equals the hop quality factor Q_H (against a filter bank combiner) to have balanced detectability.

To develop Q_H it is convenient to compare the ratio of average carrier power to noise density, \bar{C}/N_0 , required by the filter bank combiner to that required by the energy detector for equal probabilities of detection and false alarm. Then Q_H is defined so that

$$\frac{Q_M}{Q_H} = \frac{\frac{\bar{C}}{N_0} \Big|_{\text{required for energy detector}}}{\frac{\bar{C}}{N_0} \Big|_{\text{required for filter bank combiner}}} = \frac{\eta_M d_M \sqrt{\frac{W_M}{t_m}}}{\alpha \eta_H d_H \sqrt{\frac{W_p}{t_p}}}$$

or

$$Q_H = \frac{\alpha}{r_D \frac{E_b}{N_0} \sqrt{\frac{t_p}{W_p}}} \left(\frac{\eta_H d_H}{d_M} \right)$$

In summary, two quality factors, Q_M and Q_H , have been defined. The first is a measure of the covertness of a modulation technique based on observing the message as a whole. The second is based on observing the message with a near optimum receiver that exploits the hop characteristics of the waveform. In both cases it is assumed that the interceptor is aligned in time and bandwidth with the transmitted message. Again,

$$Q_M = \frac{1}{r_D \frac{E_b}{N_0} \sqrt{\frac{t_m}{W_M}}}$$

and

$$Q_H = \frac{\alpha}{r_D \frac{E_b}{N_0} \sqrt{\frac{t_p}{W_p}}} \left(\frac{\eta_H d_H}{d_M} \right).$$

IV. COVERTNESS: A PARAMETRIC ANALYSIS

It is now possible to discuss the effects on covertness of waveform design parameters. This will be accomplished by first discussing the effects of the waveform parameters on quality factors Q_M and Q_H regardless of signal processing losses. Once this is done, the combined effects of modulation parameters and implementation losses encountered in the actual demodulation process can be addressed.

Quality Factors and Waveform Parameters

To facilitate discussion of the effects of waveform parameters on quality factors, regardless of processing losses, it is convenient to normalize Q_M and Q_H with respect to $r_D E_b/N_0$. Processing losses affect the required transmitted carrier power and are reflected in the value of E_b/N_0 actually required. If quality factors are normalized, covertness trends can be discussed independently of required transmitted power. The normalized quality factors are defined as follows:

$$Q'_M = Q_M r_D \frac{E_b}{N_0} = \frac{1}{\sqrt{\frac{t_m}{W_M}}}$$

$$Q'_H = Q_H r_D \frac{E_b}{N_0} = \frac{\alpha}{\sqrt{\frac{t_p}{W_p}}} \left[\frac{\eta_H d_H}{d_M} \right].$$

Clearly, Q'_M increases as the square root of the spread bandwidth and decreases as the square root of the message duration. Unfortunately, Q'_H is not so easily analyzed. Multiplying factor $\eta_H d_H/d_M$ is a complicated function of all the system parameters, including the interceptor's probability of detection and probability of false alarm. It is necessary, therefore, to determine the effects of these parameters on Q'_H . For a wide range of parameters, plots of the normalized quality factor, based on the optimum-threshold filter bank combiner are shown in Figs. 18a through 18h. In each figure, a family of curves is plotted, one for each value of pulse duration t_p , as a function of pulse bandwidth W_p . The beginning point for each curve is the point at which no hop spreading exists. This corresponds to an intrinsic pulse bandwidth approximately equal to the reciprocal of pulse duration t_p .

It is interesting to note that for fixed values of α , t_p , and W_p there is no significant change in Q'_H over an appreciable variation in the other parameters. In other words, the total spread bandwidth, message duration, probability of detection, and probability of

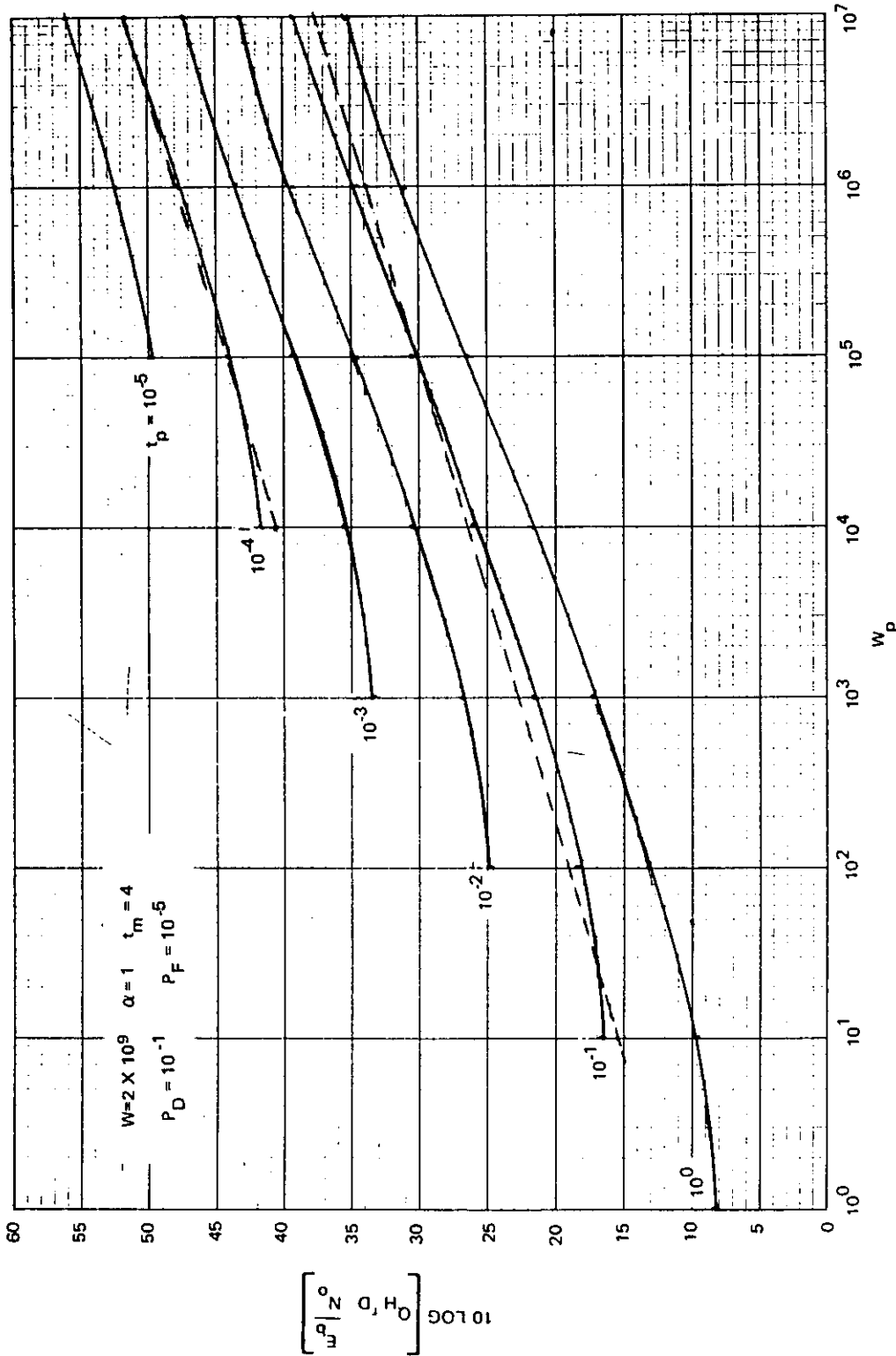


Fig. 18a—Normalized hop quality factor Q'_H vs hop bandwidth; $W = 2 \times 10^9$, $\alpha = 1$, $t_m = 4$, $P_D = 10^{-1}$, $P_{FA} = 10^{-5}$

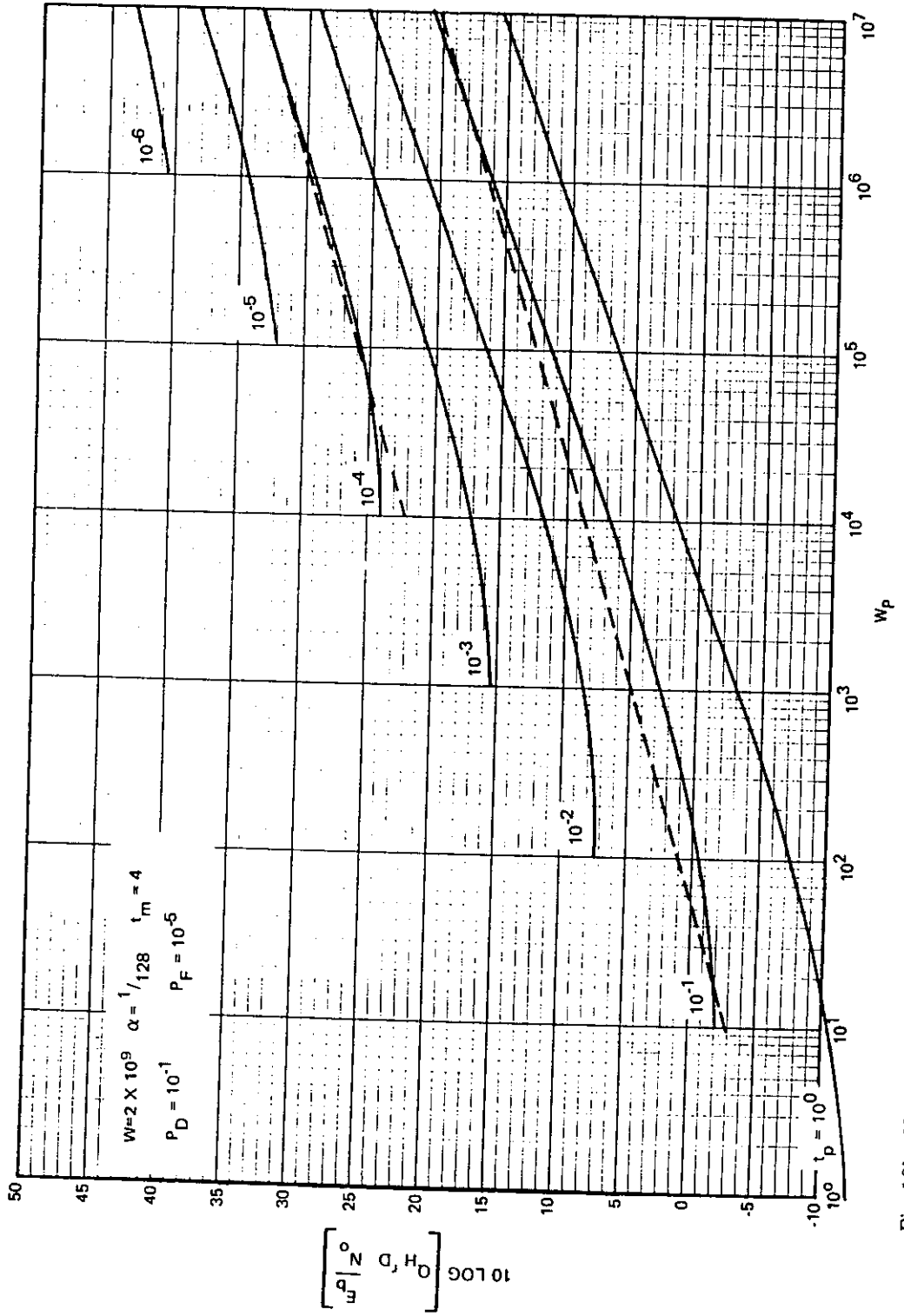


Fig. 18b—Normalized hop quality factor Q'_H vs hop bandwidth; $W = 2 \times 10^9$, $\alpha = 1/128$, $t_m = 4$, $P_D = 10^{-1}$, $P_{FA} = 10^{-6}$

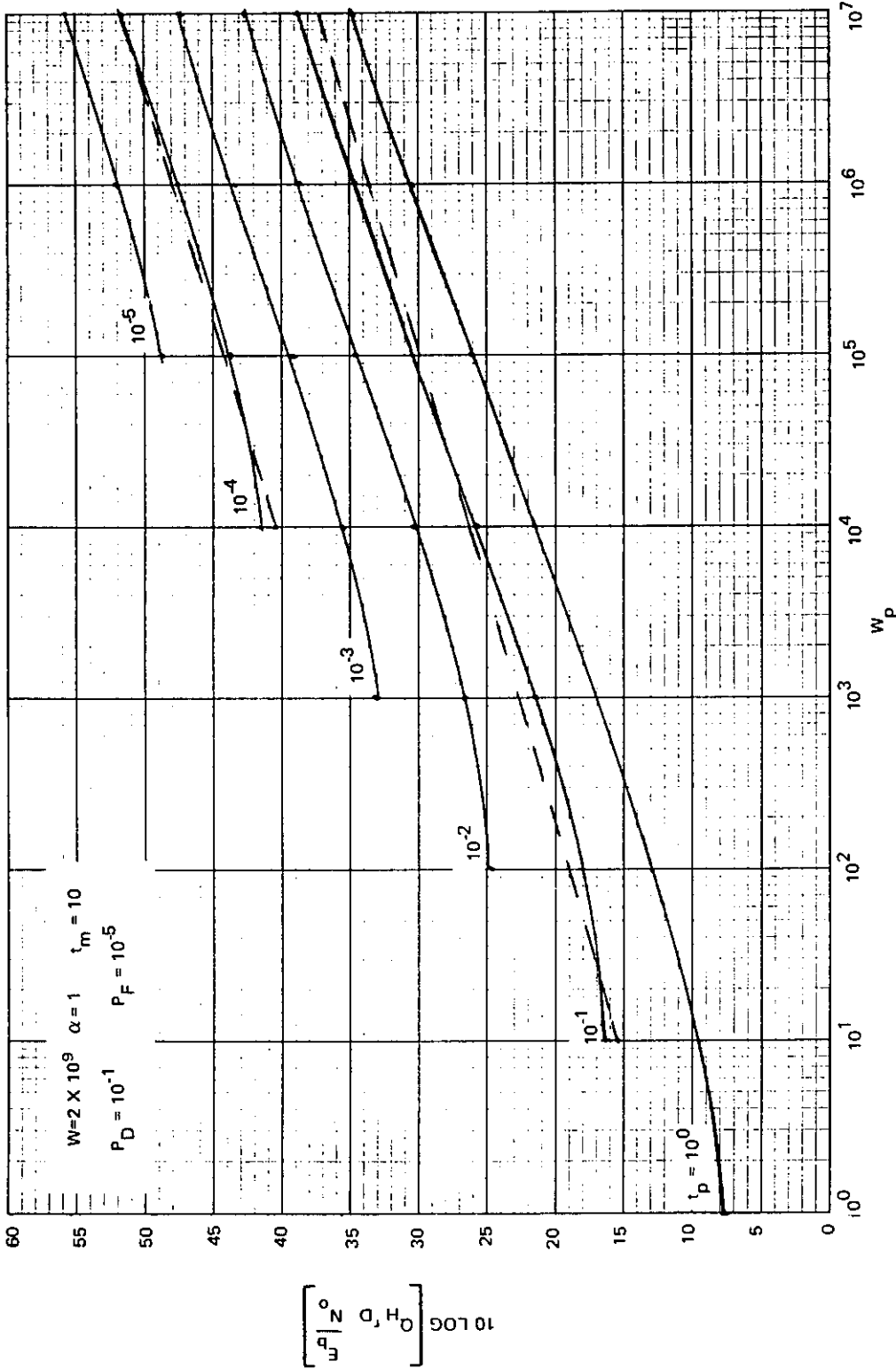


Fig. 18c—Normalized hop quality factor Q'_H vs hop bandwidth; $W = 2 \times 10^9$, $\alpha = 1$, $t_m = 10$, $P_D = 10^{-1}$, $P_{FA} = 10^{-5}$

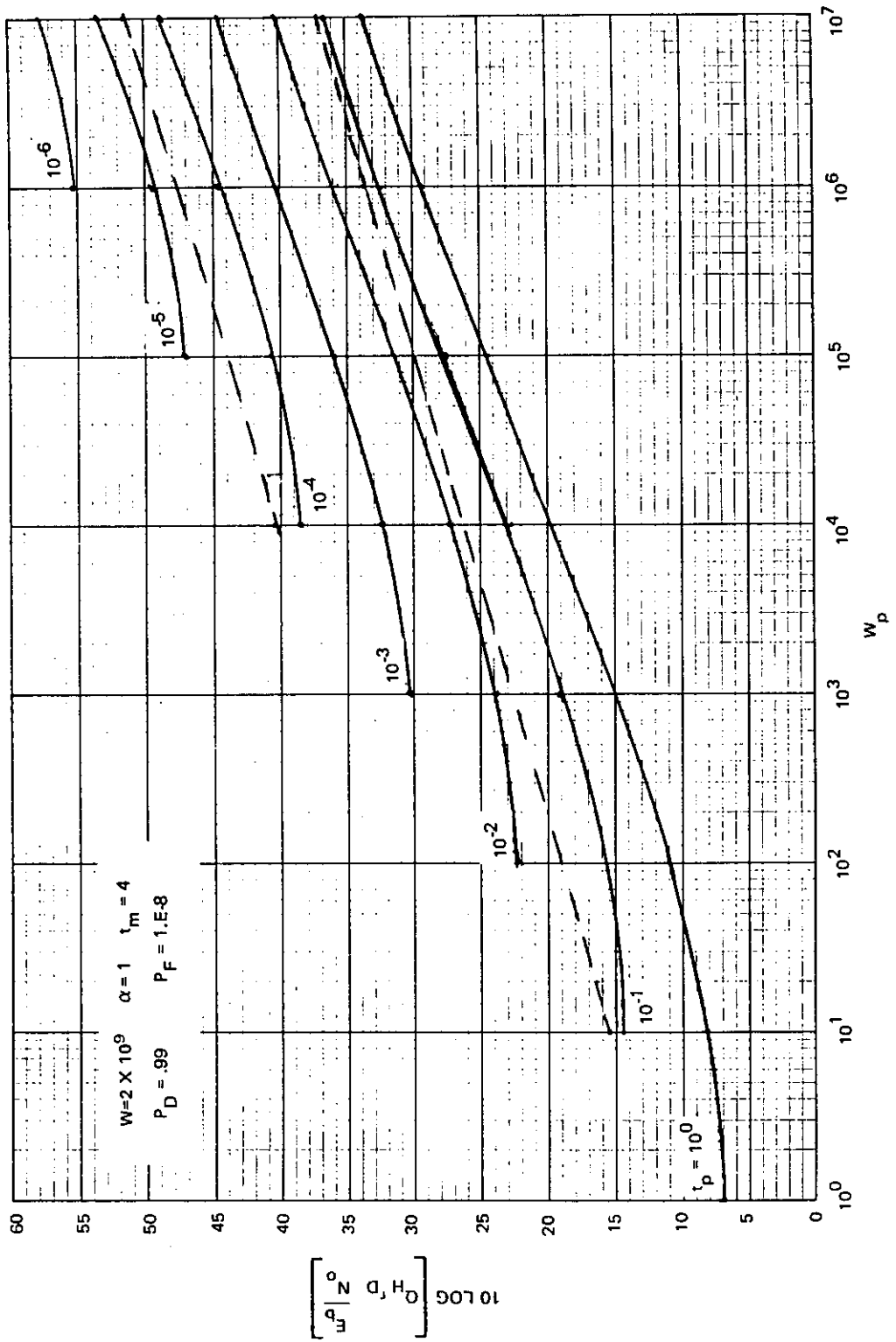


Fig. 18d—Normalized hop quality factor Q'_H vs hop bandwidth; $W = 2 \times 10^9$, $\alpha = 1$, $t_m = 4$, $P_D = 0.99$, $P_{FA} = 10^{-8}$

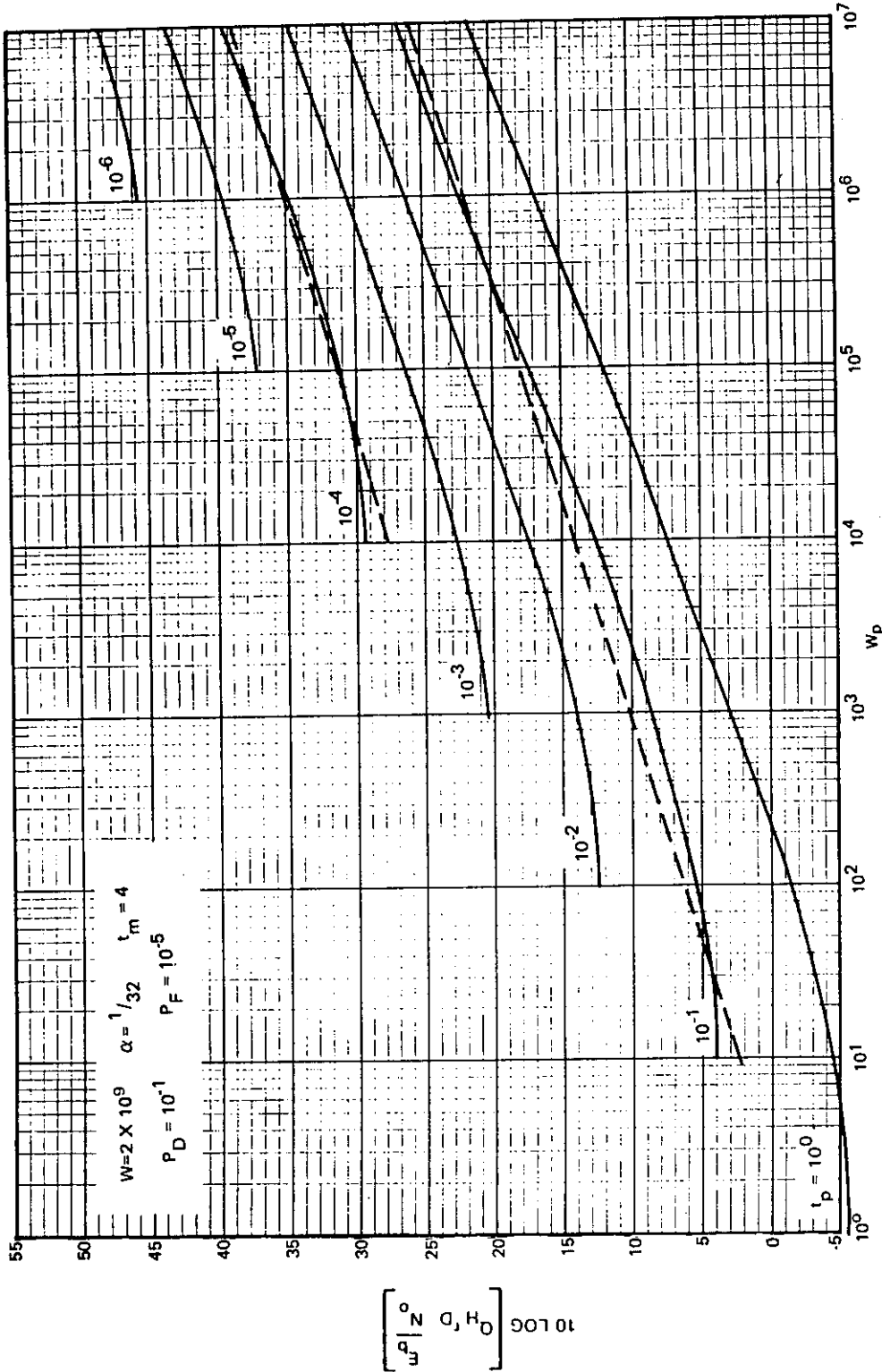


Fig. 18e—Normalized hop quality factor Q_H^0 vs hop bandwidth; $W = 2 \times 10^9$, $\alpha = 1/32$, $t_m = 4$, $P_D = 10^{-1}$, $P_F = 10^{-5}$

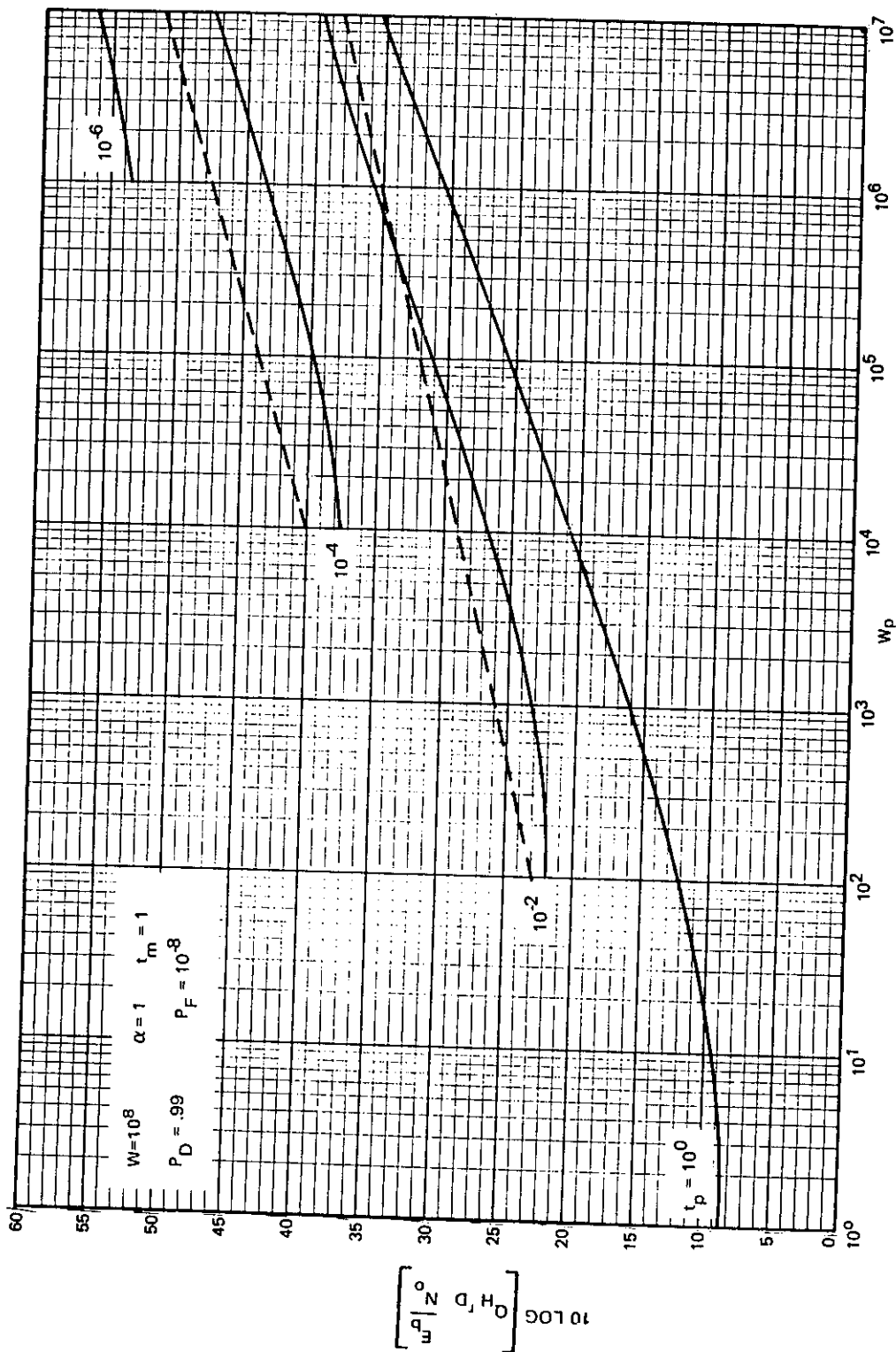


Fig. 18f—Normalized hop quality factor Q'_H vs hop bandwidth; $W = 10^8$, $\alpha = 1$, $t_m = 1$, $P_D = 0.99$, $P_{FA} = 10^{-8}$

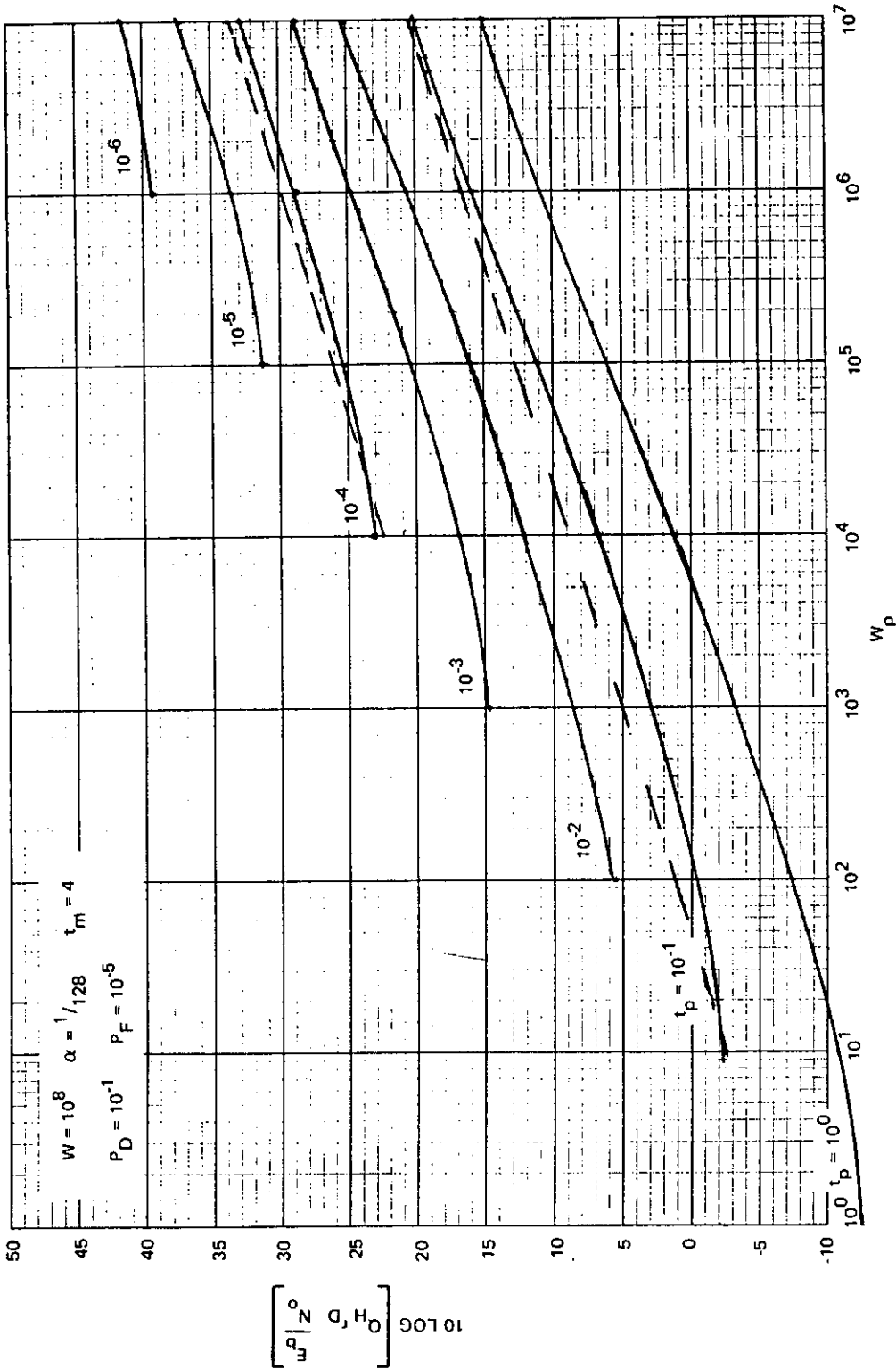


Fig. 18g—Normalized hop quality factor Q'_H vs hop bandwidth; $W = 10^8$, $\alpha = 1/128$, $t_m = 4$, $P_D = 10^{-1}$, $P_{FA} = 10^{-5}$

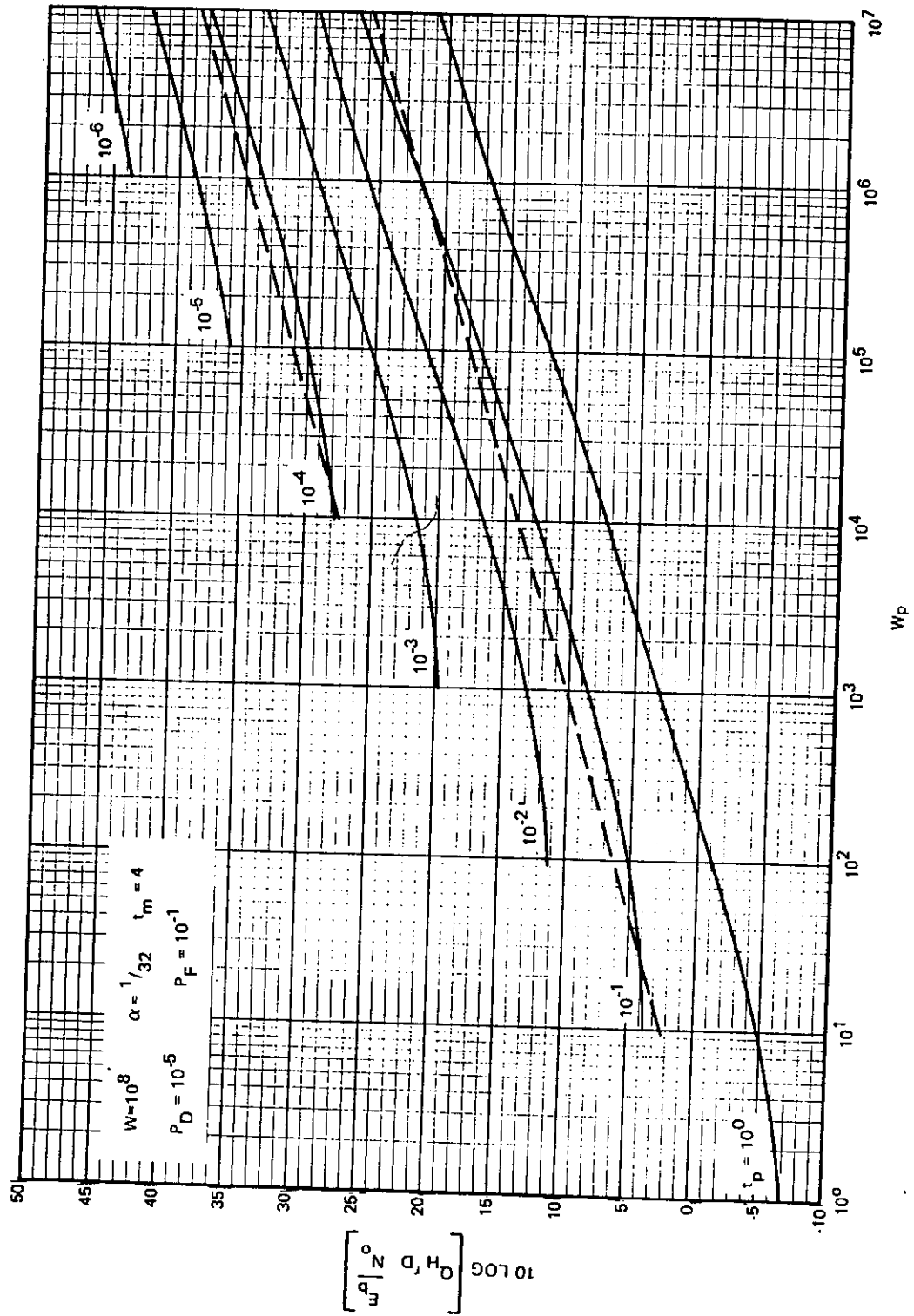


Fig. 18h—Normalized hop quality factor Q'_H vs hop bandwidth; $W = 10^8$, $\alpha = 1/32$, $t_m = 4$, $P_D = 10^{-1}$, $P_{FA} = 10^{-5}$

false alarm do not appreciably alter Q'_H . To give some feeling for the effect of each parameter, a typical curve (Fig. 18a, $t_p = 10^{-3}$) has been replotted in Figs. 19a through 19e. In each figure, the curve is plotted for several values of a single parameter while all other parameters are held constant. In every case except variations in α , Q'_H varies no more than about 2 dB. It is assumed that waveform parameters affect Q'_H independently. Clearly, this is questionable. For now, however, the assumption will be made. The way it is used and the error involved will be discussed later.

The single most important result is that the shape of the Q'_H curve does not change significantly over wide ranges of parameter values. This means that the relative change in Q'_H is nearly an invariant function of pulse duration and pulse bandwidth. Varying any or all of the other parameters only shifts the curves up or down by a fixed amount. In light of the invariant dependence on t_p and W_p , and because of the large variance in Q'_H with respect to α , it is interesting to determine, somewhat empirically, the form of this relationship. This can be done by "fitting" an approximation to the curves of Figs. 18a through 18h, as a function of α , t_p , and W_p . Here, as described, variations due to all parameters are considered independent. An approximation will be developed and its validity will be analyzed to either verify or dismiss this assumption. The dependence of Q'_H is nearly linear with the logarithm of W_p . The starting point of each curve is also very nearly a linear function of the logarithm of t_p and W_p . Variation of Q'_H , as a function of α (Fig. 20), is also linear with the logarithm. These linear approximations with the logarithm of the parameters correspond to variations of powers of the parameters themselves.

The curve fitting yields the following general form for Q'_H :

$$Q'_H = \frac{C(t_m, P_D, P_{FA}, W_M)\alpha^{0.85}}{\frac{t_p^{0.47}}{W_p^{0.37}}}$$

where $C(t_m, P_D, P_{FA}, W_M)$ is the correction factor for Q'_H as a function of the indicated parameters. Because each of these has a small effect on the value of Q'_H , a nominal value that provides a reasonable approximation to the family of curves is selected. Several values are examined, and a value of 5 is selected as a good minimization of overall error. The approximate normalized quality factor now becomes

$$Q'_H \approx \frac{5\alpha^{0.85}}{t_p^{0.47}/W_p^{0.37}}$$

The accuracy of this expression is shown by the dotted linear curves in Figs. 18a through 18h. Even in the rather extreme cases of $P_D = 0.99$ and $P_{FA} = 10^{-8}$, the approximation is still within about 3 dB of the actual values. Elsewhere it is considerably more accurate. The purpose of quality factor Q_H is to ensure that an interceptor does not, by using the filter bank combiner rather than a wideband radiometer, gain enough of an advantage in detectability to induce him to build a generally more costly and complicated receiver. Therefore, it is only necessary that Q_H reflect this advantage to within a few dB. With this in mind, the approximation to Q_H ,

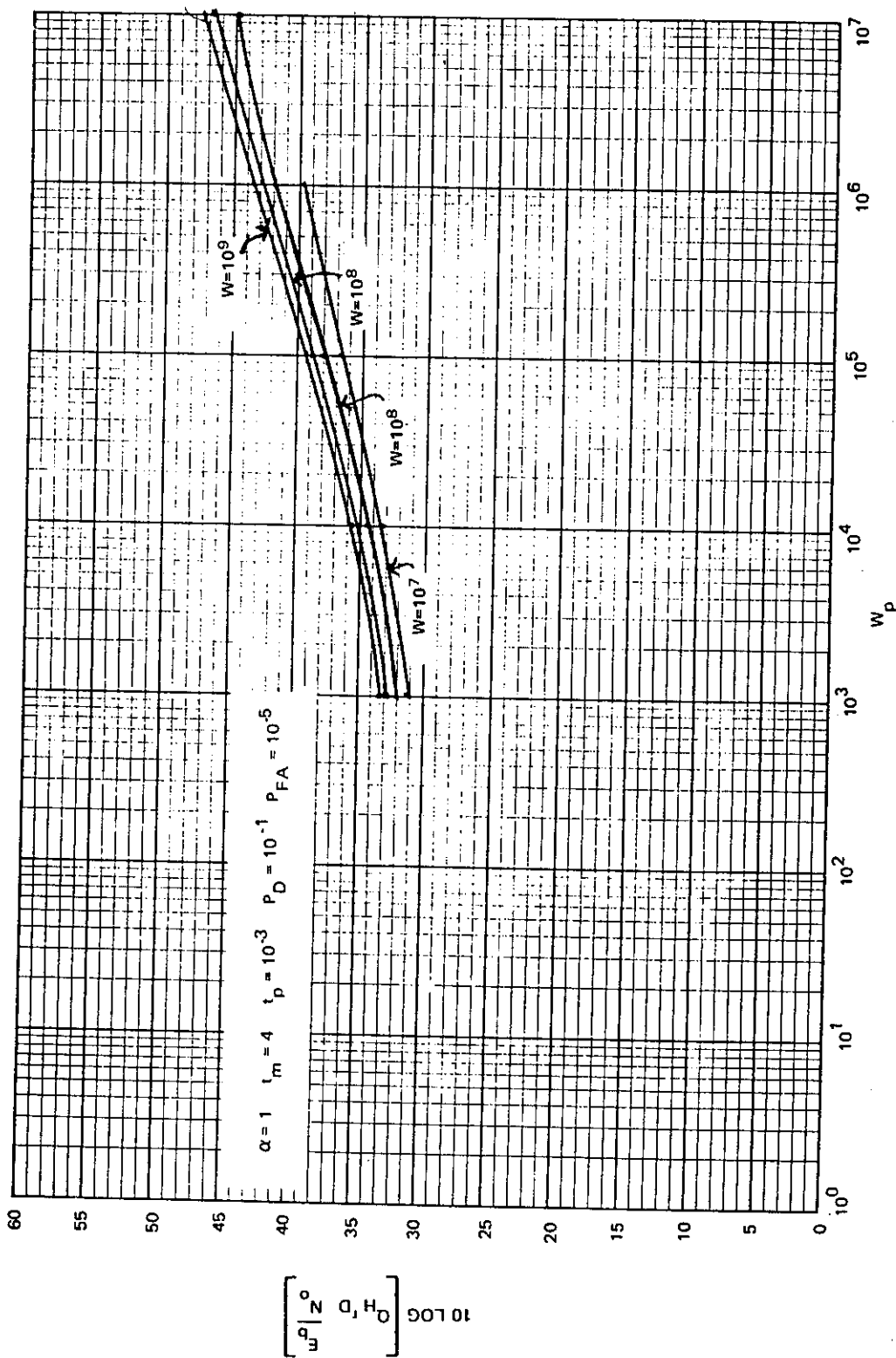


Fig. 10.—Terminal variation in α_c as a function of W

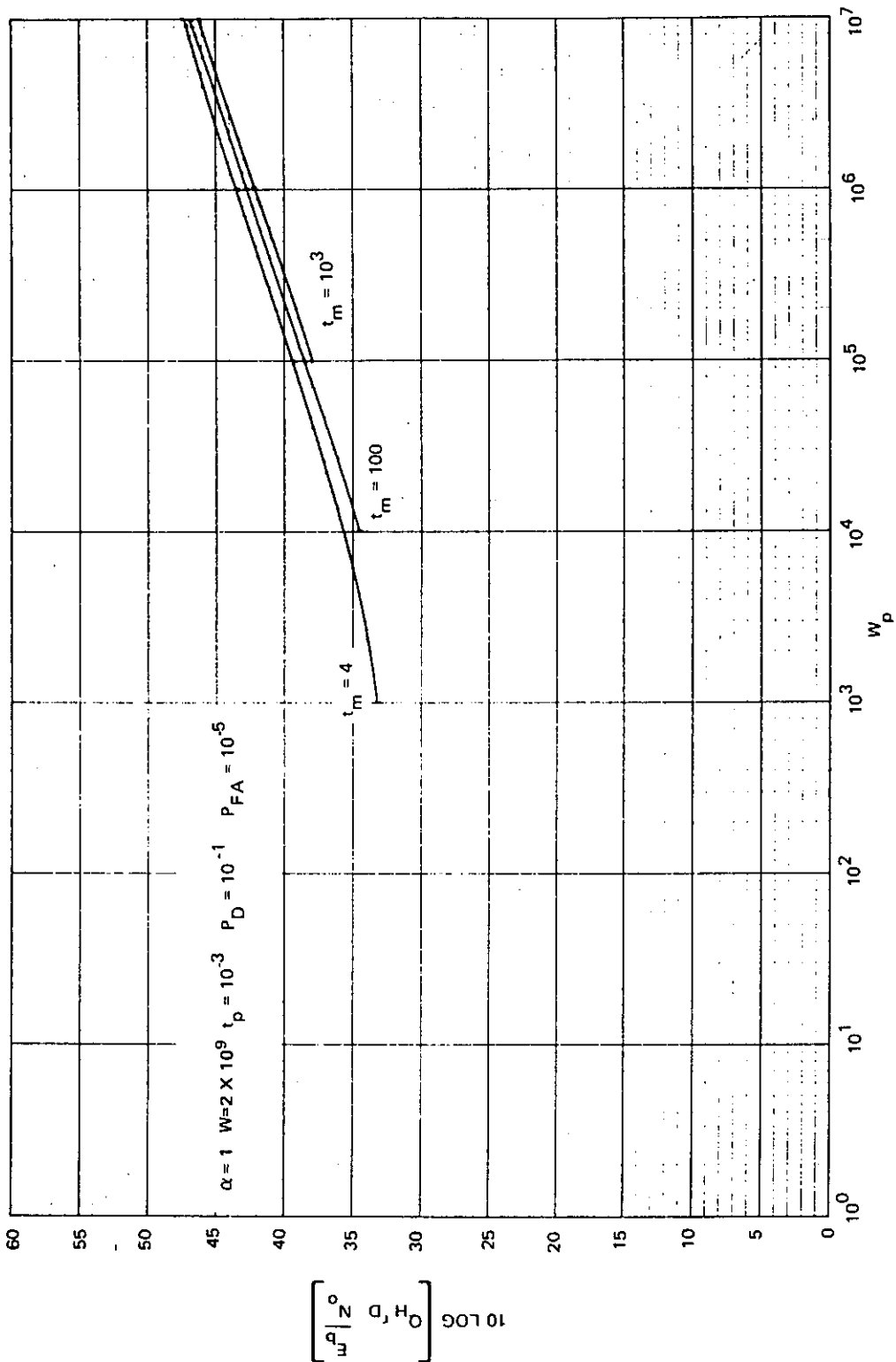


Fig. 19b—Typical variation in Q_H' as a function of t_M

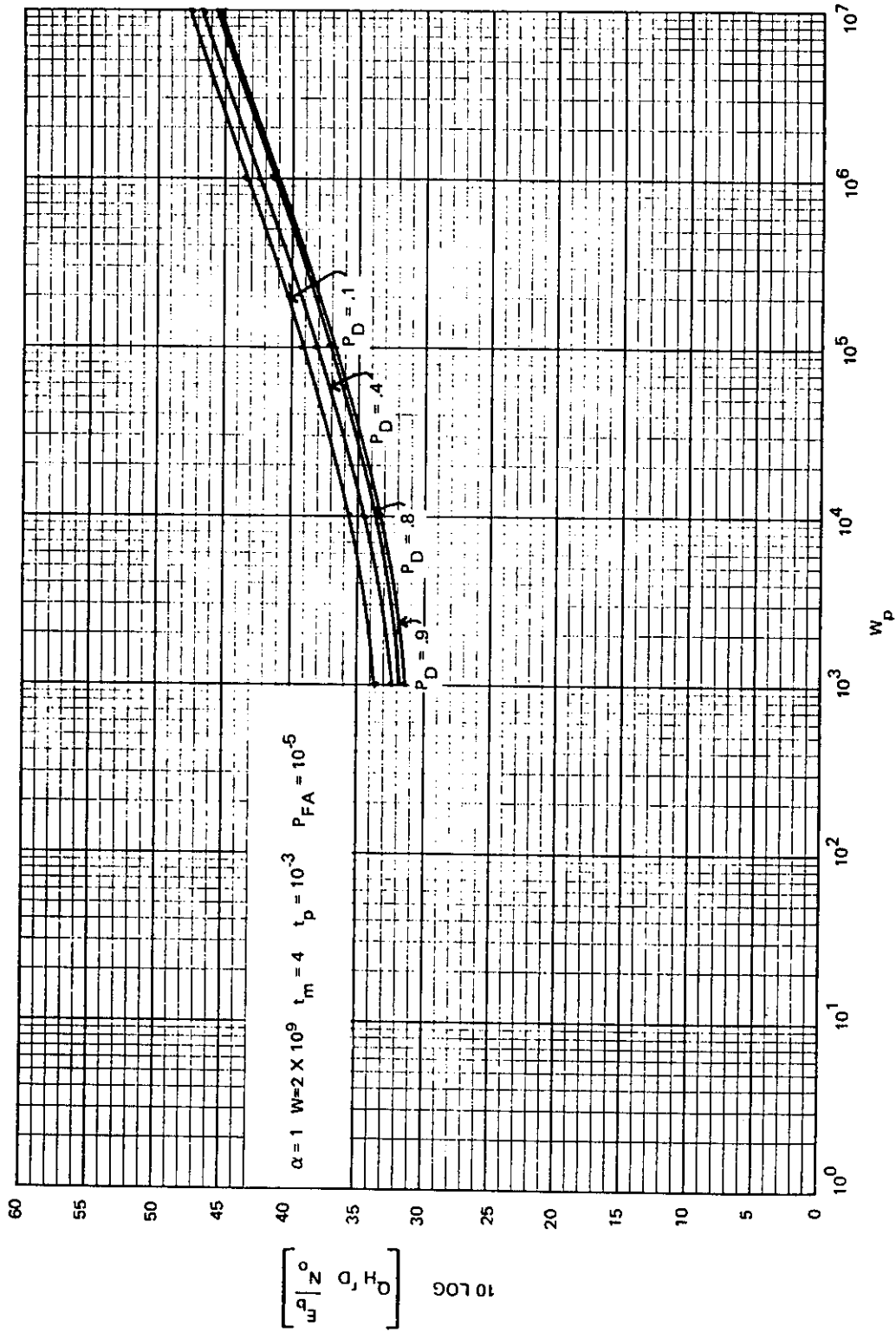


Fig. 19c—Typical variation in Q'_H as a function of P_D

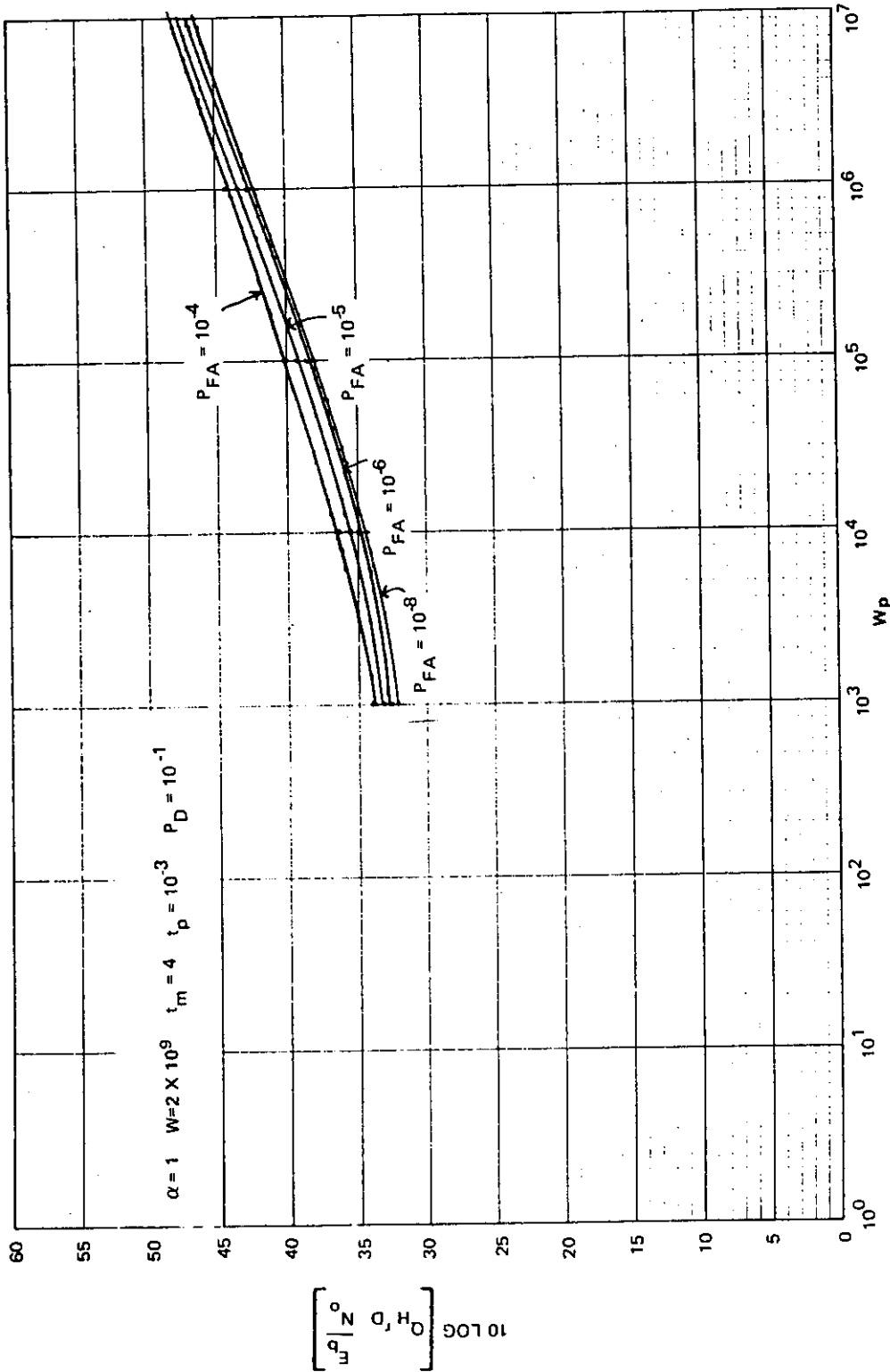


Fig. 19d—Typical variation in $Q'H$ as a function of P_{FA}

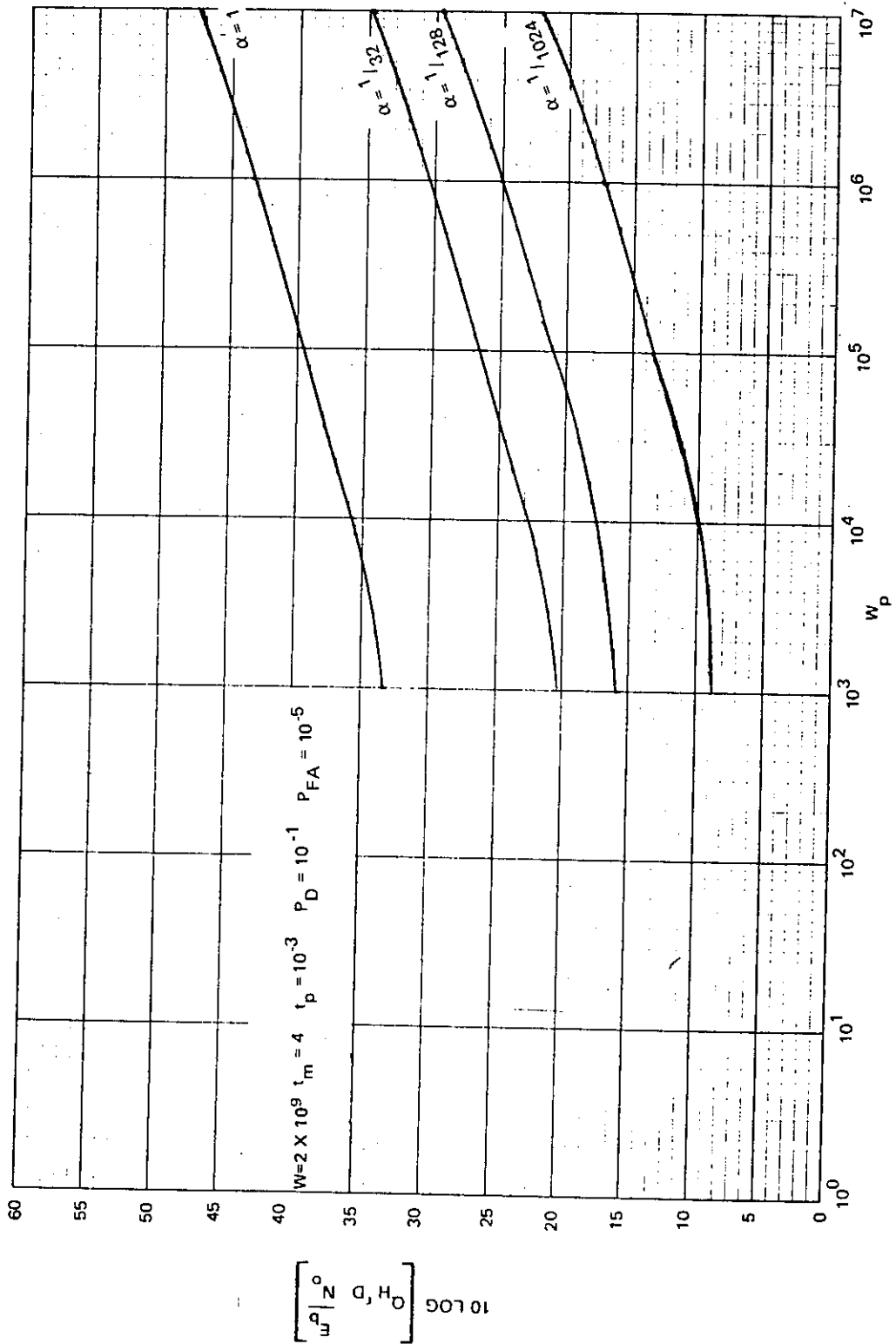


Fig. 19e—Typical variation in Q'_H as a function of α

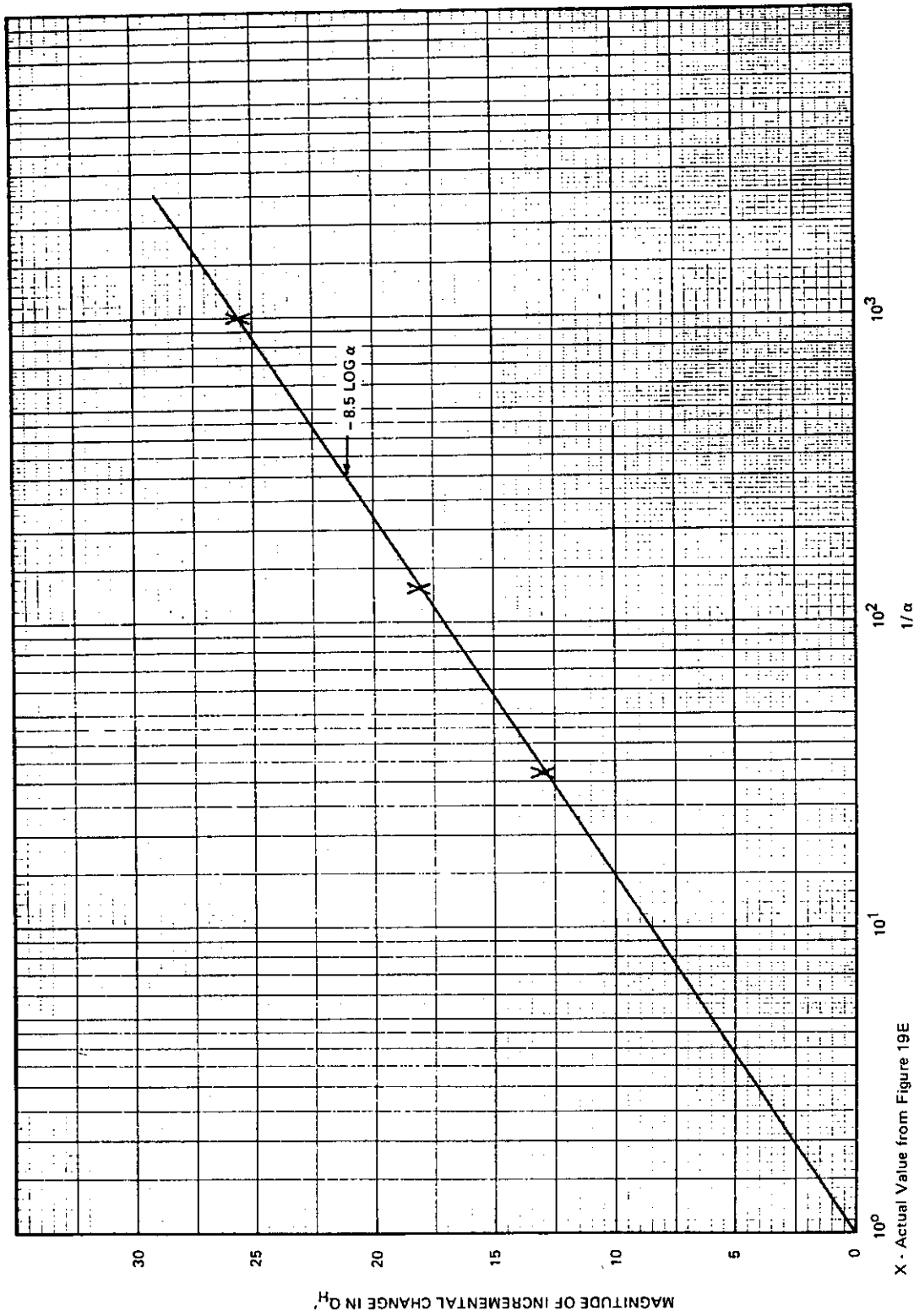


Fig. 20—Typical variation in $Q'H$ as a function of $1/\alpha$

$$Q_H = \frac{5\alpha^{0.85}}{r_D \frac{E_b}{N_0} \left(t_P^{0.47} / W_P^{0.37} \right)},$$

serves its purpose, and the original assumption of parameter independence has been mitigated.

Covertness: The Best Choice

The tools have now been developed to allow comparison of overall covertness. Basic signal processing techniques and their associated losses have been discussed. Their impact on covertness can be assessed through the quality factors. The combined effects on covertness of the choice of waveform parameters and the associated processing will now be considered. Figure 21 depicts a hierarchy of techniques that can be used in a frequency-hopped modulation scheme. The basic flow upward indicates techniques from which improvement may be derived. Each of these techniques will now be treated, and the corresponding deficiencies and benefits will be described. The progression of a numerical model will be carried through Fig. 21, which will provide some feel for the magnitude of the parameters involved. Parameters for the initial model are as follows:

modulation = binary FSK

$$r_D = 75 \text{ bits/s}$$

$$t_m = 4 \text{ s}$$

$$W_M = r_D$$

$$E_b/N_0 = 10.9 \text{ dB at a } 10^{-3}\text{-bit error rate}$$

$$N_b = \text{number of bits } (N_b = 300)$$

$$Q_M = -23.3 \text{ dB.}$$

Parameter N_b was chosen as a reasonable value for a communicator serious about covertness. It will become clear that it is the number of information bits to be transmitted that ultimately determines the maximum achievable covertness of the message. It should be remembered that Q_H is based on an approximation to the filter bank combiner performance relative to the wideband radiometer, good to within approximately 3 dB. The numbers in the numerical example will also suffer from the same error.

Pure Frequency Hopping

At the bottom of Fig. 21 is a basic message using a simple modulation, as in the numerical model. Covertness is improved by moving up to the next technique in the figure. Noncoherent frequency hopping is used to increase W_M and improve Q_M . A significant increase in covertness can be obtained over the basic message by hopping the carrier over the larger bandwidth. To maximize the contribution of W_M a total spread bandwidth of 2×10^9 Hz is used in the numerical example. This increases Q_M by $5 \log(W_M/r_D)$, or 37 dB. This is a significant improvement. For a modulation technique that uses no hop spreading or pulsed transmission, the following relations hold:

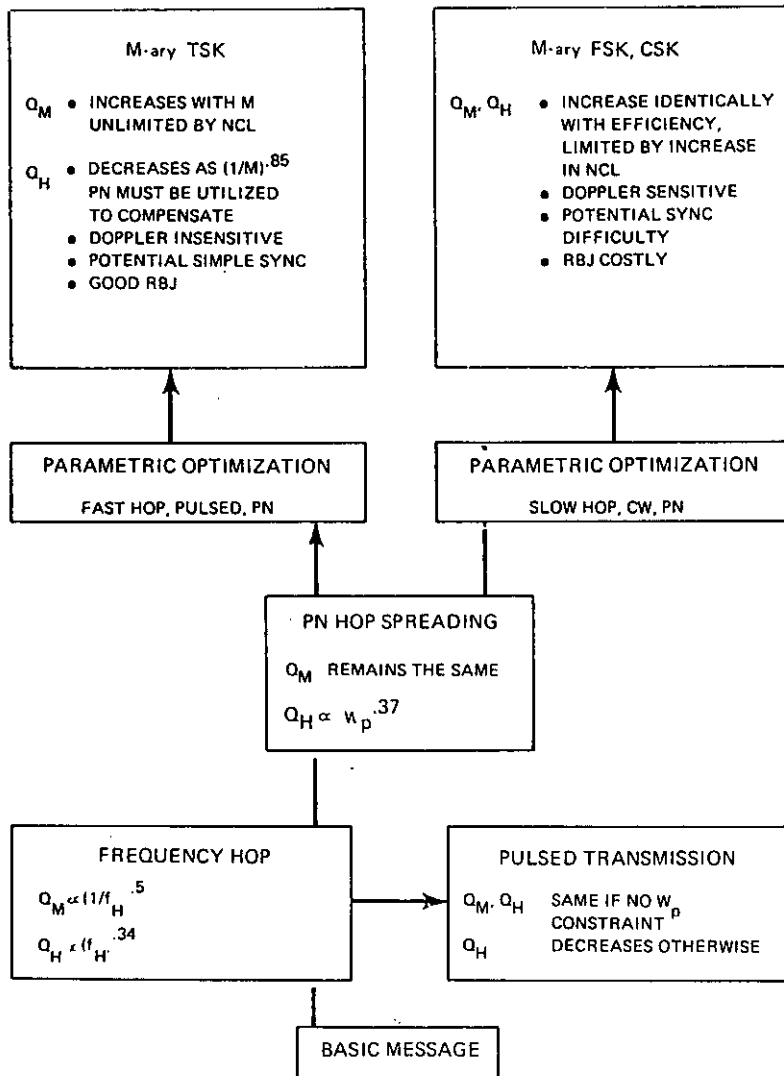


Fig. 21—Hierarchy of frequency-hopped and hybrid waveform techniques

JOHN D. EDELL

$$W_p \approx \frac{1}{t_p}$$

$$\alpha = 1$$

$$Q'_H \approx \frac{5}{r_D \frac{E_b}{N_0} t_p^{0.84}}$$

Equalizing Q_M and Q_H gives

$$Q_M = \frac{1}{r_D \frac{E_b}{N_0} \sqrt{\frac{t_m}{W_M}}} = Q_H = \frac{5}{r_D \frac{E_b}{N_0} t_p^{0.84}}$$

or

$$t_p \approx 6.8 \left[\frac{t_m}{W_M} \right]^{0.59}$$

This corresponds to a frequency-hopping rate of approximately $1/t_p$. For the numerical example,

$$f_H = \frac{1}{t_p} \approx 20,000 \text{ hops/s.}$$

The equalization of Q_M and Q_H is independent of $r_D E_b/N_0$, because this parameter affects both quality factors identically. Now examine the effects of the frequency-hopping rate on $r_D E_b/N_0$. For the numerical example a transmitted FSK symbol represents one data bit. Therefore

$$t_S = 1/r_D$$

where t_S is the transmitted symbol duration. If the frequency hopping rate is f_H , then N_H hops must be combined noncoherently to recover the energy required to detect the bit, where

$$N_H = f_H t_S = f_H / r_D.$$

For the example,

$$N_H = (20,000)(1/75) = 266 \text{ hops.}$$

An examination of the noncoherent combining loss curves indicates that for the required post-detection signal-to-noise ratio (E_b/N_0) of 10.9 dB, the loss encountered is

$$\text{NCL}|_{266} \approx 8.3 \text{ dB.}$$

NRL REPORT 8025

Now Q_M and Q_H have been equalized, but in the process the original 37-dB gain in Q_M due to W_M has been reduced by 8.3 dB. This is discouraging. Q_M can be increased by reducing the frequency-hopping rate, but this will result in a decrease in Q_H . If the hop rate is increased to increase Q_H , the noncoherent combining losses also increase, thus reducing Q_M . If this effect is taken into consideration for a pure frequency-hopped modulation, in the limiting case, the NCL changes as $\sqrt{N_H}$ or, equivalently, $\sqrt{f_H}$, and the following relationship holds:

$$Q_M \propto 1/f_H^{0.5}.$$

Because Q_H increases as $f_H^{0.84}$ while decreasing as the NCL the net result is

$$Q_H \propto f_H^{0.34}.$$

With pure frequency hopping, the full advantage of the bandwidth spreading cannot be achieved while maintaining a balanced system.

Another approach is to increase the data rate, thereby reducing the transmission time for a given number of data bits. Examination of the expression for Q_M indicates that

$$Q_M \propto \frac{1}{r_D},$$

while at the same time

$$Q_M \propto \frac{1}{\sqrt{t_m}}.$$

The NCL is approximately proportional to $1/\sqrt{r_D}$. Any increase in r_D , then, will be directly offset by decreases in t_m and the NCL, resulting in no net change in Q_M . (That is, the decrease in Q_M caused by increasing transmitter power is very nearly offset by the combined effects of the decreases in noncoherent combining loss and message transmission time.) At the same time, however, Q_H has decreased proportionally to $\sqrt{r_D}$, and the system is no longer balanced. A balanced system can be regained by increasing the hopping rate to give lower values of Q_M and Q_H than in the former balanced state.

Pulsed Transmission

Since the capabilities of pure frequency hopping have been examined and found wanting, the technique of pulsed transmission is examined. A scheme may be envisioned whereby a pure-frequency-hopped waveform could be balanced by adjusting the hop rate so that Q_M and Q_H are equal and then pulsing each transmitted hop so that more carrier power is transmitted for a shorter interval. If this pulsing corresponds to a duty cycle α , then

$$Q_H \propto \alpha^{0.85},$$

and in the pure-frequency-hop case

JOHN D. EDELL

$$Q_H \propto 1/t_p^{0.84}.$$

Thus, a decrease in t_p , which is identically equal to the duty cycle, will almost exactly offset the increase in power that must be transmitted per pulse. Equivalently, an increase in transmitted power is offset by the expanded pulse bandwidth.

Suppose the pulse, or hop, bandwidth were constrained, for example, by a fixed-rate PN sequence. Then, because

$$Q_H = \frac{5\alpha^{0.85} W_p^{0.37}}{r_D \frac{E_b}{N_0} t_p^{0.47}},$$

and t_p varies directly as the duty cycle, Q_H not only increases as $\alpha^{0.85}$ but at the same time decreases as $t_p^{0.47}$ (or $\alpha^{0.47}$). There will be a net decrease in Q_H approximately equal to $\alpha^{0.38}$. The overall message covertness is essentially the same in both cases. Thus, for pure frequency hopping, or frequency hopping in which there is a pulse bandwidth constraint, pulsing the transmitted power achieves nothing and can in fact decrease overall covertness.

Pseudonoise Hop Spreading

The next technique to be examined in Fig. 21 is pseudonoise hop bandwidth spreading. With this technique, the energy transmitted in a single pulse can be spread over a larger bandwidth than that of the basic pulse. This is directly analogous to spreading the transmitted message power over a large bandwidth. Since

$$Q_H \propto W_p^{0.37},$$

the covertness of the waveform against a filter bank combiner can be increased by increasing W_p , and there is essentially no change in message covertness other than the impact of pseudonoise sequence on synchronization time. A very fast sequence, corresponding to a high clock rate, requires very accurate time synchronization, and this can be troublesome if care is not taken to use a scheme that yields the required accuracy.

The most important aspect of the pseudonoise hop spreading is that it can be used to adjust Q_H without affecting Q_M . This is a useful quality, because it allows correction of one of the main flaws of the pure-frequency-hopping technique, the increase in noncoherent combining losses when Q_M and Q_H are balanced. By use of PN spreading, Q_M and Q_H can be equalized at a much lower hop rate than would otherwise be required. The balance will occur when

$$\frac{1}{r_D \frac{E_b}{N_0} \sqrt{\frac{t_m}{W_M}}} = \frac{5\alpha^{0.85} W_p^{0.37}}{r_D \frac{E_b}{N_0} t_p^{0.47}}$$

or

$$\frac{\alpha^{0.85} W_p^{0.37}}{t_p^{0.47}} \approx 0.2 \left(\frac{W_M}{t_m} \right)^{0.5}$$

The hop rate can be decreased, thus increasing t_p and decreasing Q_H , but this may be offset by increasing PN spreading W_p . Also, if pulsed transmission is used, W_p may be increased to offset the degradation due to decreased duty cycle, as previously discussed.

In the numerical example, let the frequency hopping rate be 1,000 hops/s instead of the 20,000 hops/s required to balance Q_M and Q_H with no hop spreading. Now the required W_p would be about 1.1 MHz. Through pseudonoise hop bandwidth spreading, then, a reduction in required hopping rate is possible. This allows a decrease in noncoherent combining losses by approximately the square root of the frequency reduction, because there will be that many fewer hops to combine per symbol. However, if such an approach is taken, yet another processing loss takes its toll—the frequency offset, or doppler loss. Recall that the loss L_D in signal power due to a frequency offset is given by

$$L_D = \left[\frac{\sin \pi \Delta f t}{\pi \Delta f t} \right]^2$$

where

Δf = frequency offset

t = integration time.

For the case at hand, the integration time is equal to the pulse duration. If continuous wave (CW) or nonpulsed ($\alpha = 1$) transmission is used, integration time corresponds to the reciprocal of the hop rate. Therefore, the slower the hop rate, the greater the sensitivity to frequency offset. For the numerical example, at a frequency hop rate of 1,000 hops/s, a frequency offset of 500 Hz causes a loss L_D of about 4 dB. Clearly then, to extract the maximum benefit from the CW waveform, slow frequency hopping* must be used, PN hop spreading must be used to equalize Q_M and Q_H , and some form of doppler or frequency tracking is necessary to reduce frequency offset losses. Widening the IF bandwidth, another approach to minimizing the frequency offset loss, was discussed in a previous section. However, it rarely saves more than a few decibels over the many that may be lost.

Now consider a pulsed waveform. A scheme can be envisioned for which the frequency-hopping rate is adjusted so that Q_M and Q_H are equal (fast hopping), but to reduce the noncoherent combining losses, the total number of pulses (hops) per symbol is not transmitted. Instead only a fraction α is actually sent. This will indeed reduce the noncoherent combining losses and increase Q_M and Q_H , but Q_H will incur an additional loss due to the increased transmitted power per hop. This loss can, in turn, be offset by PN hop spreading. Therefore Q_M and Q_H can be equalized at a relatively high level. It is interesting to note that the shortened pulse durations are much less sensitive to frequency offset than the longer CW, slow-hop pulses and that significant covertness can be achieved

*Slow frequency hopping is defined here as any hop rate significantly less than the rate at which Q_M and Q_H are equal in a pure frequency-hop waveform.

without frequency or doppler tracking. Also, pulsed waveforms have an inherent advantage in synchronization time, relative to CW waveforms, due to the higher transmitted power per pulse.

M-ary Modulation

At this point covertness has been maximized relative to waveform parameters. Either a combination of slow frequency hopping with PN hop spreading, and probably doppler tracking, or a combination of fast-hop, pulsed transmission with PN hop spreading can be used. The only remaining way to increase covertness is to use an efficient modulation, thereby reducing required transmitted power. High-order M -ary modulations provide the desired efficiency and may be implemented in either a pulsed (TSK) or CW format (FSK, CSK). Both of these techniques are displayed at the top of Fig. 21 as viable candidates for an optimal design. It is interesting to note that for a given frequency-hopping rate and alphabet size M , the TSK Q_M will always be approximately \sqrt{M} greater than the CW waveform Q_M . This is because for the CW waveform, as M increases, symbol duration and noncoherent combining losses both increase. For the TSK waveform, as M increases, noncoherent combining losses do not increase, but duty cycle $1/M$ decreases. This means that for both CW and TSK modulations, increasing M yields the same potential improvement in efficiency, but the improvement in the former case is reduced by about \sqrt{M} , due to increased noncoherent combining loss. With respect to Q_H , exactly the opposite occurs. For the CW waveform, Q_H increases exactly as Q_M due to the net reduction in required transmitted power, but the TSK Q_H is now penalized by the decreasing duty cycle α . Since,

$$\alpha = \frac{1}{M},$$

the loss in Q_H is approximately $(1/M)^{0.85}$. However, the TSK modulation is approximately \sqrt{M} more efficient than the CW waveform, so that the net result is a pulsed Q_M that is approximately $(M)^{0.35}$ less than the CW Q_M . These differences, of course, would be compensated for by slow hopping with PN spreading in the CW case, and fast hopping with PN spreading in the TSK case.

V. CONCLUSION

The parametric analysis has revealed two candidates for a low-probability-of-intercept modulation scheme: fast-hop M -ary time shift key, and slow-hop CW.* Final selection depends on other system design considerations, such as equipment complexity, cost, synchronization time, synchronization implementation complexity, and jam resistance. Without a specific design at hand, it is difficult to compare and trade off all these considerations, but a few general comments will be helpful.

*CW here indicates a larger class of modulation schemes than would be indicated by M -ary FSK or M -ary CSK. If the frequency-hop rate is reduced to a small fraction of the bit duration, then modulation techniques such as phase shift keying may be used. The ensuing comments are directly applicable to this class of modulations as well.

NRL REPORT 8025

First consider synchronization. A pulsed waveform is inherently easier to synchronize than a CW waveform because of the high peak power per pulse. The general approach to time synchronization is to dwell on a particular time hypothesis and integrate the post-detection signal power until the post-detection signal-to-noise ratio is large enough to allow an accurate decision. In a frequency-hopped waveform this is directly applicable to determining the number of hops that must be accumulated. Obviously, then, if the waveform is pulsed, each transmitted hop will have a higher peak power, and fewer hops will be necessary for achieving the same post-detection signal-to-noise ratio than if a CW waveform is used. This is not to say that a CW waveform cannot be synchronized as quickly as a TSK waveform, but it does imply that more sophisticated methods may be required.

In jam resistance, the TSK waveform again has a few advantages, mainly with respect to repeat-back and frequency-following jammers. A slow-hop modulation allows a frequency-following jammer much more time to sweep and locate the transmit frequency. For a CSK modulation, the only resistance to a jammer who knows the transmit hop frequency lies in the processing gain associated with the pseudonoise spreading of each hop. The FSK modulation can be made invulnerable to a frequency-following jammer if the symbol frequencies are independently generated. This requires an essentially independent receiver for each symbol frequency (a somewhat costly option). The TSK modulation is virtually invulnerable to a frequency-following jammer in the data mode, because the jammer has no way of knowing the transmit frequency of any time slot other than the one actually transmitted. If this slot is jammed, it can only help the receiver, since energy detection is used for demodulation. In the synchroization mode all waveforms have inherently the same vulnerability, and care must be taken.

Finally, an important consideration affecting system hardware complexity is the sensitivity of the modulation scheme to frequency offsets, or doppler effects. The TSK modulation, because of its short pulse duration, is relatively insensitive to doppler shifting, and substantial covertness may be obtained without active doppler tracking.* The CW waveform, if it is to achieve its full potential, requires some form of active tracking.

Clearly, serious concern must be given to the governing constraints on system design before an optimum modulation technique is selected.

ACKNOWLEDGMENTS

The author wishes to thank R. A. LeFande of NRL for offering his original work as a basis for this report, which is an extension and refinement of his ideas. The author is greatly indebted to C. A. Hoffman of NRL for performing the extensive numerical analysis, D. G. Woodring of NRL for general advice and consultation on the subject, and R. H. Early and J. D. Sawdey of Booz, Allen Applied Research for their technical suggestions and assistance in revision of the draft.

REFERENCES

1. A.J. Viterbi, *Principles of Coherent Communication*, McGraw-Hill, New York, 1966.

*This statement is made on the premise that some form of doppler prediction is used.

JOHN D. EDELL

2. J.V. DiFranco and W.L. Rubin, *Radar Detection*, Prentice-Hall, Inc., Englewood Cliffs, N.J., 1968.
3. S.L. Bernstein, "Error Rates for Square Law Combining Receivers," MIT Technical Note 1971-31, 1971.
4. H. Taub and D.L. Schilling, *Principles of Communication Systems*, McGraw-Hill, New York, 1971, pp. 286-288.
5. H.L. Van Trees, *Detection, Estimation and Modulation Theory*, Part I, Wiley, New York, 1968.
6. W.W. Peterson, et al., "Theory of Signal Detectability," *IRE Trans. PGIT-4*, 171-212 (Sept. 1954).
7. John Sam Lee, "Phase-Incoherent Synchronization in Frequency-Hopping Communication Systems," NRL Report 7560, Apr. 27, 1973.
8. G.E. Uhlenbeck and J.L. Lawson, eds., *Threshold Signals*, McGraw-Hill, New York, 1968.
9. R.A. Dillard, "Vulnerability of Low Detectability Communications to Energy Detection," Naval Electronics Laboratory Center, San Diego, Calif., NELC/TR 1748, 1971.

Appendix A

FILTER BANK COMBINER PERFORMANCE

A block diagram of the filter bank combiner detector is shown in Fig. A1. The receiver consists of a bank of energy detectors, one centered at each of the N possible frequency channels, with integration times matched to pulse duration t_p and bandwidths matched to pulse bandwidth W_p . A decision is made in each channel, and the outputs are logically "OR'd," summed over the number M of frequency-hop intervals, and finally compared to a threshold k . If the sum exceeds the threshold, a detection is announced.

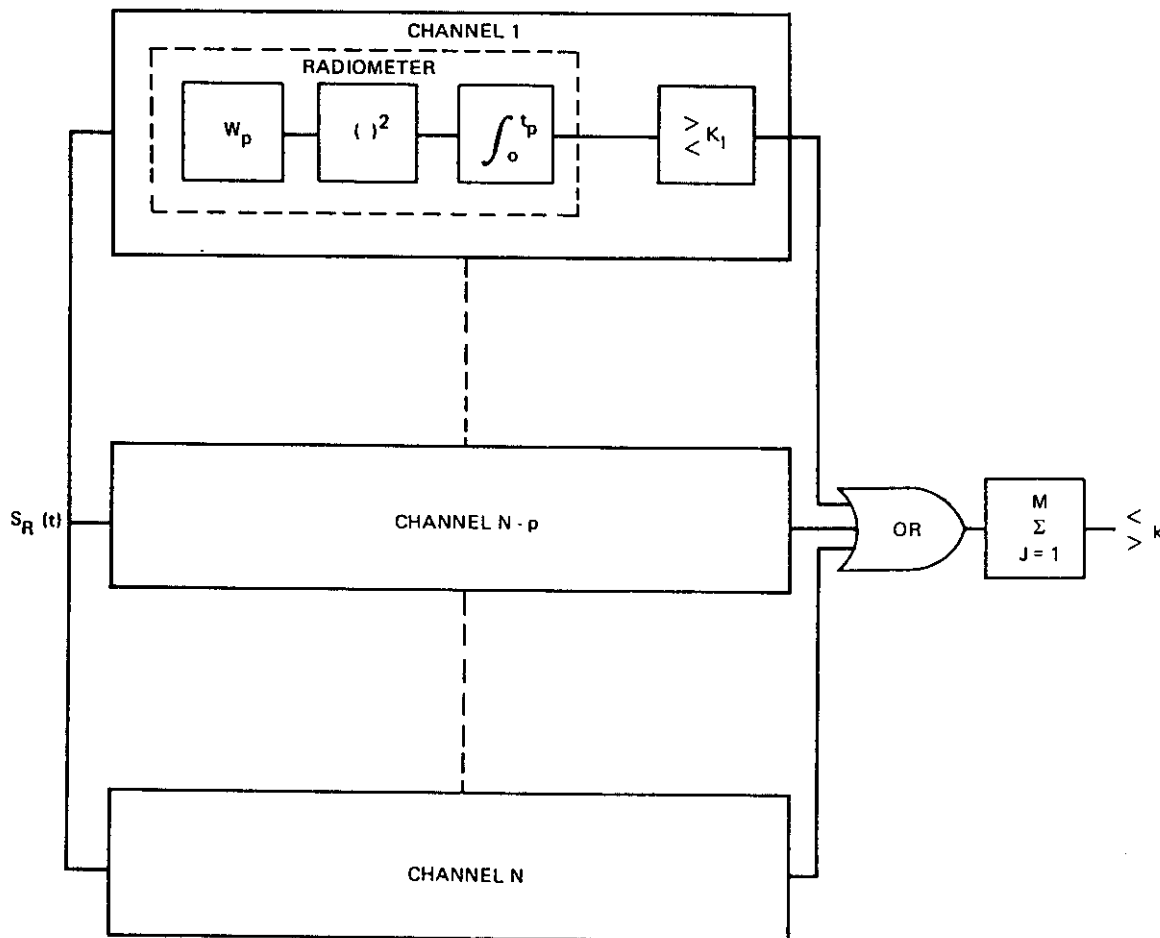


Fig. A1—Filter bank combiner

The average ratio of carrier power to noise density required at the input to the filter bank combiner, assuming that the receiver is aligned in time with the hop intervals and observes for duration t , is given as

$$\begin{aligned} \left. \frac{\bar{C}}{N_0} \right|_{\text{required for Hop Detector}} &= \eta_H \alpha \left[\left\{ Q^{-1}(P_{FAI}) - Q^{-1}(P_{DI}) \right\} \sqrt{\frac{W_p}{t_p}} \right] \\ &= \eta_H d_H \alpha \sqrt{\frac{W_p}{t_p}} \end{aligned}$$

where

α = duty cycle

P_{FAI} = probability of false alarm for an individual channel

P_{DI} = probability of detection for an individual channel

$d_H = Q^{-1}(P_{FAI}) - Q^{-1}(P_{DI})$

η_H = correction factor for Gaussian statistics.

This equation is based on the Gaussian performance model for a wideband radiometer, corrected by η_H to yield accurate values. Overall probability of detection P_D and probability of false alarm P_{FA} , for the observation interval t , are given by the following formulas:

$$P_D = \sum_{J=k}^{D_1} \binom{D_1}{J} (P_{DI})^J (1 - P_{DI})^{D_1 - J}$$

$$P_{FA} = \sum_{J=k}^{D_2} \binom{D_2}{J} \left[1 - (1 - P_{FAI})^N \right]^J \left[(1 - P_{FAI})^N \right]^{D_2 - J}$$

where

D_1 = number of opportunities to detect an individual pulse per message
 = number of pulses per message actually transmitted
 = $\alpha t / t_p$

D_2 = total number of parallel decisions per message
 = total number of opportunities for a false alarm per message interval
 = t / t_p

W = total observed spread bandwidth

NRL REPORT 8025

W_p = bandwidth of a transmitted pulse

P_D = probability of detecting the message using a wideband radiometer

P_{FA} = probability of false alarm for a wideband radiometer

k = hop detector decision threshold

$$\binom{D}{J} = D!/J!(D-J)!$$

The expression for P_D ignores the unlikely event of a false alarm occurring during the observation interval when a message is actually present, thereby aiding detection.

Curves showing the required average input C/N_0 are shown in Figs. A2 through A7 for the simple $k = 1$ threshold, for a wide range of waveform parameters. Curves of Figs. A8 through A15 show the required average C/N_0 for an optimized threshold k , for the same range of parameters. The curves indicate that the difference between the $k = 1$ and optimized k thresholds ranges from a few tenths of a decibel to as much as 3 dB, depending on the particular parameters.

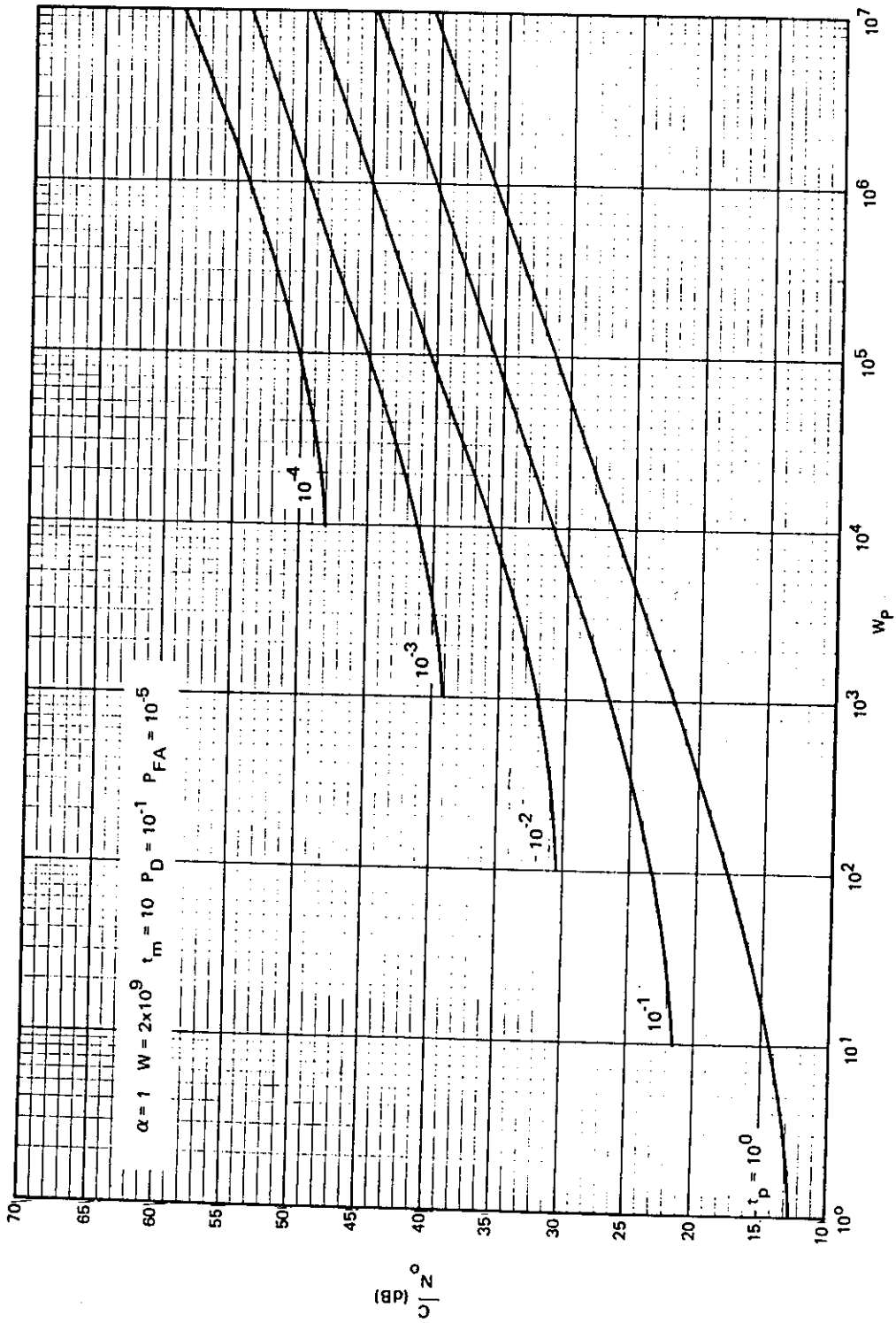


Fig. A2—Average required input C/N_0 for simple $k = 1$ threshold; $W = 2 \times 10^9$, $\alpha = 1/128$, $t_m = 4$, $P_D = 10^{-1}$, $P_{FA} = 10^{-5}$

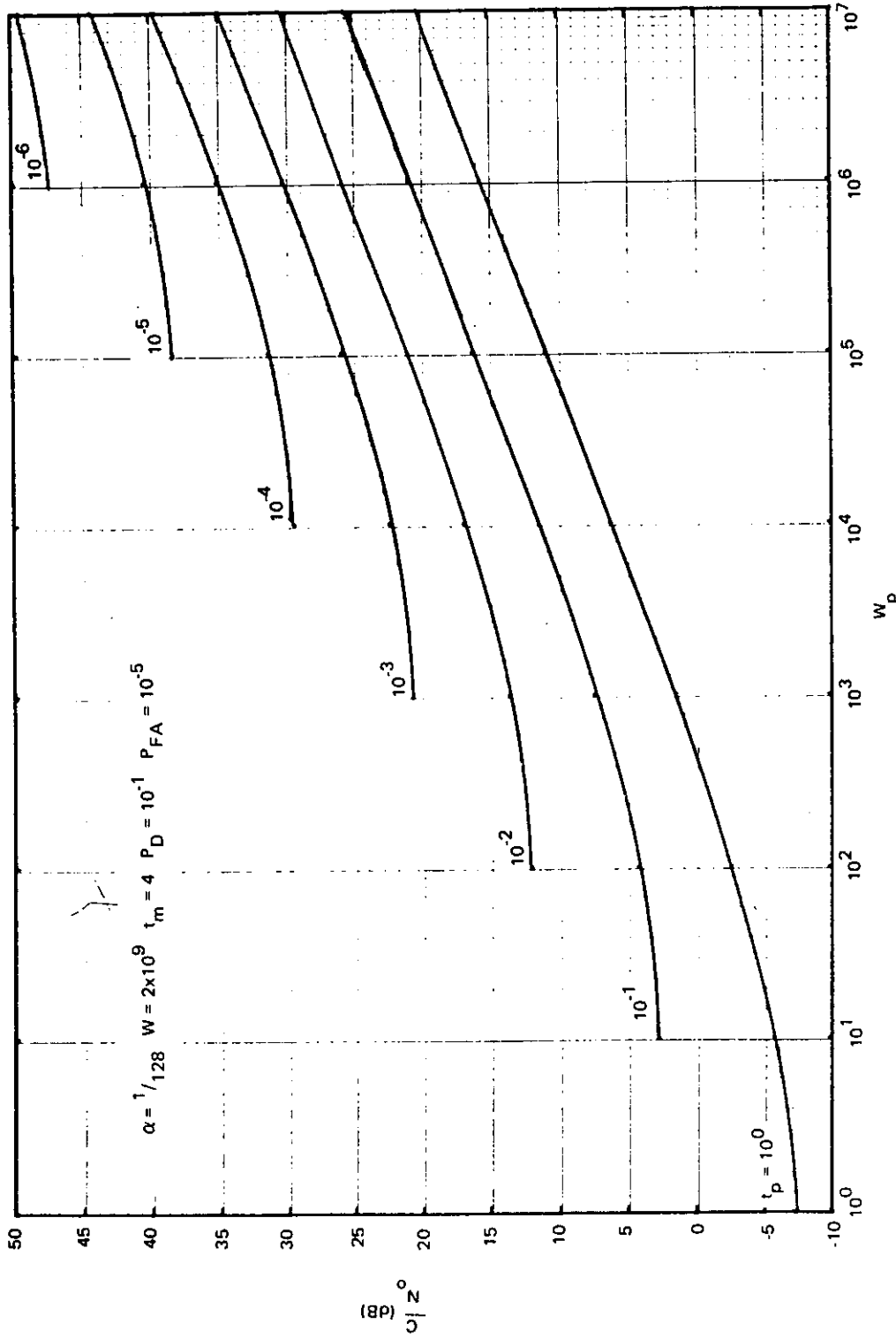


Fig. A3—Average required input C/N_0 for simple $k = 1$ threshold; $W = 2 \times 10^9$, $\alpha = 1$, $t_m = 10$, $P_D = 10^{-1}$, $P_{FA} = 10^{-5}$

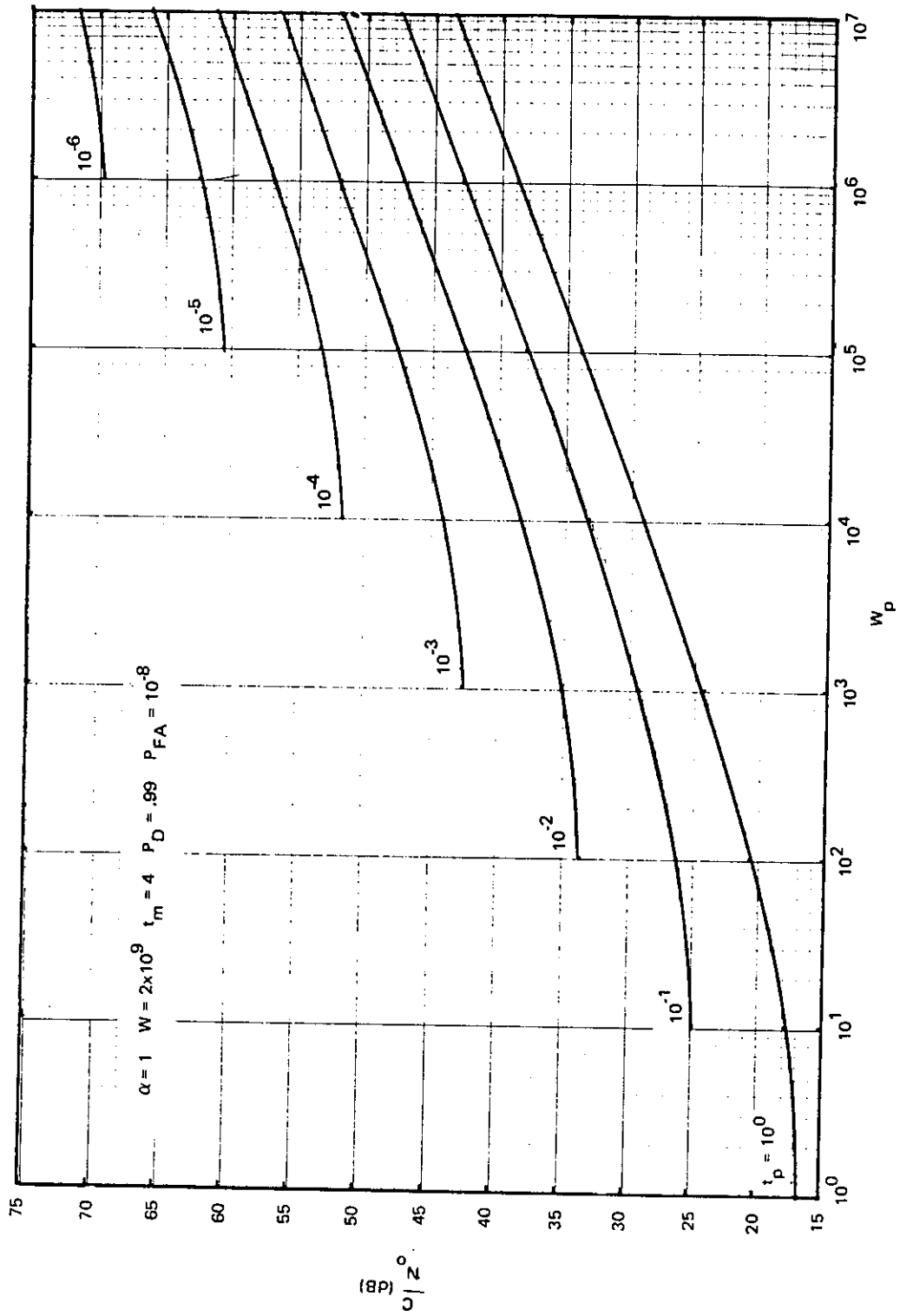


Fig. A4—Average required input C/N_0 for simple $k = 1$ threshold; $W = 2 \times 10^9$, $\alpha = 1$, $t_m = 4$, $P_D = 0.99$, $P_{FA} = 10^{-8}$

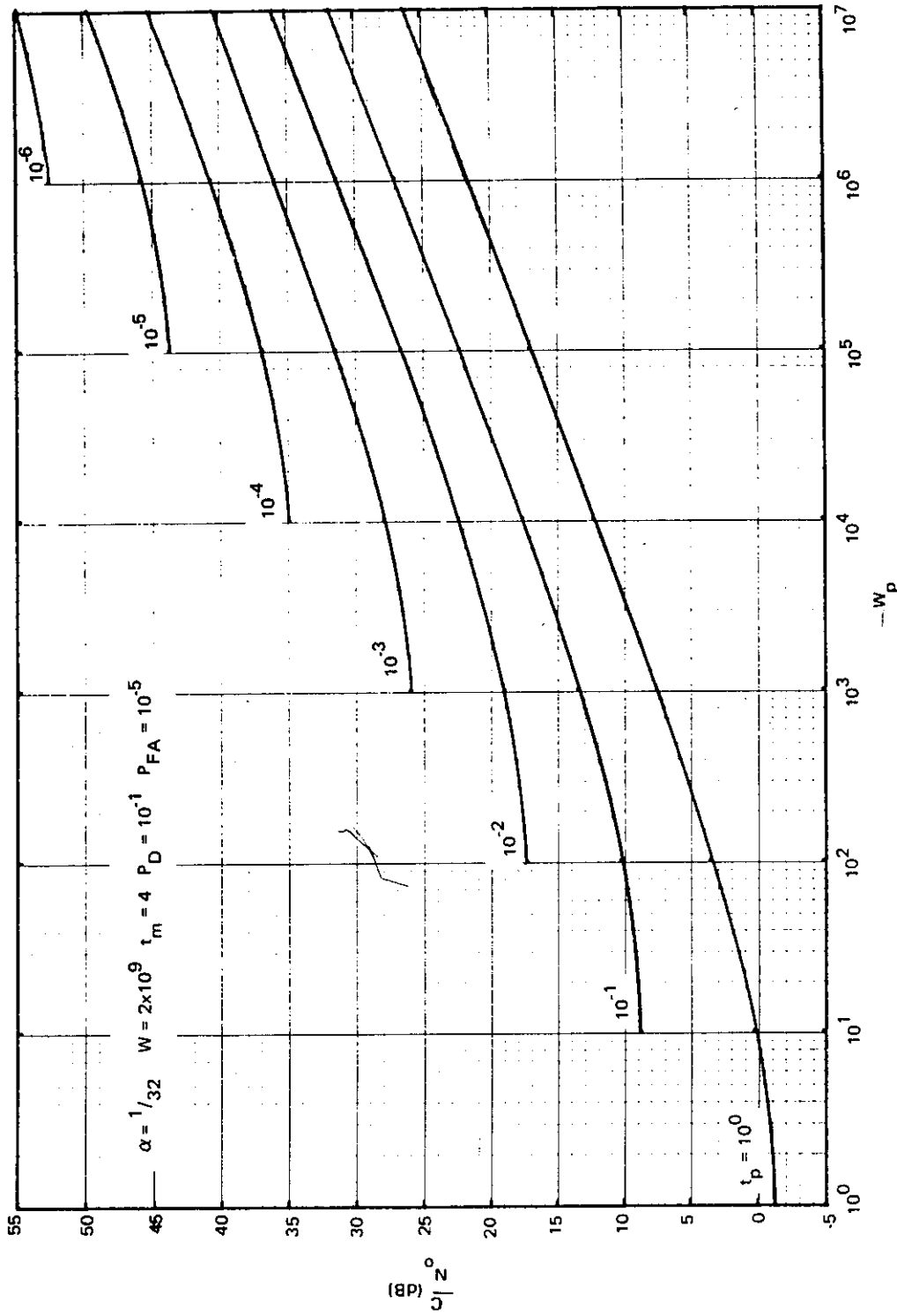


Fig. A5--Average required input C/N_0 for simple $k = 1$ threshold; $W = 2 \times 10^9$, $\alpha = 1/32$, $t_m = 4$, $P_D = 10^{-1}$, $P_{FA} = 10^{-5}$

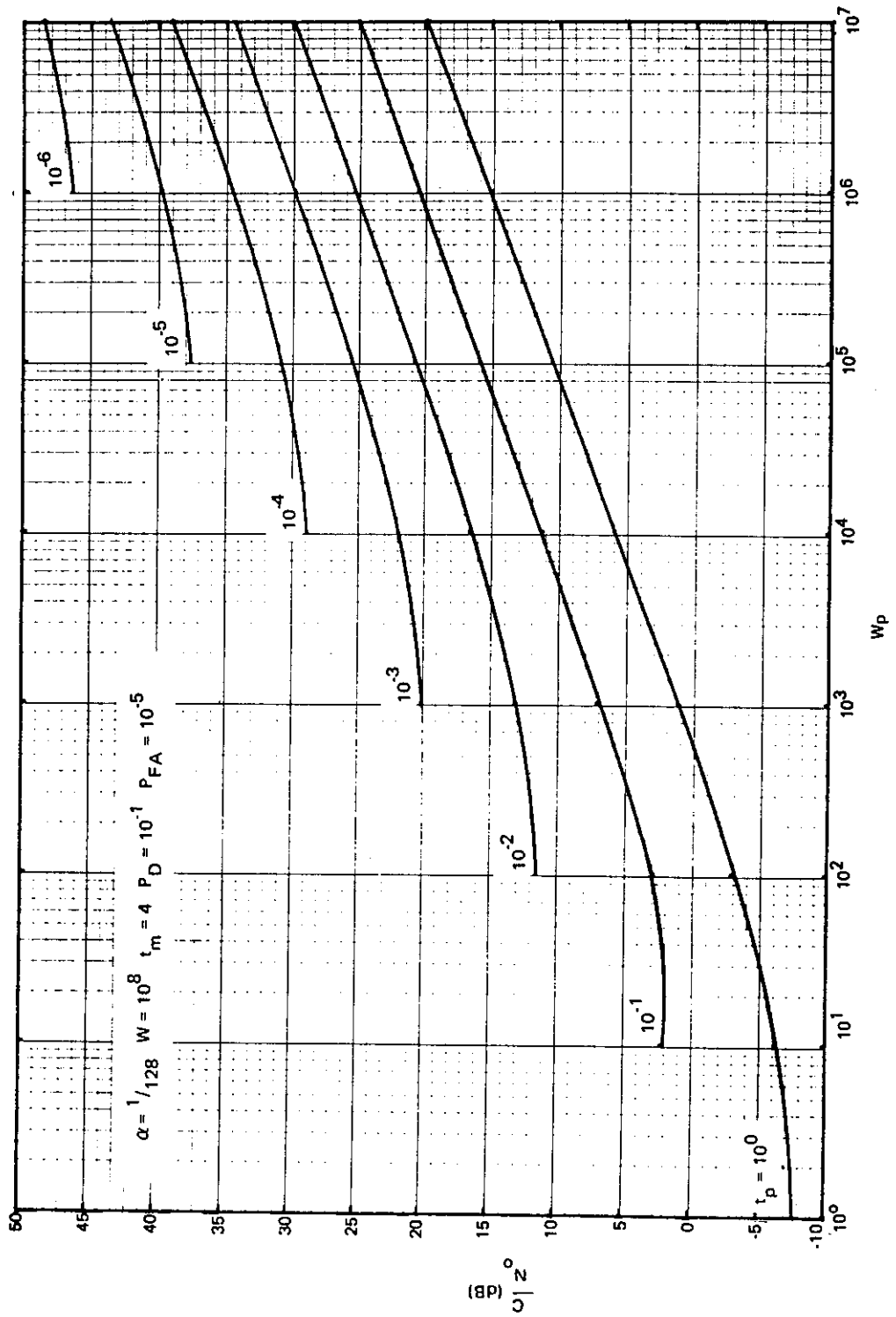


Fig. A6—Average required input C/N_0 for simple $k = 1$ threshold; $W = 10^8$, $\alpha = 1/128$, $t_m = 4$, $P_D = 10^{-1}$, $P_{FA} = 10^{-5}$

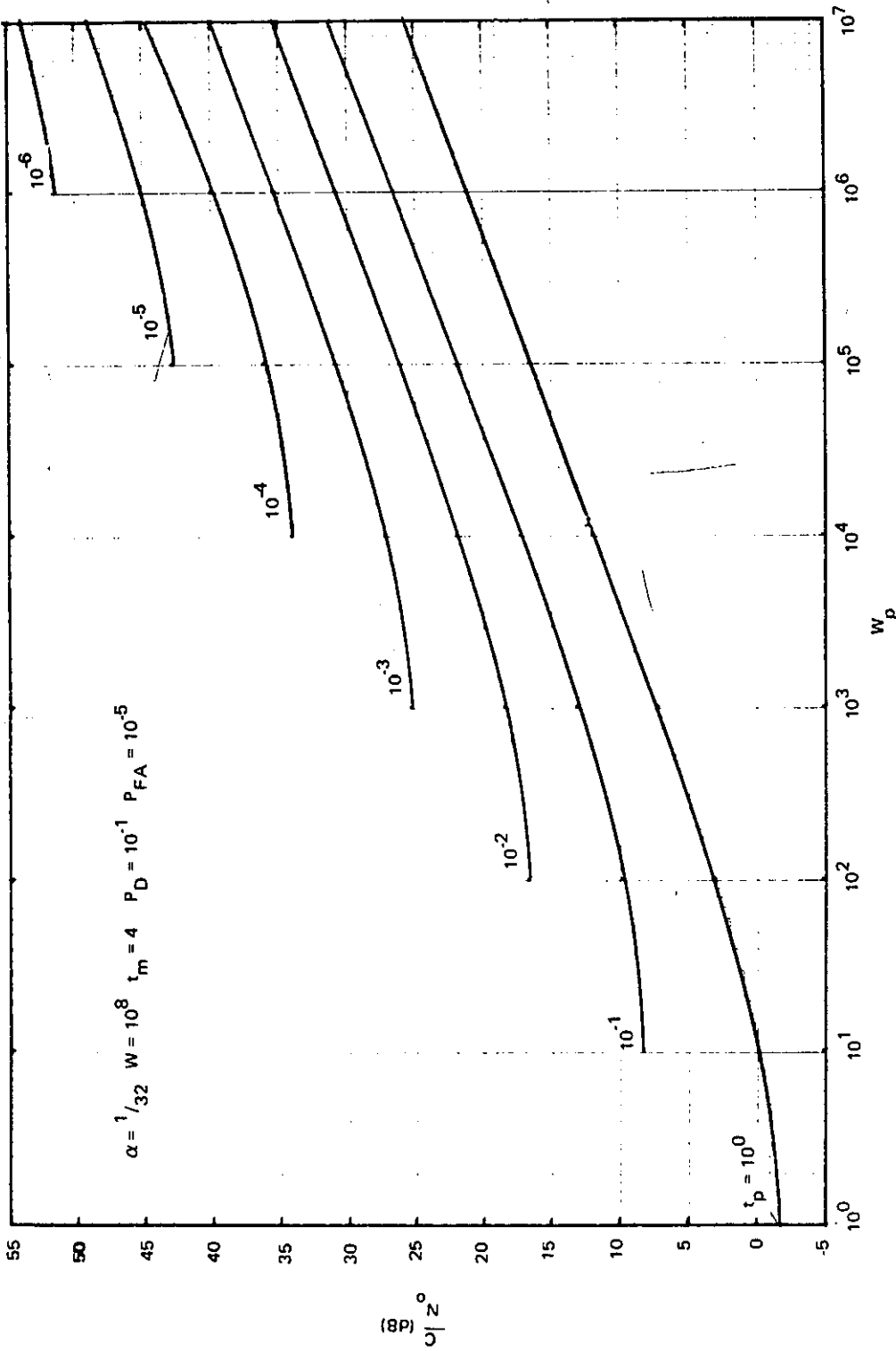


Fig. A7—Average required input C/N_0 for simple $k = 1$ threshold; $W = 10^8$, $\alpha = 1/32$, $t_m = 4$, $P_D = 10^{-1}$, $P_{FA} = 10^{-5}$

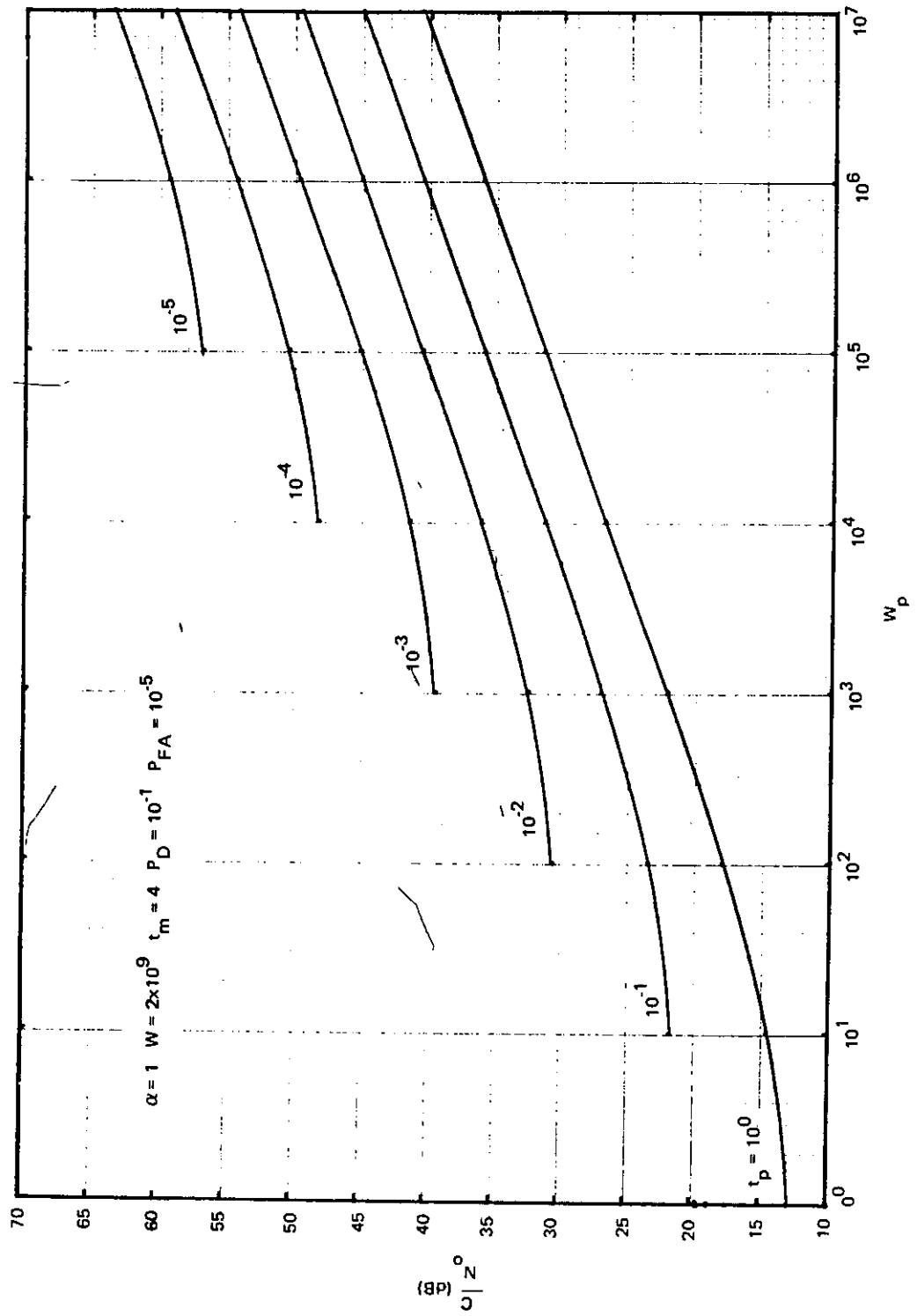


Fig. A8—Average required input C/N_0 for simple $k = 1$ threshold; $W = 2 \times 10^9$, $\alpha = 1$, $t_m = 4$, $P_D = 10^{-1}$, $P_{FA} = 10^{-5}$

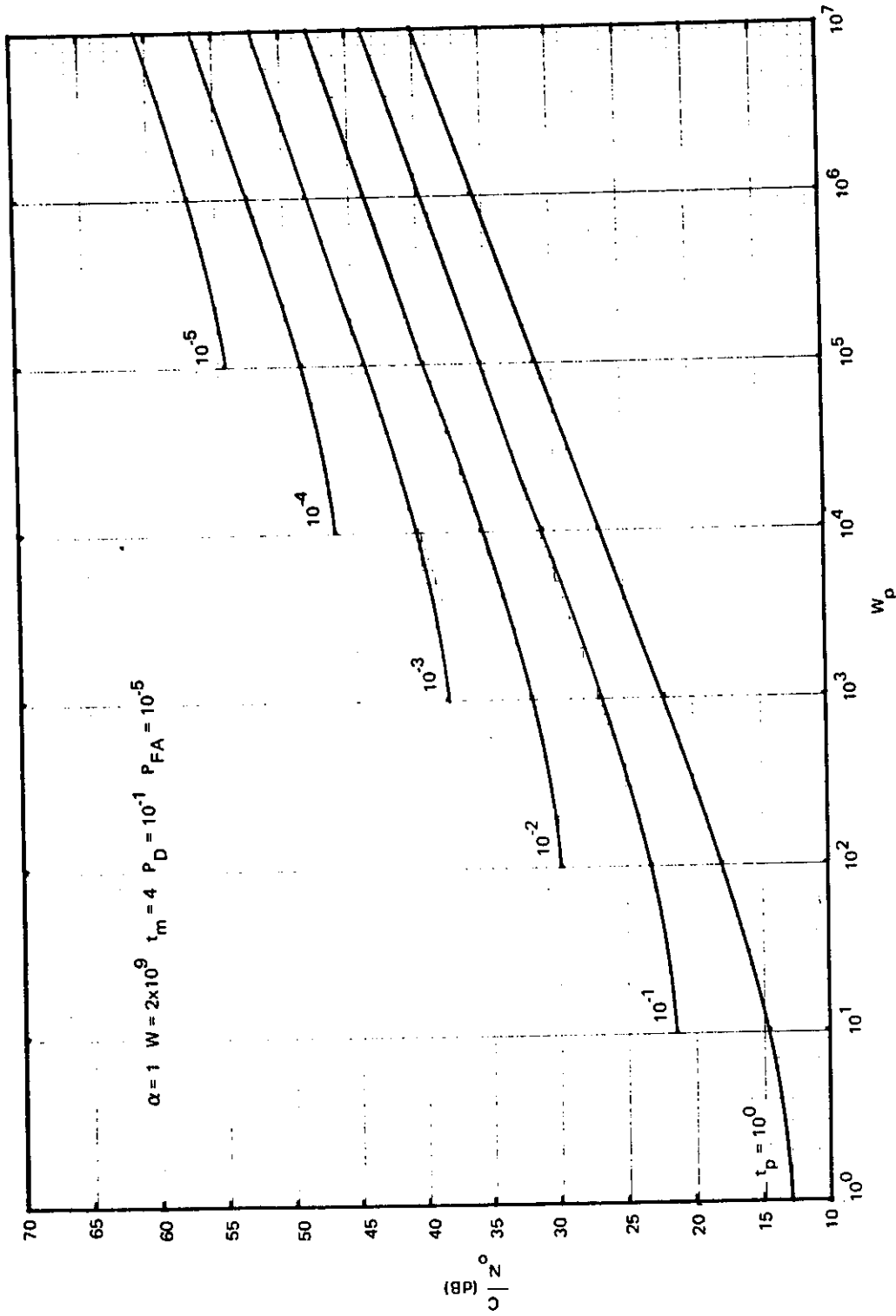


Fig. A9—Average required input C/N_0 for optimized threshold k ; $W = 2 \times 10^9$, $\alpha = 1$, $t_m = 4$, $P_D = 10^{-1}$, $P_{FA} = 10^{-5}$

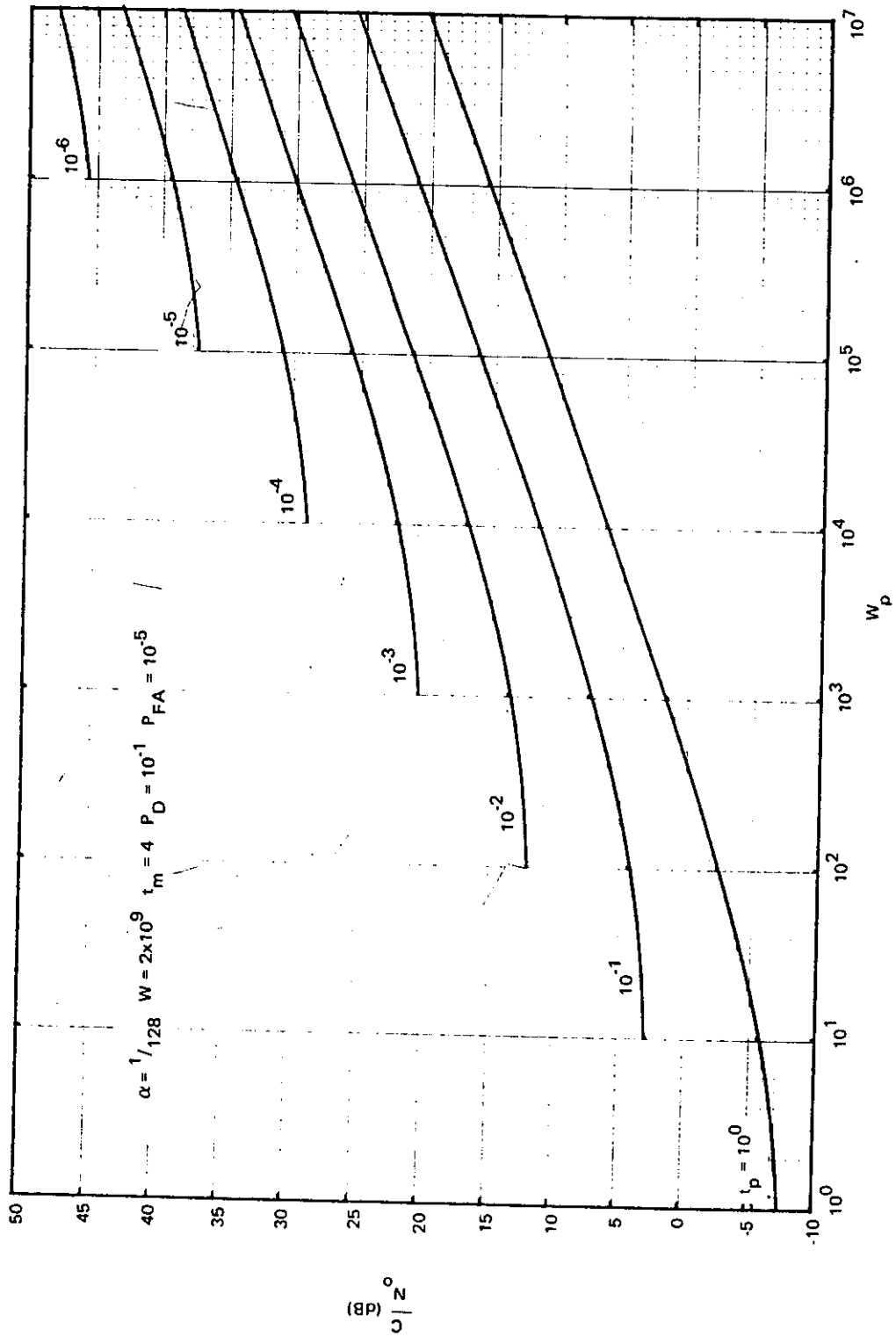


Fig. A10—Average required input C/N_0 for optimized threshold k ; $W = 2 \times 10^9$, $\alpha = 1/128$, $t_m = 4$, $P_D = 10^{-1}$, $P_{FA} = 10^{-5}$

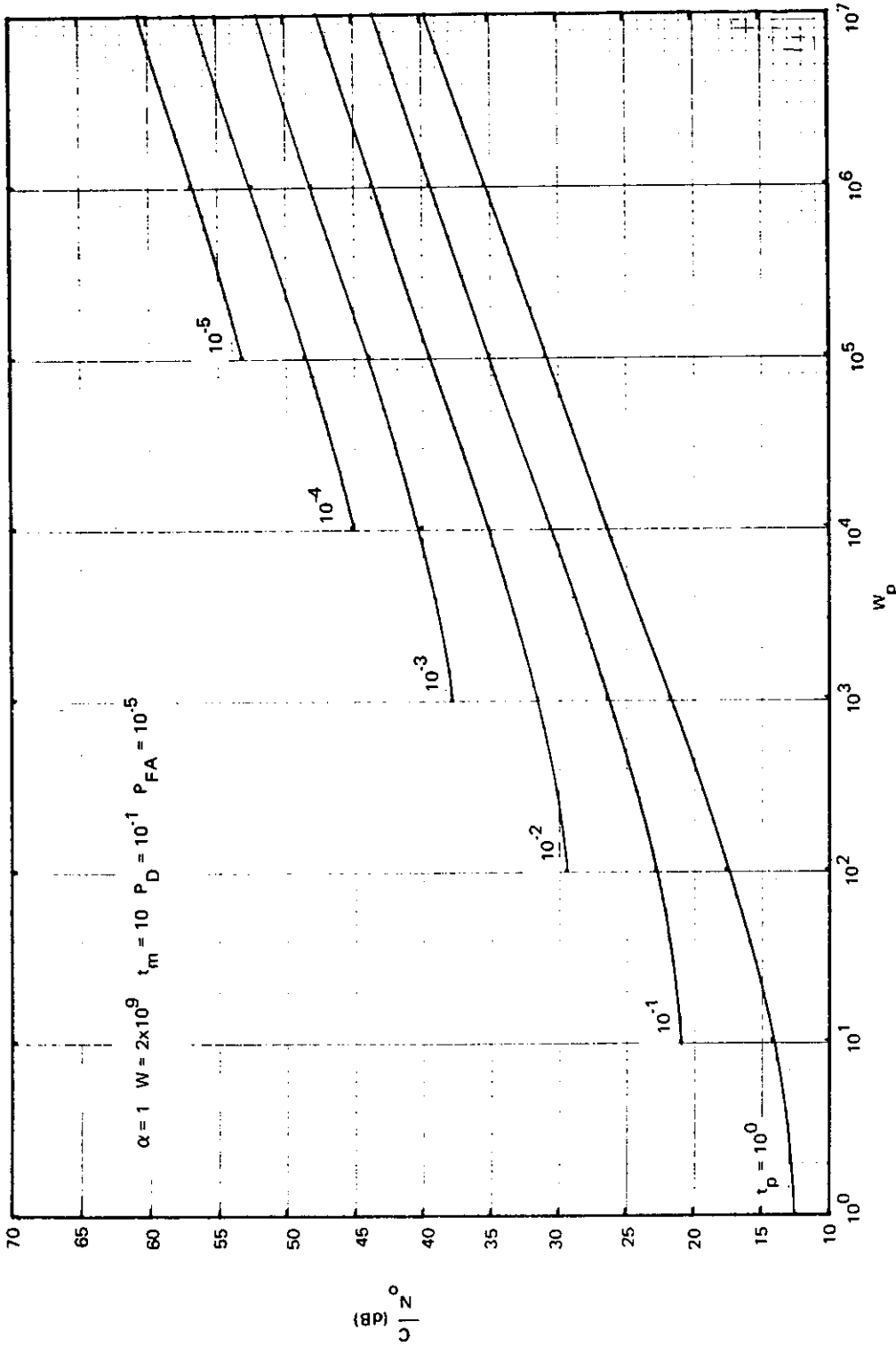


Fig. A11—Average required input C/N_0 for optimized threshold k ; $W = 2 \times 10^9$, $\alpha = 1$, $t_m = 10$, $P_D = 10^{-1}$, $P_{FA} = 10^{-5}$

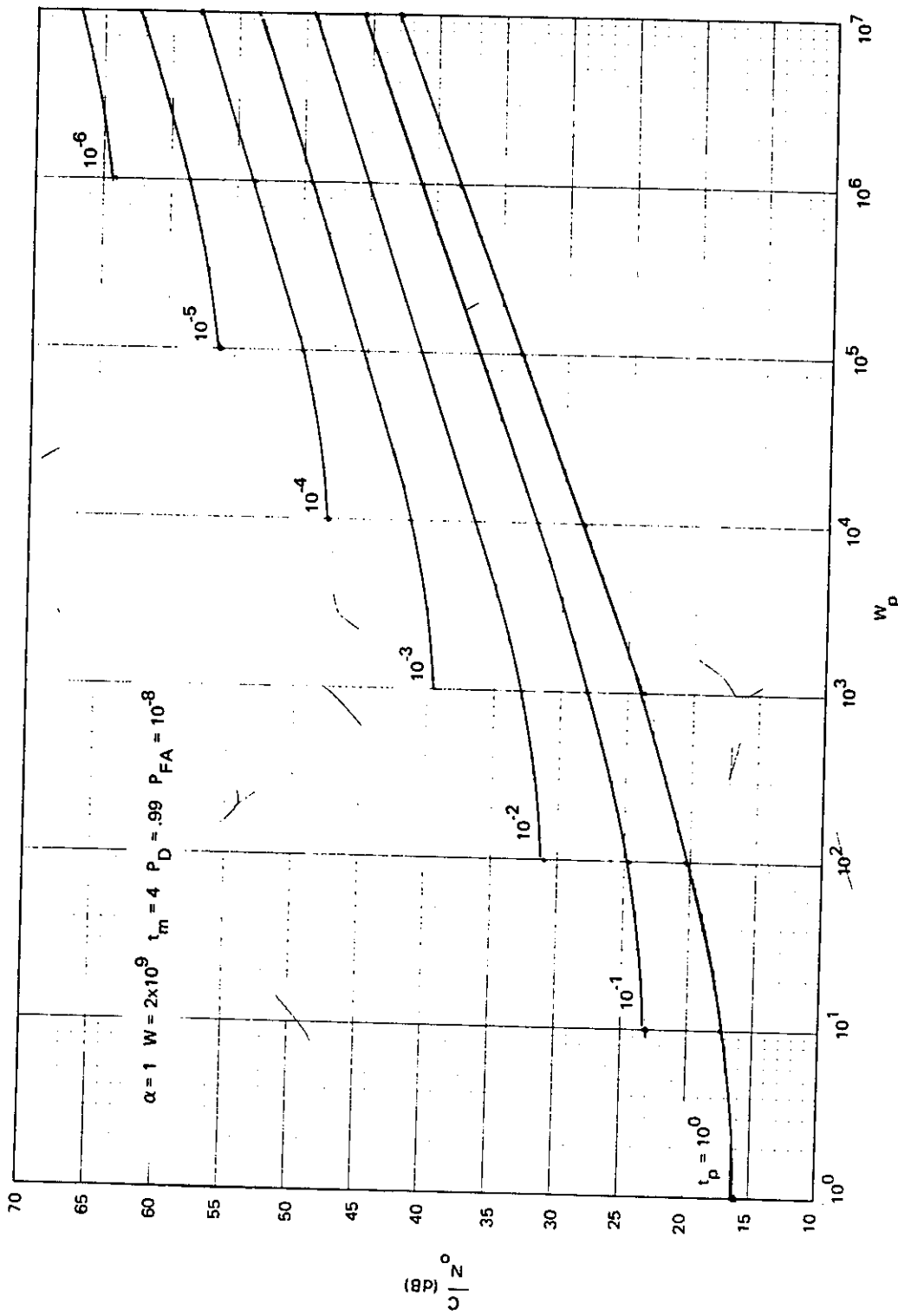


Fig. A1.2—Average required input C/N_0 for optimized threshold k ; $W = 2 \times 10^9$, $\alpha = 1$, $t_m = 4$, $P_D = 0.99$, $P_{FA} = 10^{-8}$

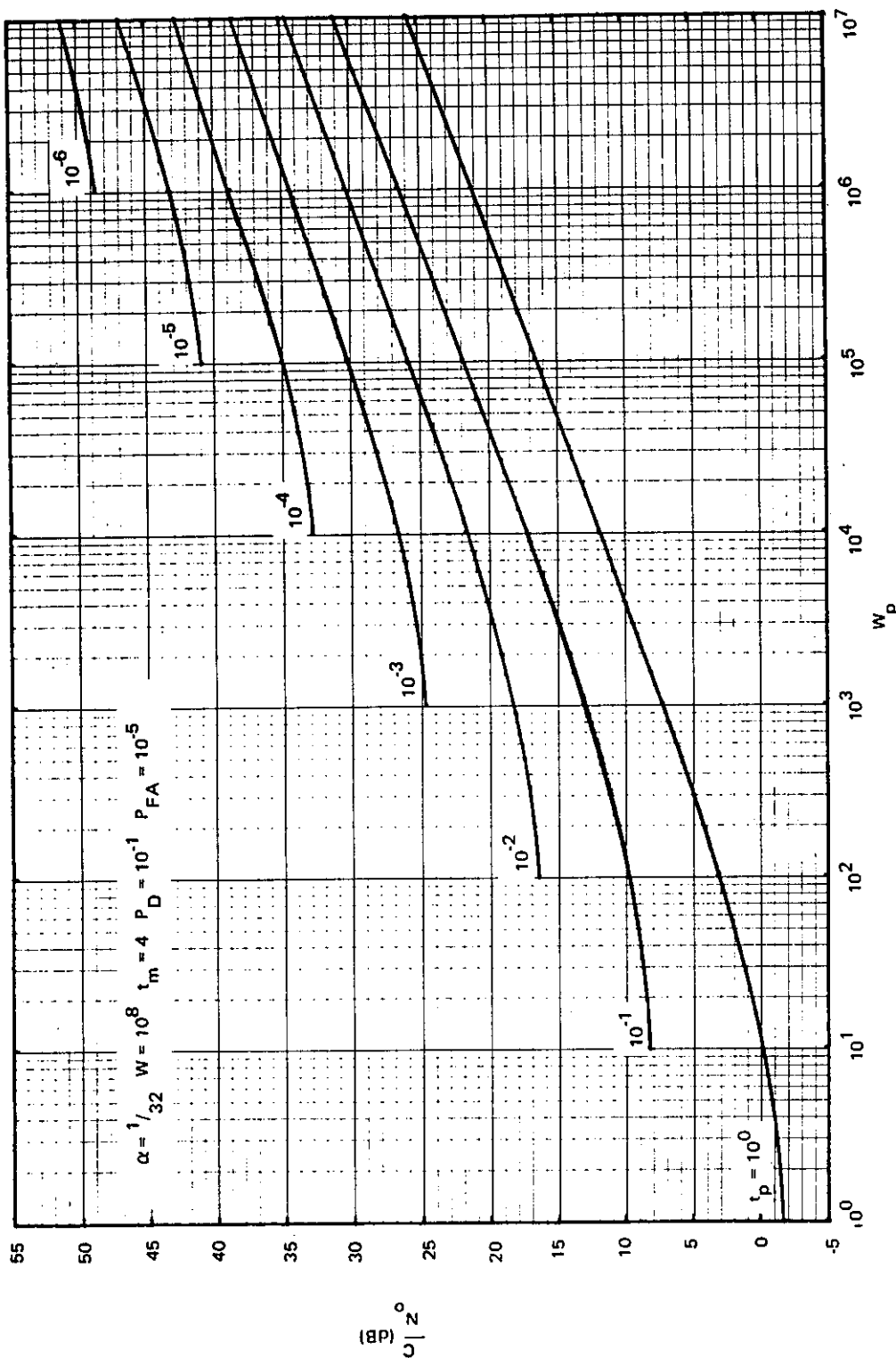


Fig. A13—Average required input C/N_0 for optimized threshold k ; $W = 10^8$, $\alpha = 1/32$, $t_m = 4$, $P_D = 10^{-1}$, $P_{FA} = 10^{-5}$

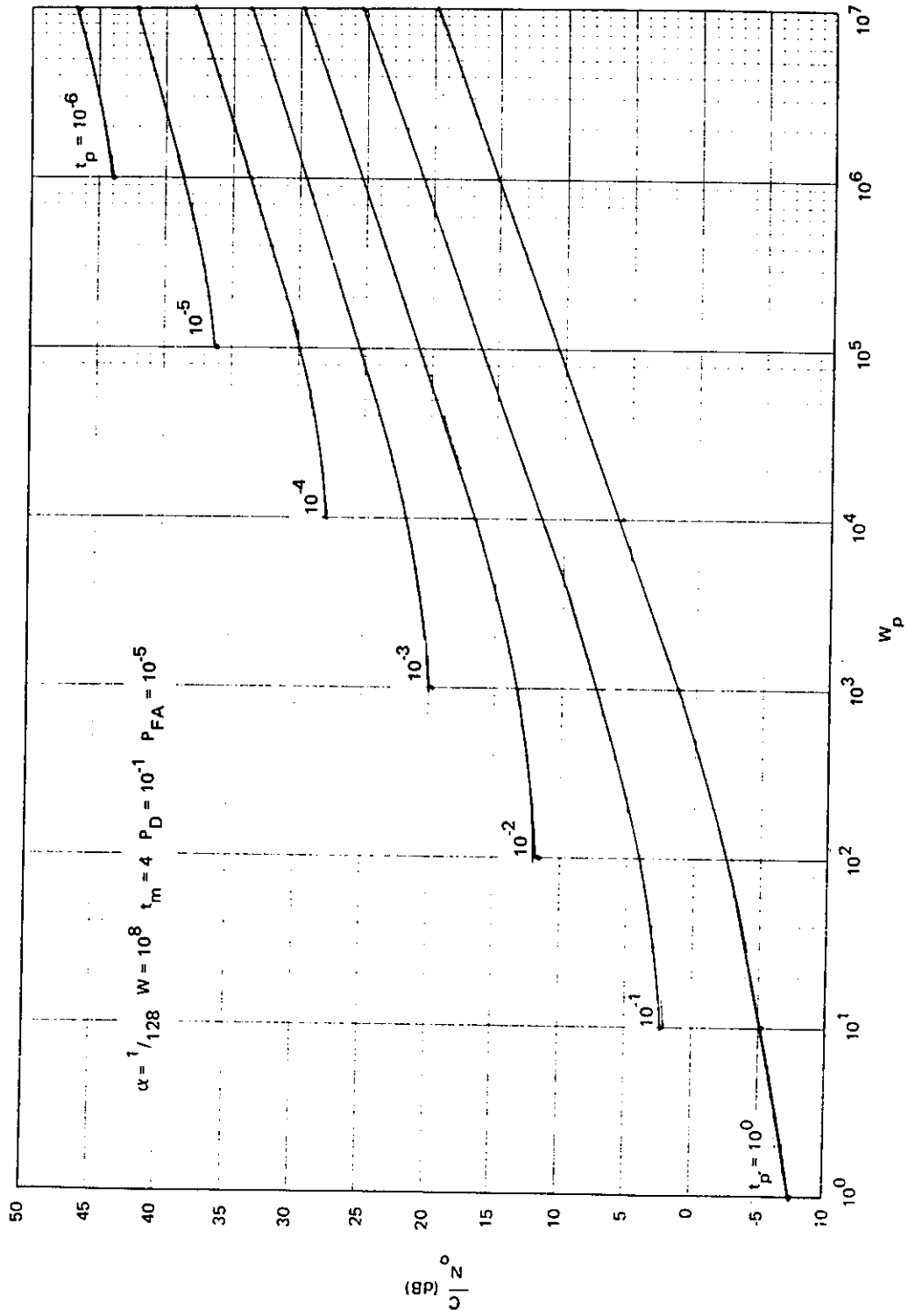


Fig. A.14—Average required input C/N_0 for optimized threshold k ; $W = 10^8$, $\alpha = 1/128$, $t_m = 4$, $P_D = 10^{-1}$, $P_{FA} = 10^{-5}$

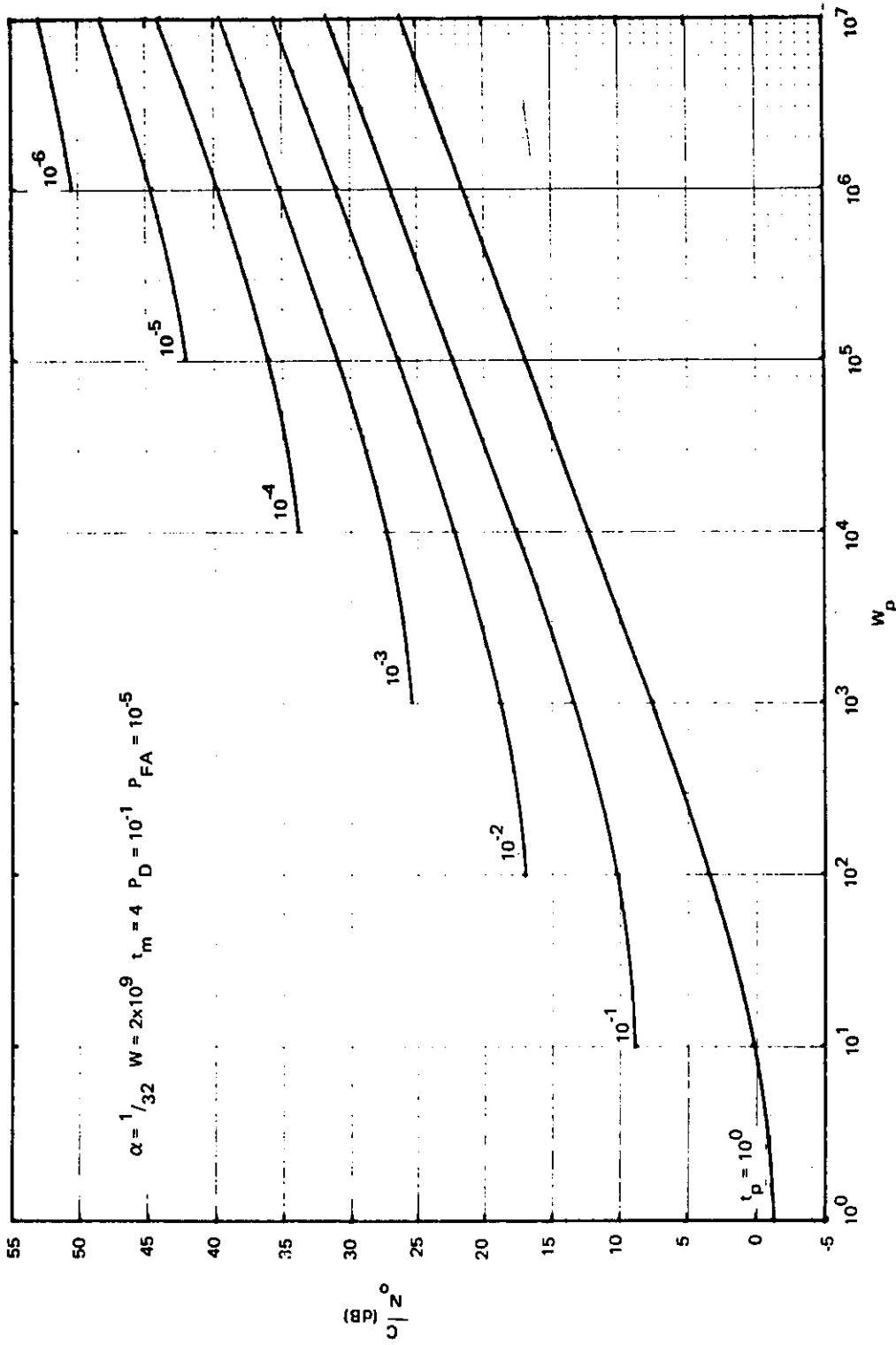


Fig. A15—Average required input C/N_0 for optimized threshold k ; $W = 2 \times 10^9$, $\alpha = 1/32$, $t_m = 4$, $P_D = 10^{-1}$, $P_{FA} = 10^{-5}$

SYMBOLS

A	carrier amplitude
B	noise bandwidth
$C(\dots)$	correction factor
$\frac{C}{N_0}$	ratio of input carrier power to noise power density
D_1	number of pulses per message actually transmitted
D_2	total number of parallel decisions per message
$\frac{E}{N_0}$	ratio of signal energy to noise density
$\frac{E_b}{N_0}$	ratio of bit energy to noise density
$\frac{E_s}{N_0}$	ratio of symbol energy to noise density
$\frac{E_H}{N_0}$	ratio of energy per hop to noise density
$F(\dots)$	$\frac{C}{N_0}$ predicted by accurate chi-square statistics
f_H	rate at which a carrier is switched or hopped
Δf	frequency offset
$G(\dots)$	$\frac{C}{N_0}$ predicted by equal-variance Gaussian approximation
G_{LR}	gain of listener's antenna
G_R	gain of receive antenna
G_T	transmitting antenna gain of terminal
$G_T(L)$	gain of transmitting antenna in direction of listener
$I_0(\cdot)$	modified Bessel function of the first kind of order zero
k	Boltzmann's constant
L_D	frequency offset loss
L_i	noncoherent combining loss
\ln	natural logarithm
L_U	uplink path loss
$L_U(L)$	path loss to listener
M	total number of hops per message

NRL REPORT 8025

M_C	reliable communications margin
N	total number of frequency cells to which a carrier can be switched
N_I	in-phase noise
N_0	noise power spectral density
N_Q	quadrature noise
$n(t)$	noise random process
P_b	probability of bit error
P_D	probability of detection
P_{DI}	probability of detection for an individual channel
P_{FA}	probability of false alarm
P_{FAI}	probability of false alarm for an individual channel
P_s	probability of symbol error
P_T	transmitter power
Q_H	hop quality factor
Q_M	message quality factor
r_D	data rate
$\frac{S}{N}$	signal power to noise power ratio
$s(t)$	transmitted signal
$S_0(t)$	output signal
$S_R(t)$	received signal
t	integration time
t_m	duration of a message
t_p	dwel time of a single hop
T_L	listener's receiving system temperature
T_R	receiving system noise temperature
W_p	bandwidth occupied by a single hop
W_s	total spread-spectrum bandwidth
α	duty cycle
η	correction factor for Gaussian statistics
Γ_L	$\frac{C}{N_0}$ at input to listener's receiver
ϕ_i	phase of carrier frequency ω_i
ω_i	carrier frequency transmitted during hop interval i